9-23-2020

Real-Time Time-Dependent Electronic Structure Theory

Xiaosong Li
University of Washington, Seattle

Niranjan Govind
Pacific Northwest National Laboratory

Christine Isborn
UC Merced

A. Eugene Deprince
Florida State University

Kenneth Lopata
Louisiana State University

Recommended Citation

Li, X., Govind, N., Isborn, C., Deprince, A., & Lopata, K. (2020). Real-Time Time-Dependent Electronic Structure Theory. *Chemical Reviews, 120* (18), 9951-9993. https://doi.org/10.1021/acs.chemrev.0c00223

CHEMICAL REVIEWS

pubs.acs.org/CR

Review

Real-Time Time-Dependent Electronic Structure Theory

Xiaosong Li,* Niranjan Govind,* Christine Isborn,* A. Eugene DePrince, III,* and Kenneth Lopata*

Cite This: https://dx.doi.org/10.1021/acs.chemrev.0c00223

Read Online

ACCESS | Metrics & More | Article Recommendations

ABSTRACT: Real-time electronic structure methods provide an unprecedented view of electron dynamics and ultrafast spectroscopy on the atto- and femtosecond time scale with vast potential to yield new insights into the electronic behavior of molecules and materials. In this Review, we discuss the fundamental theory underlying various real-time electronic structure methods as well as advantages and disadvantages of each. We give an overview of the numerical techniques that are widely used for real-time propagation of the quantum electron dynamics with an emphasis on Gaussian basis set methods. We also showcase many of the chemical applications and scientific advances made by using real-time electronic structure calculations and provide an outlook of possible new directions.

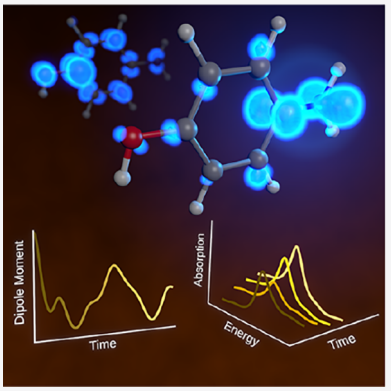

CONTENTS

1. Introduction A
2. Theory of Real-Time Time-Dependent Electronic Structure Methods C
   2.1. Real-Time Time-Dependent Hartree−Fock and Density Functional Theory C
      2.1.1. The Adiabatic Approximation in TDDFT E
      2.1.2. Accuracy of TDHF and TDDFT F
   2.2. Real-Time Time-Dependent Semi-Empirical Methods G
   2.3. Real-Time Time-Dependent Configuration-Interaction Methods G
   2.4. Real-Time Time-Dependent Coupled-Cluster Methods H
   2.5. Real-Time Time-Dependent Two-Component and Relativistic Methods K
   2.6. Real-Time Methods in Complex and Non-equilibrium Environments L
3. Numerical Techniques M
   3.1. Basis Set Representations M
   3.2. Time Propagation Methods M
   3.3. Signal Processing N
4. Application of Real-Time Time-Dependent Electronic Structure Methods P
   4.1. UV/Vis Spectroscopy P
   4.2. X-ray Absorption Spectroscopy Q
   4.3. Excited State Absorption and Emission Q
   4.4. Charge Transfer, Plasmon Excitations, and Exciton Dynamics R
   4.5. Nonlinear Properties and Multidimensional Spectroscopy U
   4.6. Spin and Magnetization Dynamics W
   4.7. Electronic Circular Dichroism and Magnetic Circular Dichroism W
   4.8. Electron Dynamics in Strong Fields X
5. Outlook Y
Author Information Z
   Corresponding Authors Z
   Notes Z
   Biographies Z
Acknowledgments AA
References AA

1. INTRODUCTION

Real-time electronic structure theory explicitly considers the time dependence of a quantum electronic system by evolving the time-dependent Schrödinger or Dirac equation, eq 1, in the time domain,

$$i\frac{\partial \Psi(\mathbf{r}, t)}{\partial t} = \hat{H}(\mathbf{r}, t)\Psi(\mathbf{r}, t) \quad (1)$$

In eq 1 and throughout this Review, atomic units are used. The nonequilibrium condition of the Hamiltonian under external

Received: March 25, 2020

perturbation gives rise to the time-evolution of the wave function or the electron density that underlies all response properties of a quantum electronic system. A complementary approach, not reviewed here, is frequency-domain response theory, which has been widely applied to chemical systems with remarkable success. Instead, this Review focuses on the time-dependent electronic wave function or density, explicitly propagated in the time domain.

Historically, the early work for explicitly time-dependent solutions of the time-dependent Schrödinger equation began in the late 70s and early 80s in the field of nuclear physics with a mean-field time-dependent Hartree−Fock (TDHF) approximation for studies of nuclear collisions and their scattering profiles.[1−5] In 1990, Cederbaum and coworkers laid the groundwork for propagating correlated electronic wave functions in real time with the development of the multiconfigurational time-dependent Hartree (MCTDH) method.[6] In 1994, Micha and Runge used a density-matrix-based real-time time-dependent Hartree−Fock (RT-TDHF) approach with a traveling atomic orbital basis for describing electron rearrangement during atomic collisions.[7] However, despite these developments, real-time methods did not become a practical computational tool for many years because the explicit time propagation of correlated electronic wave functions remained computationally expensive and the Hartree−Fock approach lacks important electron correlation effects.

In 1996, Bertsch and Yabana, for the first time, developed and applied the real-time time-dependent density functional theory (RT-TDDFT) approach within the local density approximation (LDA) for studies of dynamic response properties.[8] Their efforts in explicitly time-dependent electronic structure theory,[9−11] combined with the advent of usable real-space density functional theory (DFT) codes,[12−14] have led to great interest in real-time methods in the condensed matter physics community. However, the application of RT-TDDFT in the quantum chemistry and spectroscopy communities remained limited due to the lack of implementations of RT-TDDFT within the generalized gradient approximation (GGA) and hybrid GGA approximations, the modern day workhorses for computational chemistry and materials science. In 2005, Li and Schlegel introduced an efficient implementation of RT-TDHF[15] in a Gaussian-type atomic orbital basis, followed by an RT-TDDFT extension[16] by Li and Isborn in 2007 that could use generalized hybrid density functionals which include exact exchange. The development of real-time electronic structure theory in an atomic orbital basis, which allows for low-cost, accurate simulations of molecular spectroscopies and electronic dynamics using GGA and generalized hybrid functionals, has led to many Gaussian basis set-based real-time implementations in widely used codes in the quantum chemistry community capable of handling both small and large molecular and finite cluster systems.[17−23] With the development of scalable plane-wave and real-space grid-based implementations,[24−27] simulations of large-scale condensed phase systems have also become possible.

With advancements in computing power and numerical algorithms, there has been renewed interest in explicit time propagation of correlated methods such as multiconfigurational self-consistent-field (MCSCF),[28−32] configuration interaction (CI),[33−39] algebraic diagrammatic construction,[40−46] and coupled cluster (CC)[22,35,37,47−55] theories. Although wave-function-based real-time techniques scale poorly compared to RT-TDDFT, they afford systematically improvable accuracy and allow for accurate simulations of electronic dynamics in strong fields. Alternatively, correlated electron dynamics can be modeled through the time evolution of the one-electron reduced density matrix (RDM)[56−60] or the two-electron RDM,[61,62] as opposed to the wave function, but such methods are plagued by *N*-representability[63] problems resulting from the truncation of the Bogoliubov−Born−Green−Kirkwood−Yvon (BBGKY)[64−67] hierarchy of equations of motion for the RDMs.[61,62]

Motivated by the need for an explicit and accurate description of electron spin interaction with internal (e.g., spin−spin and spin−orbit) and external (e.g., magnetic field) perturbations, there has been a growing interest in extending real-time methods beyond the framework of the time-dependent Schrödinger equation. In 2014, Li and coworkers introduced a nonrelativistic real-time time-dependent two-component method to simulate electron spin dynamics.[68] This work demonstrated that the *ab initio* simulation of electron spin dynamics requires at least two components in the description of electronic degrees of freedom. In 2015, Repisky and Ruud presented the first fully relativistic four-component RT-TDDFT (4c-RT-TDDFT),[69] followed by a formally equivalent relativistic two-component implementation (2c-RT-TDDFT) by Li in 2016.[70] The development of these real-time time-dependent Dirac methods has enabled the computational investigation of magnetic and spin−orbit effects in molecular spectroscopy and electronic dynamics.

The nonrelativistic Hamiltonian for an *N*-electron system interacting with a time-dependent electromagnetic field is defined as

$$\hat{H}(\mathbf{r}, t) = \sum_{i}^{N} \left(\frac{1}{2}\boldsymbol{\pi}^2 - U(\mathbf{r}_i, t) \right) + \sum_{i<j}^{N} \frac{1}{|\mathbf{r}_i - \mathbf{r}_j|} + V_{\text{ext}} \tag{2}$$

where the first term includes the electron kinetic energy and the coupling to the field, the second term is the electron−electron repulsion term V_{ee}, and V_{ext} includes the electron−nuclear attraction term and other external potentials such as the system−bath interaction. The external electromagnetic perturbation is usually treated classically and defined by a vector potential $\mathbf{A}(\mathbf{r}, t)$ and a scalar potential $U(\mathbf{r}, t)$. $\boldsymbol{\pi} = \mathbf{p} + \mathbf{A}$ is the generalized momentum that includes the vector potential $\mathbf{A}$ along with linear momenta $\mathbf{p}$. This term gives rise to the electron kinetic energy and electron-field coupling. Note that in some cases, the electron-field interaction is included in the V_{ext} term but here we include this coupling by incorporating the vector and scalar potentials in eq 2. The majority of this Review focuses on approximate solutions to the time-dependent Schrödinger equation and their scientific applications. Development of practical real-time methods within the time-dependent Dirac framework is an emerging direction and some aspects will be discussed in Section 2.5.

Eq 2 is the general form of the nonrelativistic Hamiltonian that drives electronic dynamics via the time-dependent Schrödinger equation. Real-time methods, like other *ab initio* methods, must numerically solve the underlying Schrödinger or Dirac equation (eq 1) through mean-field approximations, such as Hartree−Fock (HF) and DFT, or wave-function-based techniques, such as CC and CI. For treating large systems, low-cost semiempirical approaches, continuum models, or molecular mechanics can be used to simulate responses from the complex environment. The fundamental theory and mathematical *ansatz* of these techniques will be reviewed in Sections 2.1−2.6. In addition, real-time methods must also rely on robust numerical

https://dx.doi.org/10.1021/acs.chemrev.0c00223
Chem. Rev. XXXX, XXX, XXX−XXX

techniques and representations (Section 3) to explicitly integrate the quantum system in time and resolve quantum observables from time signals without introducing nonphysical behavior.

Most scientific applications of real-time methods concern electronic responses to external perturbations, such as an electromagnetic field [$\mathbf{A}(\mathbf{r}, t)$ and $U(\mathbf{r}, t)$], electron−nuclear coupling (V_{Ne}), and system-bath coupling (V_b). These perturbations give rise to the spectroscopic signatures, population transfer, and energetic decay of an electronic system. In the absence of these driving forces, time-evolution of an electronic wave function will exhibit either coherent oscillations that travel through phase space in the case of a pure coherent wave function or remain stationary in the case of an eigenstate. Real-time electronic structure theory is thus a powerful tool for simulating diverse chemical phenomena, many of which will be reviewed in Section 4.

Applications of real-time methods span the field of spectroscopy, including valence-electron UV/vis and photoelectron spectroscopy,[9,10,15,18,34,69−88] circular dichroism,[89−94] core−electron X-ray absorption,[49,95−98] nonlinear optical response,[14,99,100] photoionization,[71,101−115] and magnetization dynamics.[68,116,117] Real-time electronic structure methods have also found utility in studies of molecular electronics,[118−127] optimal control,[117,128−131] as well as coherence and charge-transfer dynamics.[16,132−151] To probe chemical processes in complex environments, real-time electronic dynamics have been coupled to polarizable[32,152] and nonpolarizable molecular mechanical layers,[74,153] implicit solvation models,[138,139,154−157] quantum subsystems,[158] and thermal baths in an open quantum system formalism.[20,150,159−165] Recently, the coupling of a molecule to a quantized electromagnetic field,[166−174] real-time quantum electrodynamics (QED), has led to first-principles studies of photon absorption and emission and simulations of cavity QED experiments.

The focus of this Review is on real-time electronic structure; thus, we do not focus on nuclear motion. However, because different electronic structure methods lend themselves to different ways of coupling with nuclear motion, it is worth briefly mentioning some of these methods here. See extensive reviews[175−180] and references therein for more in-depth discussions and an overview of mixed quantum-classical dynamics methods. Exact electron−nuclear dynamics are obtainable via solution of the full time-dependent Schrödinger equation for the entire (electronic plus nuclear) system: a computationally prohibitive prospect for all but the smallest of molecules with only a few active electrons.[181] Various approximate methods have been introduced with the aim of achieving reliable results at lower costs.[7,132,182−211] Two of the most widely used methods are trajectory surface hopping and the Ehrenfest approach.[184,189] These mixed quantum-classical formalisms use the classical equation-of-motion for nuclear degrees of freedom and quantum mechanical evolution of the time-dependent electronic wave function, such as RT-TDHF, RT-TDDFT, TD-CC, TD-CI, etc., but differ in how the electronic potential energy surface is computed. Trajectory surface hopping methods, introduced specifically to account for the branching of trajectories due to electron−nuclear coupling, often use fitted potential surfaces or compute electronic forces and couplings on-the-fly.[184,189,212−225] Surface hopping therefore does not generally make use of real-time electronic structure. Analogous methods can also be built from nuclear motion on the ground state electronic surface, which can provide time-evolving ground state occupied and virtual orbitals to be used for time-domain surface hopping methods;[226,227] these techniques ignore feedback from the excited state population to the nuclear motion as well as ignoring all electronic coherences between states that are captured by real-time electronic structure methods.

In contrast, the Ehrenfest approach naturally couples to real-time electronic structure methods, propagating the nuclei as classical particles subject to a force from a weighted average of all the electronic states of the system (see refs 16, 128, 129, 135, 175, 188, 201, 210, and 228−237).The time-evolving expansion coefficients of the electronic wave function, which are governed by the electronic time-dependent Schrödinger equation, determine the weights in the average of the potential energy surfaces. This method can avoid explicit computations of the excited states by representing the wave function as a superposition state, while still accounting for electronic nonadiabaticity, making the Ehrenfest dynamics an excellent approach for simulating dense manifolds of electronic states. Indeed, for methods based on real-time propagation of the electron density, such RT-TDHF and RT-TDDFT, excited states and their respective populations are ill-defined; evolving the classical nuclei on this electronic superposition state yields Ehrenfest dynamics. The drawback of the Ehrenfest approach is the restriction to motion on a single average potential energy surface, which can lead to nonphysical results, such as overcoherence, particularly in the asymptotic limit.[209,238−243] Recently, Fedorov and Levine proposed a systematically improvable multiple cloning approach to mitigate issues arising from long-time propagation of Ehrenfest dynamics on unphysical mean-field surfaces.[237]

In this Review, we highlight the theory of various real-time electronic structure methods as well as advantages and disadvantages of each. We give an overview of the numerical techniques that should be considered for real-time electron propagation with a focus on Gaussian basis set approaches, and we showcase many of the chemical applications for real-time electronic structure calculations.

2. THEORY OF REAL-TIME TIME-DEPENDENT ELECTRONIC STRUCTURE METHODS

We use the following notations throughout the rest of this Review:

- $K, L, \ldots$ are Slater determinants.
- $i, j, k, l, \ldots$ are occupied molecular orbitals.
- $a, b, c, d, \ldots$ are virtual molecular orbitals.
- $p, q, r, s, \ldots$ are general molecular orbitals.
- $\mu, \nu, \ldots$ are atomic orbitals.

All equations use atomic units with $e^2 = \hbar = m_e = 1$. Primed notations (e.g., $\mathbf{F}'$, $\mathbf{P}'$) are used for matrices in the orthonormal basis and unprimed notations for matrices (e.g., $\mathbf{F}$, $\mathbf{P}$) in the atomic orbital (AO) basis.

2.1. Real-Time Time-Dependent Hartree−Fock and Density Functional Theory

Many excellent articles, reviews, and books exist focusing on details of TDDFT within both the linear response matrix formulation and within the real-time electronic propagation formulation.[146,244−252] We refer the reader to these works to gain a more detailed perspective of the theoretical underpinnings of TDDFT, including details of the Runge−Gross[253] and the van Leeuwen[254] proofs of mappings from the density to the potential that show that all time-dependent properties can be

https://dx.doi.org/10.1021/acs.chemrev.0c00223
Chem. Rev. XXXX, XXX, XXX−XXX

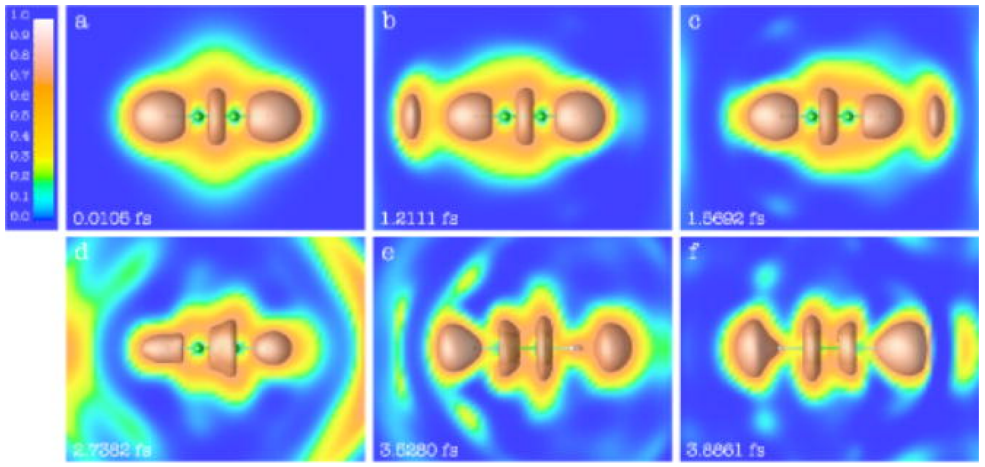

Figure 1. Snapshots of the time-dependent electron localization function of acetylene during application of a laser pulse. The electronic transition is from a bonding π to an antibonding π^* state. Adapted with permission from ref 260. Copyright (2005) American Institute of Physics.

extracted from the time-evolving electron density. Here, we especially wish to highlight similarities and differences between RT-TD Hartree−Fock (RT-TDHF) and RT-TDDFT. We therefore initially present these two methods on an equal footing within a molecular orbital or Kohn−Sham (KS) picture, which is required by Hartree−Fock and by generalized KS hybrid DFT methods due to the inclusion of exact exchange, before focusing on some of the relevant issues specific to RT-TDDFT.

For both TDDFT and TDHF within an orbital basis, a set of time-dependent one-particle equations is given by

$$i\frac{\partial}{\partial t}\phi_i(\mathbf{r}, t) = \hat{H}(\mathbf{r}, t)\phi_i(\mathbf{r}, t) \tag{3}$$

where i runs over all N electrons and the time-dependent electron density is

$$n(\mathbf{r}, t) = \sum_{i=1}^{N} |\phi_i(\mathbf{r}, t)|^2 \tag{4}$$

Although numerous theoretical differences exist between TDDFT and TDHF as discussed in the citations listed above, the main, practical difference is the treatment of the electron−electron repulsion term V_{ee} in the Hamiltonian $\hat{H}(\mathbf{r}, t)$ in eq 2. For both TDHF and TDDFT, V_{ee} depends on the time-dependent density or the time-dependent orbitals, and therefore becomes a time-dependent operator.

For Hartree−Fock, V_{ee} contains Coulomb and exchange operators that describe average electron−electron interactions within the single particle picture

$$V_{ee}^{HF}(\mathbf{r}, t)\phi_i(\mathbf{r}, t) = \left[\sum_j^N \int d\mathbf{r}' \frac{\phi_j^*(\mathbf{r}', t)\phi_j(\mathbf{r}', t)}{|\mathbf{r} - \mathbf{r}'|}\right]\phi_i(\mathbf{r}, t) - \left[\sum_j^N \int d\mathbf{r}' \frac{\phi_j^*(\mathbf{r}', t)\phi_j(\mathbf{r}, t)}{|\mathbf{r} - \mathbf{r}'|}\right]\phi_i(\mathbf{r}', t) \tag{5}$$

where the first term provides an average Coulombic electron−electron interaction and the second term describes the nonlocal exchange contribution to the energy that results from the use of a Slater determinant for describing an antisymmetric wave function. Both terms depend only on the instantaneous orbitals at time t. The missing electron−electron interaction energy in Hartree−Fock theory is called the correlation energy, the lack of which arises from the mean-field single particle approximation.

For density functional theory, the electron−electron interaction term V_{ee} contains the same average Coulombic electron−electron interaction (often called the Hartree term in the physics community), which can also be written in terms of the electron density $n(\mathbf{r}, t)$, and an exchange-correlation term V_{xc}

$$V_{ee}^{DFT}(\mathbf{r}, t)\phi_i(\mathbf{r}, t) = \left[\int d\mathbf{r}' \frac{n(\mathbf{r}', t)}{|\mathbf{r} - \mathbf{r}'|} + V_{xc}[n; \Psi_0, \Phi_0]\right]\phi_i(\mathbf{r}, t) \tag{6}$$

where the unknown exchange-correlation potential V_{xc} is formally a function of: the electron density n at all points in space and at all previous points in time, Ψ_0 the initial many-body wave function, and Φ_0 the initial state to be used for the noninteracting Kohn−Sham wave function. Unlike TDHF theory, TDDFT up to this point is formally exact. Although the Coulomb/Hartree energy contains contributions from each electron in orbital ϕ_i interacting with itself as part of the total density n, this erroneous self-interaction energy should be exactly canceled in the exchange contribution of V_{xc}, as it is for the exact nonlocal exchange in Hartree−Fock theory.

The Liouville equation generalizes the time-dependent Schrödinger equation to

$$i\frac{\partial\hat{\rho}(t)}{\partial t} = [\hat{H}(\mathbf{r}, t), \hat{\rho}(t)] \tag{7}$$

where $\hat{\rho}(t)$ is the density operator and $\hat{H}(\mathbf{r}, t)$ is the time-dependent many-body Hamiltonian. This expression is only valid for Hermitian Hamiltonians, i.e., without complex absorbing potentials. The time-dependent molecular orbitals ϕ_i are often created from a linear combination of basis functions $\{\chi_\mu\}$ as $\phi_i = \sum_\mu c_{\mu,i}(t)\chi_\mu$, where $c_{\mu,i}(t)$ are the time-dependent coefficients. The elements of the Hartree−Fock or DFT density matrix $\mathbf{P}$ are then given in this basis by

$$P_{\mu\nu}(t) = \sum_p f_p c_{\mu,p}^*(t)c_{\nu,p}(t) \tag{8}$$

where f_p is the occupation of orbital p. Transforming the density matrix $\mathbf{P}$ to the orthonormal basis and now writing it as $\mathbf{P}'$ in this basis, we can then express the TDHF or TDDFT equation as

https://dx.doi.org/10.1021/acs.chemrev.0c00223
Chem. Rev. XXXX, XXX, XXX−XXX

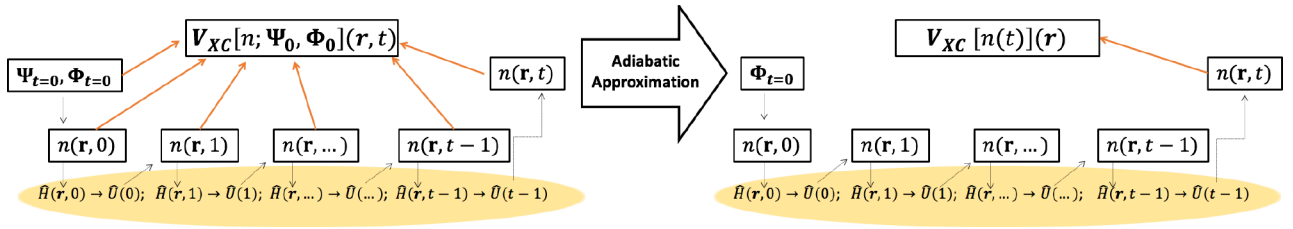

Figure 2. The commonly used adiabatic approximation in TDDFT uses only the instantaneous electron density $n(\mathbf{r}, t)$ as an input to the exchange-correlation potential, ignoring the dependence on the electron density at all previous points in time.

$$i\frac{\partial P'(t)}{\partial t} = [H'(t), P'(t)] \tag{9}$$

where $\mathbf{H}'(t)$ is the Hamiltonian matrix (integrated over $\mathbf{r}$), here the Fock matrix for TDHF or the Kohn–Sham matrix for TDDFT, in the orthonormal basis.

This equation is a starting point for both solving for the density response in the frequency domain via a matrix formulation, usually by keeping only the terms that are first order in the perturbation to obtain the linear response,[255−258] and for propagating the electron density in the time domain by numerical integration.[259] Real-time propagation reveals time-resolved electron distributions responding to a perturbation, such as the electron density of an acetylene molecule under the influence of an applied laser pulse as shown in Figure 1.[260]

However, a key challenge with RT-TDHF and RT-TDDFT is that the Hamiltonian becomes time-dependent, not just from the time-dependent perturbation, but from the dependence of the Hartree–Fock and DFT Hamiltonian on the time-dependent density in the Coulomb/Hartree and exchange-correlation potentials. This time-dependence of V_{ee} contrasts with correlated electronic dynamics methods wherein the exact form of V_{ee} is used and the only source of time dependence in the Hamiltonian is the external perturbation. The time-dependence of the Hartree–Fock/DFT Hamiltonian creates a nonlinear equation, which exhibits a host of inaccuracies for the RT-TDHF method and for the RT-TDDFT method with the common approximations to V_{xc}. These inaccuracies include unphysical peak-shifting,[77,261−266] incorrect Rabi oscillations,[84,267,268] and incorrect charge-transfer dynamics.[140,252,269] Because TDDFT is formally exact, these inaccuracies derive from the practical implementation of TDDFT, which requires approximations in choosing the form of the initial Kohn–Sham state Φ_0 and in choosing the form of the exchange-correlation potential V_{xc}. In practice, the initial Kohn–Sham state Φ_0 is usually chosen to be a single Slater determinant constructed from the single particle orbitals ϕ_i, as in Hartree–Fock theory. A recently developed formulation where the number of Kohn–Sham orbitals and their occupations are updated on the fly shows promise for alleviating some of the inaccuracies of RT-TDDFT.[268] The most common approximation to V_{xc} is to ignore all previous time-dependence on the electron density and to use the instantaneous electron density with a V_{xc} parametrized or derived for the ground state: $V_{xc}[n;\ \Psi_0,\ \Phi_0](\mathbf{r},\ t) = V_{xc}[n(t)](\mathbf{r})$. This adiabatic approximation, which ignores all memory dependence of the electron density, is equivalent to a frequency-independent kernel in linear response theory.

2.1.1. The Adiabatic Approximation in TDDFT. Formally, RT-TDDFT electron density propagation is exact, assuming the use of the exact time-dependent exchange-correlation potential. In contrast, RT-TDHF is inherently approximate because electron correlation effects are formally missing from the Hamiltonian and therefore from the electron propagation. The phase information encoded in the orbitals leads to some incorporation of memory via the exact exchange energy contribution in TDHF or in orbital-dependent TDDFT, but these memory effects[270,271] do not fix the dramatic errors in the RT-TDHF and RT-TDDFT electron dynamics. The exact V_{xc}, which would yield the exact electron density propagation, formally depends on the density at all points in time, as well as the initial wave function and initial Kohn–Sham state.[272,273] However, this memory dependence of the potential at time t on the density at all previous points in time $t' < t$ is not well-understood. As a result of this lack of knowledge, almost all TDDFT calculations ignore the history dependence of the electron density completely, with some notable exceptions discussed below. The dependence of V_{xc} on the initial wave function and Kohn–Sham state is usually ignored as well. Therefore, in almost all applications, RT-TDDFT is used within the adiabatic application, in which V_{xc}, usually a ground state functional, only uses input from the instantaneous electron density (see Figure 2).

Despite its widespread use for modeling charge transfer in complex systems, RT-TDDFT as it is used in practice within the adiabatic approximation suffers from a number of deficiencies for small model systems. The RT-TDDFT method within the adiabatic approximation is not able to capture Rabi oscillations, where if an electric field of frequency resonant with an allowed transition is applied to the system, single electron transitions occur between the states.[84,267] For RT-TDDFT, a field that is initially resonant with an energy gap will no longer be resonant as soon as electron density transfers out of the ground state. As a result, the electron transfer into the excited state is not complete when the electric field is applied, limiting RT-TDDFT's applicability to model pump–probe spectroscopy and non-equilibrium dynamics. Intricately connected with this issue is the incorrect extent and rate of charge transfer within RT-TDDFT for the exactly solvable Hubbard dimer. For this system, in addition to obtaining the exact dynamics, the dynamics were also simulated within the adiabatically exact approximation, revealing that the error is in fact due to the adiabatic approximation rather than any errors in the exchange or correlation functional for the instantaneous electron density.[140,269] Note that using the adiabatically exact functional is a nontrivial task, but recent progress in numerically constructing the exact Kohn–Sham potential for a given density makes this possible for model systems with smooth potentials (see Figure 3).[274−279] The lack of time-dependence within the adiabatic approximation, which corresponds to a lack of frequency-dependence in the frequency domain used with linear response theory, was shown by Maitra, Cave, and Burke in 2004 to be linked to the lack double excitations within TDDFT.[280] However, Li and Isborn in 2008 showed that although RT-TDDFT cannot capture the response of two-electron

https://dx.doi.org/10.1021/acs.chemrev.0c00223
Chem. Rev. XXXX, XXX, XXX−XXX

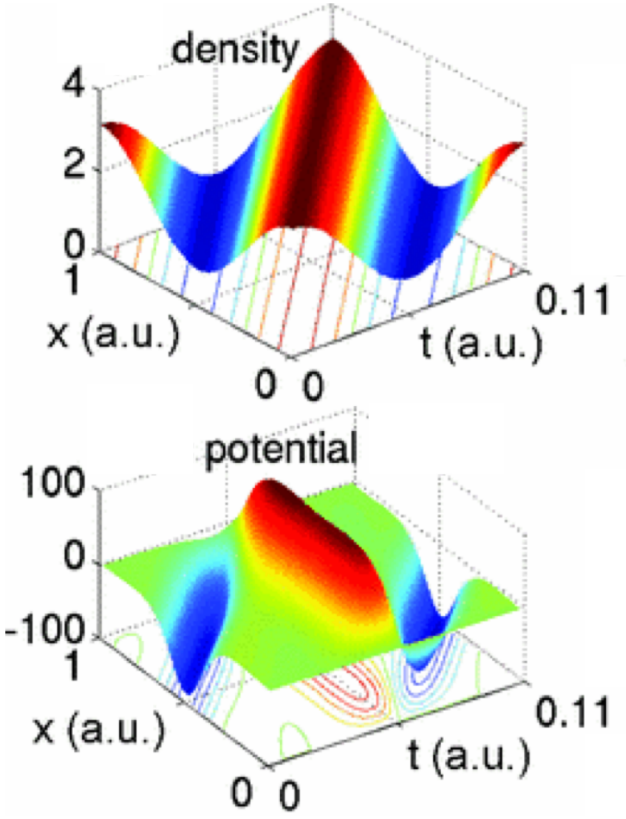

Figure 3. Density and corresponding correlation potential in atomic units created from density-potential mapping. Adapted with permission from ref 277. Copyright (2013) American Physical Society.

excitations, it can recover the electron density of closed-shell doubly excited states.[77]

Another related problem observed with approximate RT-TDDFT is the phenomena of peak-shifting within the computed absorption spectra.[77,261−266] Although the energy of the spectral peaks computed with RT-TDDFT agree with the energy of the resonances computed from linear response theory within the matrix formulation of TDDFT if a ground state electron density is used as a reference, as the electron density evolves away from the ground state the peaks in the absorption spectrum unphysically shift in energy. This spurious shift is due to the changing character of the evolving electron density. Both RT-TDDFT within the adiabatic approximation and RT-TDHF suffer from the problems of incorrect Rabi oscillations and peak-shifting; these problems are due to the nonlinear nature of the potential, which depends on the time-dependent electron density. Thus, a challenge in going beyond the adiabatic approximation requires that any time-dependence built into V_{xc} repair this resonance condition.[265,266]

Previous studies have attempted to explore the time-dependence of the V_{xc}, with some progress in developing time-dependent potentials via the current TDDFT formalism.[281−289] Very recent work by Maitra and coworkers has introduced a new class of nonadiabatic approximations to V_{xc} that are functionals of the one-body reduced density-matrix and the exchange-correlation hole.[290,291] The dependence of the density evolution on the initial Kohn−Sham state going beyond a single Slater determinant has also been recently explored.[292] All efforts to go beyond the adiabatic approximation require careful attention to exact conditions.[265,290,293−296]

In contrast to RT-TDDFT and RT-TDHF, for correlated wave-function-based time-dependent approaches there is no dependence of the Hamiltonian on the electron density, and therefore no unphysical peak-shifting. Wave-function-based methods instead propagate the time-dependent coefficients corresponding to different electronic states, rather than time-dependent orbitals. The adiabatic approximation of RT-TDDFT becomes less justified as the electron density is propagated away from the ground state, which is the case for many nonequilibrium and pump−probe simulations. Although correlated wave-function-based methods often have greater computational expense than RT-TDDFT for complex systems, they have the potential to perform better at modeling these far-from-ground state phenomena.

To evolve the system from an excited state, an alternative to propagating the system with a resonant laser pulse is to instead initialize the system in an excited state. This technique offers a way to partially bypass some of the problems with adiabatic TDHF/TDDFT for resonant processes and allows for computation of excited state dynamics and nonlinear properties. The accuracy of the technique, however, hinges on the preparation of an initial state that yields physically meaningful dynamics and avoids undesirable broadband excitation due to the rapid change in potential. Additionally, there are as-of-yet unaddressed formal problems such as the initial-state dependence for TDDFT.[273,297] The simplest approach for preparing an initial state close to an excited state is to directly manipulate the orbital populations without relaxation, either by promoting an electron to an unoccupied orbital,[136] or by removing it to emulate valence or core-level ionization.[298] An improvement on this approach is to instead propagate from a state computed from the linear-response eigenvectors.[86,299] Another approach is to converge the system in the presence of a static field, typically to create a charge separated state. Van Voorhis and coworkers introduced a constrained DFT (cDFT),[300] which minimizes the energy with the constraint that particular fragments of a system have a particular charge. This gives an initial state with improved intramolecular charge migration dynamics as compared to an orbital hole. This is due to reduced self-interaction errors with cDFT.[301]

2.1.2. Accuracy of TDHF and TDDFT. Many reviews,[245,249,251,252,302] books,[247,248] and benchmarking studies[250,303−312] highlight the accuracy and pitfalls of TDDFT for common approximations for V_{xc} for various excited state properties. Although these reviews mostly focus on the more common linear response matrix formulation of TDDFT rather than real-time TDDFT, the accuracy for real-time and linear response formulations will be similar, assuming that the ground state electron density is used as a reference in both cases. Thus, the use of these functionals for TDDFT calculations can be expected to work well for the valence excited states of medium-sized organic molecules, although qualitatively incorrect transitions are predicted for thiophene and thienoacenes.[313]

TDDFT with standard approximate functionals has larger errors in modeling other kinds of excited states, including those with charge-transfer, Rydberg, or double excitation character. Approximate local exchange in DFT leads to a lack of Coulombic attraction between the excited electron and hole in TDDFT, so that charge-transfer transitions are generally much too low in energy.[245,314−316] These spuriously low-energy charge-transfer transitions are particularly problematic when computing the excitation energies of a molecule in explicit solvent.[317−320] The charge-transfer problem can be remedied

https://dx.doi.org/10.1021/acs.chemrev.0c00223
Chem. Rev. XXXX, XXX, XXX−XXX

using exact exchange,[316] with long-range corrected hybrid functionals and optimally tuned functionals providing much improved treatment of charge-transfer excitations.[304,321−326] Rydberg transitions are also often too low in energy using approximate TDDFT methods[302,327−331] because the V_{xc} does not exhibit the correct $-1/r$ limit as the distance r between an electron to the nucleus becomes large. Both TDHF and the usual adiabatic approximations for V_{xc} in TDDFT yield singly excited states and therefore give a very poor description for states that have doubly excited character. Such mixed states are often important for describing surface crossings, conical intersections, and extended conjugated systems.[280,302,332−337] For modeling core−electron excitations, there is a consistent improvement in the absolute values of the calculated excitation energies with increasing Hartree−Fock exchange.[95,338−340] Particularly, short-range exchange has been shown to be an important component of hybrid functionals applied to core excitations. Both TDHF and TDDFT should be used with extreme caution in modeling open-shell systems such as transition metal complexes[341−343] or systems with multireference character where a single Slater determinant provides a poor starting reference.

2.2. Real-Time Time-Dependent Semi-Empirical Methods

Semiempirical methods have a long history.[344] With the growing interest in excited state properties and dynamics of large molecular systems, these methods have been revisited in recent years. The first examples of semiempirical methods (i.e., the Hückel[345] and Pariser−Parr−Pople (PPP) methods), were limited to the description of π networks in organic systems. This treatment was later extended by Hoffman to both π and σ bonding.[346] Subsequently, Pople and Segal developed a series of semiempirical Hamiltonians based on HF theory, namely, the complete neglect of differential overlap (CNDO),[347,348] intermediate neglect of differential overlap (INDO),[349] and neglect of diatomic differential overlap (NDDO).[350] The INDO (INDO/S) Hamiltonian was further reparametrized by Zerner and coworkers in order to evaluate UV/vis spectra for organic systems within the frameworks of configuration interaction with single excitations (CIS) and the random phase approximation (RPA),[351−355] respectively. Since then, this approach has been used for a broad range of systems including organic electronics, organic dyes, conjugated polymers, biological molecules and nanoparticles.[356−368] INDO/S parameters are now available for transition metals, lanthanides, and actinides.[369−372] More recent improvements to the INDO/S method, INDO/X, have also been reported by Voityuk.[373] Other approximate methods include the modified neglect of diatomic overlap (MNDO)[374,375] and its parametrized model 3 (PM3) or MNDO-PM3 methods.[376,377] The semipirical density functional tight binding (DFTB) method,[378−380] which is formally based on DFT, has also been extensively developed over the last two decades.

Despite this long history, real-time formulations of semiempirical methods have only been reported within the last two decades. The PPP Hamiltonian, which includes the important Coulomb interaction among π electrons, is particularly useful for studies of electronic properties of conjugated molecules. Mukamel and coworkers have successfully developed and employed real-time PPP Hamiltonian for studies of spectroscopic signals and electron dynamics of conjugated organic molecules.[381−385] Bartell et al.[386] and Ghosh et al.[387] have reported real-time time-dependent implementations of the PM3 and INDO/S methods using the Liouville superoperator approach and Chebyshev time propagation framework to study the time-dependent response to a weak pulse. They studied the UV/vis spectra of a range of molecules, including large systems like the tyrosine chromophore in the ubiquitin protein (Figure 4), the betanin dye molecule in the presence of methanol and water, and the Nile Red chromophore in a variety of solvents (acetone, ethanol, toluene and *n*-hexane). Both approaches yield spectra that are comparable in quality to those obtained from RT-TDDFT simulations or experiment. Large scale real-time DFTB simulations have also been used to model electron dynamics in complex systems such as solvated nanodroplets,[148] plasmonic nanoantennas,[388,389] and dye TiO_2 nanoparticle hybrids for charge injection,[390,391] such as those shown in Figure 5.

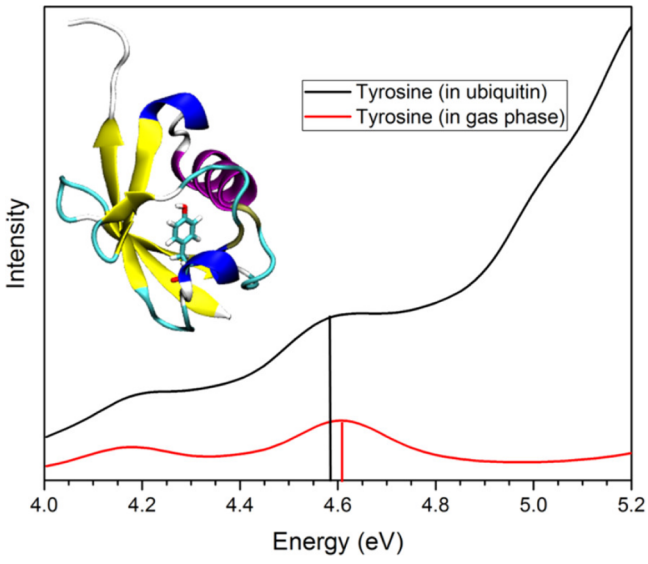

Figure 4. RT-INDO/S spectra of tyrosine in the gas phase and in the ubiquitin protein environment. The experimentally observed small red shift within the protein environment is qualitatively reproduced. Adapted with permission from ref 387. Copyright (2017) American Chemical Society.

2.3. Real-Time Time-Dependent Configuration-Interaction Methods

Time-evolved multiconfigurational wave functions are ideally suited for modeling time-resolved spectroscopies or excited-state properties in strong perturbations, in part, because they do not exhibit the deficiencies of RT-TDDFT that result from the

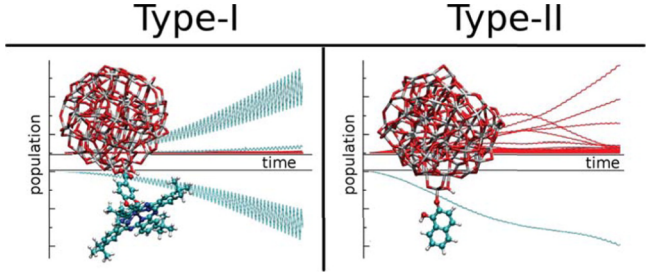

Figure 5. Population evolution of dyes involved in both direct (type-I) and indirect (type-II) photoinjection into TiO_2 were studied with real-time DFTB. Adapted with permission from ref 390. Copyright (2012) American Chemical Society.

https://dx.doi.org/10.1021/acs.chemrev.0c00223
Chem. Rev. XXXX, XXX, XXX−XXX

use of approximate adiabatic exchange-correlation functionals of the density.

The conceptually simplest multiconfigurational wave function approach is time-dependent configuration interaction (TD-CI), wherein the wave function $\Psi(t)$ is expressed as a linear combination of electron configurations $\{\Phi_K\}$:

$$\Psi(t) = \sum_K C_K(t)\Phi_K \tag{10}$$

Here, $\{C_K(t)\}$ are time-dependent CI expansion coefficients, and $\{\Phi_K\}$ represent electronic configurations (Slater determinants or configuration state functions). If all configurations are included in the wave function expansion, TD-CI gives the exact description of the dynamics of a many-electron system,

$$i\dot{\mathbf{C}}(t) = \mathbf{H}(t)\mathbf{C}(t) \tag{11}$$

The total number of configurations in the determinant-based full CI framework is

$$N_{\text{det}} = \binom{N_{\text{orb}}}{n_e} \tag{12}$$

where N_{orb} and n_e are the total number of orbitals and electrons, respectively, in the system. Because the full TD-CI method is exponentially complex, the CI expansion is often truncated in terms of either the excitation operator (e.g., singles and doubles)[33,35−39,106,392,393] or the space used to construct the full CI basis (e.g., the complete active space (CAS) approach).[28−30,32,107,110,394−396] As the size of the truncated space increases, the time-evolution of the approximate wave function approaches the asymptotic limit of the full TD-CI solution. As an example, the CAS Hamiltonian is given in the determinant basis as

$$H_{KL}(t) = \langle K|\sum_{tu} h^c_{tu}\hat{E}_{tu} + \frac{1}{2}\sum_{tuvw}(tu|vw)(\hat{E}_{tu}\hat{E}_{vw} - \delta_{uv}\hat{E}_{tw})|L\rangle$$
$$h^c_{tu} = h_{tu} + \sum[(tu|ii) - (ti|iu)] \tag{13}$$

where t, u, v, and w label the orbitals of the active space, and h_{pq} and $(pq|rs)$ represent one- and two-electron integrals, respectively. $\hat{E}_{pq}$ is a spin-adapted excitation operator

$$\hat{E}_{pq} = \hat{a}^\dagger_{p\alpha}\hat{a}_{q\alpha} + \hat{a}^\dagger_{p\beta}\hat{a}_{q\beta} \tag{14}$$

defined in terms of the creation $(\hat{a}^\dagger)$ and annihilation $(\hat{a})$ operators of second quantization, respectively.

The TD-CI wave function can be propagated in the basis of eigenstates of the CI Hamiltonian, in which case the time-evolution operator can be expressed as a unitary matrix. However, this approach requires that the Hamiltonian be fully diagonalized to obtain all CI states; the transition dipoles between all states must then also be computed. This approach is computationally expensive and generally infeasible, with the exception of very small systems or small CAS problems. On the other hand, the time-consuming matrix-vector product in eq 11 can be computed within the determinant basis *on-the-fly*,[32,396,397] which reduces memory requirements and allows for the consideration of more complete CI expansions and the study of larger systems.

The CI wave function can be expanded in terms of excited determinants derived from restricted, unrestricted, or noncollinear mean-field reference functions. When a truncated CI expansion is used with a Slater determinant basis, the CI wave functions inherits any broken symmetries associated with the reference configuration. In a variational treatment, symmetry breaking can be advantageous in that it may lower the energy of the system. However, unphysical bright transitions to different spin states may arise from the broken symmetry wave function, and these features should be removed from calculated spectra and electric properties. Given a reference that is an eigenfunction of both $\hat{S}_z$ and $\hat{S}^2$, spin-adapted configuration state functions (CSFs), which are also eigenfunctions of these operators, are an appealing alternative to excited determinants when expanding the CI wave function. Within a CSF basis, the CI wave function will also be an eigenfunction of $\hat{S}_z$ and $\hat{S}^2$, and the effective CI space will be smaller because the Hamiltonian can be block-diagonalized according to spin state.[33,38,39]

TD-CI electron dynamics have been used to model photoionization,[28,106−108,110,112−115,393,398,399] linear spectroscopies,[32,35,39,392,394,400] and nonlinear optical responses.[29,30,37,38,107,392,393] Time-dependent configuration interaction singles (TD-CIS) is the most commonly used multiconfigurational approach. TD-CIS is particularly useful when the underlying chemical processes are mostly driven by single-electron dynamics, such those in linear optical response and photoionization. Unfortunately, TD-CIS tends to overestimate both static and dynamic hyperpolarizabilities due to a lack of electron correlation in the description of the ground state.[37,38,392,393]

In the nonlinear and nonperturbative regime, it is important that the wave function include configurations which are multiply substituted, relative to the reference configuration. As such, the use of a complete-active-space CI (CASCI) formalism becomes advantageous. TD-CASCI has been used to investigate population dynamics and simulate spectroscopies.[32,396] This active-space approach has been generalized to the restricted active space (RAS) CI formalism which allows treatment of larger systems but possesses the drawback of a loss of size extensivity.[108] In TD-CASCI, the choice of initial orbitals is of key importance. This has recently been highlighted by Liu et al.,[32] who investigated the effect of different initial orbitals in the TD-CASCI calculation of absorption spectra.[32] Similarly, in the numerical grid implementation of the time-dependent truncated CI approach, pseudo-orbitals based on HF orbitals have been demonstrated to be a decent orbital basis for the study of strong-field ionization, photoionization, and X-ray IR pump probe ionization.[108]

Recent years have also seen the development of TD-CASSCF, where the wave function obeys the time-dependent variational principle by allowing variations in both the CI coefficients and the orbitals;[28,31,394,399,401] this approach contrasts with TD-CASCI wherein the orbitals remain fixed. This technique has also been extended to the RAS partitioning, allowing a detailed analysis of the role that multielectron excitations play in the description of nonlinear properties, as well as the study of high harmonic generation spectra and ionization of carbon and beryllium atoms.[29,30]

2.4. Real-Time Time-Dependent Coupled-Cluster Methods

As discussed in Section 2.3, wave-function-based time-domain approaches do not exhibit many of the well-known failures of RT-TDDFT, making them desirable candidates for modeling strong or long-time light-matter interactions. However, real-time methods built upon the configuration interaction expansion of the wave function suffer from their own problems. For example, the lack of correlation effects in TD-CIS often

https://dx.doi.org/10.1021/acs.chemrev.0c00223
Chem. Rev. XXXX, XXX, XXX−XXX

renders it unreliable (e.g., for estimating dynamic and static hyperpolarizabilities[37,38,392,393]). A truncated CI scheme such as CI with single and double excitations (CISD) is neither size extensive nor particularly accurate, and multiconfigurational CI is exponentially complex. On the other hand, coupled-cluster (CC)-based approaches are highly accurate, rigorously size extensive when truncated at any excitation order, and can be realized in polynomial time.

The ground-state (CC) coupled-cluster wave function is given by

$$|\Psi_{CC}\rangle = e^{\hat{T}}|\Phi_0\rangle \tag{15}$$

where $|\Phi_0\rangle$ represents a single-determinant reference function, and $\hat{T}$ is the cluster operator, defined in second-quantized notation as

$$\hat{T} = \sum_{ia} t_i^a \hat{a}_a^\dagger \hat{a}_i + \frac{1}{4}\sum_{ijab} t_{ij}^{ab} \hat{a}_a^\dagger \hat{a}_b^\dagger \hat{a}_j \hat{a}_i + \ldots \tag{16}$$

If the cluster operator is not truncated, full CC theory is numerically equivalent to the full CI. Further, as mentioned above, CC theory has the useful property that it is rigorously size extensive should eq 16 be truncated to any excitation order (i.e., at the level of single and double excitations, as in CCSD[402]). The CC ground-state energy and cluster amplitudes are determined using a projection approach that is nonvariational and which slightly complicates the evaluation of properties because the Hellman−Feynmann theorem cannot be applied. The complete parametrization of the ground state thus requires a generalized Hellman−Feynmann theorem and a stationary Lagrangian function of the form

$$L = \langle \tilde{\Psi}_{CC}|\hat{H}|\Psi_{CC}\rangle \tag{17}$$

where

$$\langle \tilde{\Psi}_{CC}| = \langle \Phi_0|e^{-\hat{T}}(1 + \hat{\Lambda}) \tag{18}$$

and $\hat{\Lambda}$ represents a de-excitation operator, defined as

$$\hat{\Lambda} = \sum_{ia} \lambda_a^i \hat{a}_i^\dagger \hat{a}_a + \frac{1}{4}\sum_{ijab} \lambda_{ab}^{ij} \hat{a}_i^\dagger \hat{a}_j^\dagger \hat{a}_b \hat{a}_a + \ldots \tag{19}$$

The non-Hermiticity of this formalism and the fact that both right- and left-hand CC wave functions are required to define ground-state properties play important roles in the extension of CC theory to the time domain.

Given a time-dependent Hamiltonian operator, $\hat{H}(t)$, the simplest way to achieve a time-dependent CC (TD-CC) theory is to build time-dependence into the right-hand CC wave function $[\hat{T} \rightarrow \hat{T}(t)]$ while ignoring the non-Hermiticity of the theory and assuming that the underlying molecular orbitals are independent of time. Under these assumptions, which define the TD-CC formalism of Huber and Klamroth,[47] the time-dependent Schrödinger equation can be left-multiplied by $e^{-\hat{T}(t)}$ to obtain

$$i\hbar e^{-\hat{T}(t)}\frac{\partial}{\partial t}e^{\hat{T}(t)}|\Phi_0\rangle = e^{-\hat{T}(t)}\hat{H}(t)e^{\hat{T}(t)}|\Phi_0\rangle \tag{20}$$

and programmable expressions for the time derivatives of the cluster amplitudes can then be obtained upon considering the Baker−Campbell−Hausdorff expansions of both the similarity-transformed Hamiltonian and time derivative operators that arise in eq 20.[403] Few groups follow this precise scheme, though, for two reasons. First, a correct description of time-dependent properties (e.g., the energy, dipole moment, etc.) requires knowledge of the time-evolution of both the right- *and* left-hand CC wave functions. Indeed, the CC wave functions should satisfy a time-dependent bivariational principle,[404] and the complete specification of the time evolution of the system requires the integration of both the time-dependent Schrödinger equation and its complex conjugate. Second, Huber and Klamroth[47] observed that, in practical computations at the time-dependent CCSD (TD-CCSD) level of theory, the lack of time-dependence of the orbitals apparently leads to numerical instabilities that emerge when considering either large basis sets or intense external electric fields. Pedersen and Kvaal[405] later confirmed intense-field-induced instabilities within a more sophisticated TD-CCSD formalism that evolved both the *t*- and λ-amplitudes.

Regarding the time-evolution of the molecular orbitals, in the 1970s, Hoodbhoy and Negele[403,406] and Schönhammer and Gunnarsson[407] separately proposed that the orbitals underlying the TD-CC wave function should evolve in time, with the former authors suggesting that the CC amplitudes could be evolved within the orbital basis defined by the equations of motion of TDHF theory. In 2012, Kvaal[404] refined these ideas with his orbital adaptive TD-CC (OATDCC) hierarchy, which employs time-varying biorthogonal orbitals and interpolates between the MCTDHF and TDHF approaches when the cluster operator is chosen to include all excitation levels or none, respectively. A similar treatment, based upon time-varying orthonormal orbitals, can be found in the time-dependent orbital-optimized CC (TD-OCC) method of Sato et al.,[50] although it should be noted that, for systems with more than two electrons, orbital-optimized CC theory does not converge to the full CI limit.[408]

Some aspects of the structure of both the OATDCC with double excitations (OATDCCD) and TD-OCC with double excitations (TD-OCCD) approximations resemble those of Huber and Klamroth's TD-CCSD, with two significant exceptions. First, OATDCC and TD-OCC ignore single-particle transitions in the cluster operator, as they are rendered redundant through the time dependence of the orbitals. Second, and more significantly, the TD-CC scheme of Huber and Klamroth considers only the time evolution of the *t*-amplitudes (that define the right-hand CC wave function), whereas OATDCC and TD-OCC evolve both the *t*- and λ-amplitudes (as does the TD-CCSD approach of Pedersen and Kvaal[405]). Huber and Klamroth attempted to circumvent the need to consider the time evolution of λ-amplitudes by defining time-dependent quantities in terms of an approximate CISD wave function, constructed from TD-CCSD amplitudes. However, observables computed in this way incorrectly assume complex values upon interaction of the system with an oscillating electric field. On the other hand, Pedersen and Kvaal[405] demonstrated that a time-dependent formalism that respects the non-Hermiticity of CC theory will retain physically meaningful (i.e., real) observables; small imaginary contributions to quantities such as the energy are purely numerical artifacts that can be removed through the use of a suitable integrator.

The nonlinear nature of the cluster operator leads to complicated equations for the time-evolution of the cluster amplitudes. The complexity of these equations and any related potential numerical issues can be avoided by keeping the cluster amplitudes fixed at their time-independent, ground-state values and considering time-evolution of the system only at the equation-of-motion CC[409−411] (EOM-CC) level of

https://dx.doi.org/10.1021/acs.chemrev.0c00223
Chem. Rev. XXXX, XXX, XXX−XXX

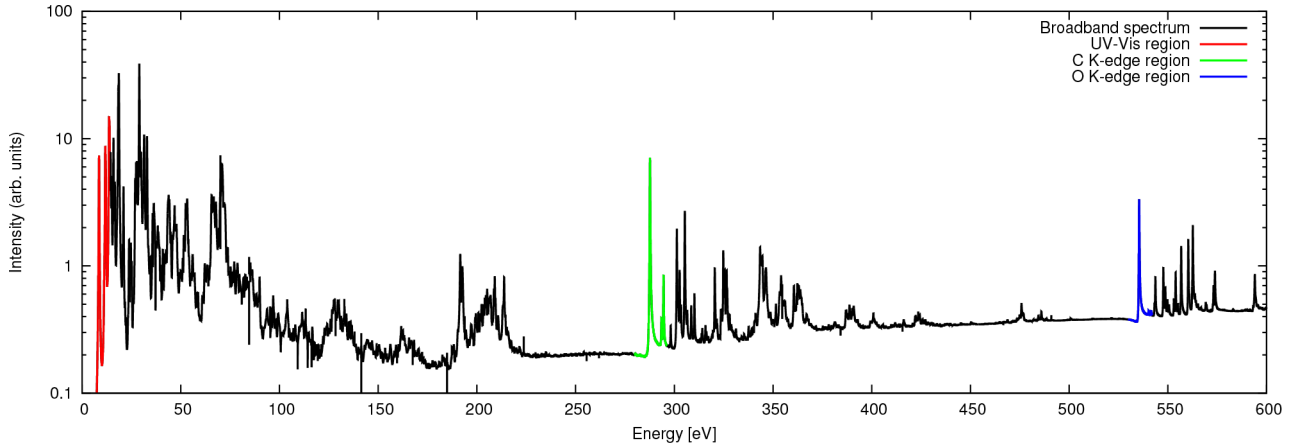

Figure 6. Broadband absorption spectrum for carbon monoxide computed at the TD-EOM-CCSD/aug-cc-pVTZ level of theory. Adapted with permission from ref 49. Copyright (2017) American Chemical Society.

theory.[22,35,37,49,52,53] Within the conventional EOM-CC framework, the *I*th electronic state is represented by

$$\hat{R}_I|\Psi_{CC}\rangle = \left(r_0 + \sum_{ia} r_i^a \hat{a}_a^\dagger \hat{a}_i + \frac{1}{4}\sum_{ijab} r_{ij}^{ab} \hat{a}_a^\dagger \hat{a}_b^\dagger \hat{a}_j \hat{a}_i + ...\right) e^{\hat{T}}|\Phi_0\rangle \tag{21}$$

where the expansion coefficients r_0, r_i^a, etc., comprise the (right-hand) eigenvectors of the normal-ordered similarity-transformed Hamiltonian,

$$\bar{H}_N = e^{-\hat{T}}\hat{H}e^{\hat{T}} - E_{CC} \tag{22}$$

Here, E_{CC} represents the energy associated with the ground-state CC wave function, which is recovered in the EOM framework with $r_0 = 1$. The non-Hermitian nature of the similarity-transformed Hamiltonian implies that these right-hand eigenfunctions comprise one-half of a biorthogonal set of functions; the complementary left-hand eigenfunctions are

$$\langle\tilde{\Psi}_{CC}|\hat{L}_I = \langle\Phi_0|e^{-\hat{T}}\left(l_0 + \sum_{ia} l_a^i \hat{a}_i^\dagger \hat{a}_a + \frac{1}{4}\sum_{ijab} l_{ij}^{ab} \hat{a}_i^\dagger \hat{a}_j^\dagger \hat{a}_b \hat{a}_a + ...\right) \tag{23}$$

In this representation, a general time-dependent wave function can be represented by right- and left-hand states

$$|\Psi(t)\rangle = \hat{R}(t)e^{\hat{T}}|\Phi_0\rangle \tag{24}$$

and

$$\langle\tilde{\Psi}(t)| = \langle\Phi_0|e^{-\hat{T}}\hat{L}(t) \tag{25}$$

whose time evolution are governed by the time-dependent Schrödinger equation and its complex conjugate, respectively.

We are aware of only two examples of laser-driven electron dynamics described by time-dependent EOM-CC (TD-EOM-CC). In 2011, Sonk et al.[35] used TD-EOM-CC with single and double excitations (TD-EOM-CCSD) to explore the response of butadiene to short, intense laser pulses, and in 2012 Luppi and Head-Gordon[37] applied TD-EOM-CCSD to model high harmonic generation in H_2 and N_2. In both cases, the time-dependent wave function was expanded in the basis of field-free eigenstates of the similarity-transformed Hamiltonian. In this basis, the transition dipole matrix that comprises the field interaction is not Hermitian, which could potentially lead to dynamics that do not conserve the norm of the wave function. The similarity-transformed Hamiltonian is also not strictly Hermitian, even though it is diagonal in this basis. In both refs 35 and 37 the non-Hermitian components of the matrices are disregarded. The largest difference between the two formalisms described in these papers is that Sonk et al., having Hermitized the similarity-transformed dipole matrix, employed a propagation scheme suitable for a Hermitian theory (that is, the time-dependent state is characterized by only a single wave function), whereas Luppi and Head-Gordon retained distinct left- and right-hand time-dependent wave functions.

Nascimento and DePrince[22,49] have also developed a TD-EOM-CC formalism with a slightly more limited scope than those discussed above. In their work, the linear absorption line shape function given by Fermi's Golden Rule is obtained from the Fourier transform of a dipole autocorrelation function. This treatment is similar to that employed decades earlier in the context of fluorescence and Raman spectroscopy[412−414] and in the vibrational coupled-cluster approach proposed by Prasad in 1988.[415]

It can be shown[22,49] that each Cartesian component of a linear absorption line shape function can be expressed as the Fourier transform of a dipole autocorrelation function defined as

$$I_\xi(\omega) = \int_{-\infty}^{\infty} dt e^{-i\omega t}\langle\tilde{M}_\xi(t)|M_\xi(0)\rangle \tag{26}$$

Here, $\langle\tilde{M}_\xi(0)|$ and $|M_\xi(0)\rangle$ are left- and right-hand dipole functions defined at time $t = 0$ by

$$\langle\tilde{M}_\xi(0)| = \langle\Phi_0|(1 + \hat{\Lambda})\bar{\mu}_\xi \tag{27}$$

and

$$|M_\xi(0)\rangle = \bar{\mu}_\xi|\Phi_0\rangle \tag{28}$$

respectively, and $\bar{\mu}_\xi$ represents the ξth component ($\xi \in x,y,z$) of the similarity-transformed dipole operator ($\bar{\mu}_\xi = e^{-\hat{T}}\hat{\mu}_\xi e^{\hat{T}}$). A dipole strength function, $S(\omega)$, which is formally equivalent to the oscillator strengths which arise within conventional EOM-CC theory, can then be obtained from the real part of this line shape as

$$S(\omega) = \frac{2}{3}\omega\sum_\xi \mathrm{Re}\{I_\xi(\omega)\} \tag{29}$$

https://dx.doi.org/10.1021/acs.chemrev.0c00223
Chem. Rev. XXXX, XXX, XXX−XXX

Nascimento and DePrince applied this formalism to the evaluation of UV/vis absorption spectra[22] at the TD-EOM approximate second order coupled-cluster (CC2)[416] level of theory and X-ray absorption fine structure[49] at the TD-EOM-CCSD level of theory. As with other real-time approaches, one of the benefits of TD-EOM-CC is that broad-band absorption spectra can be generated from a single time-domain simulation (for each Cartesian component of the absorption line shape function). For example, Figure 6 illustrates a TD-EOM-CCSD absorption spectrum for carbon monoxide that spans 600 eV. More recently, Nascimento and DePrince have generalized this moment-based TD-EOM-CC formalism to other linear electronic spectroscopies, demonstrating, for example, the numerical equivalence of electronic circular dichroism spectra generated at the TD-EOM-CC and conventional EOM-CC levels of theory.[52] Further, DePrince, Li, and their coworkers[53] have also recently extended TD-EOM-CC theory to the description of relativistic effects within the exact two-component[98,417−431] framework.

Closely related to time-dependent CC theory is the time-dependent algebraic diagrammatic construction (ADC) approach,[40−46,432] which has been applied to a variety of problems, including ultrafast charge[40,45] and energy[43,44] migration, metastable states,[41,42] and X-ray absorption spectroscopy.[46] The ADC formalism is Hermitian and its extension to the time domain is thus slightly less complicated than that of CC theory.

2.5. Real-Time Time-Dependent Two-Component and Relativistic Methods

Conventional electronic structure methods are incapable of simulating time-dependent spin precession. The reason for this shortcoming is the common choice to align electronic spins (anti)parallel with respect to each other within the electron configuration. In single-reference techniques, such as unrestricted Hartree−Fock and spin-density density functional theories, this choice leads to spin orbitals that are eigenfunctions of the spin operator $\hat{S}_z$. As a result, the number of spin-up and spin-down electrons will be conserved throughout any dynamical process.

To obtain a proper description of spin precession, one must consider the full vector form of the time-dependent magnetization $\mathbf{m}(\mathbf{r})$. The dynamics of $\mathbf{m}(\mathbf{r})$, which corresponds to the spin quantization axis, requires a noncollinear spin electronic structure framework, such as that provided by two-component or generalized Hartree−Fock/Kohn−Sham methods.[68,433−450] Smooth transitions between various spin configurations are enabled through the spinor basis,

$$\psi_k(\mathbf{x}, t) = \begin{pmatrix} \phi_k^{\alpha}(\mathbf{r}, t) \\ \phi_k^{\beta}(\mathbf{r}, t) \end{pmatrix} \tag{30}$$

where the spatial functions $\{\phi_k^{\alpha}(\mathbf{r},t)\}$, $\{\phi_k^{\beta}(\mathbf{r},t)\}$, are expanded in terms of a common set of basis functions $\{\chi_\mu(\mathbf{r})\}$

$$\phi_k^{\alpha}(\mathbf{r}, t) = \sum_{\mu} c_{\mu k}^{\alpha}(t)\chi_\mu(\mathbf{r}) \tag{31}$$

$$\phi_k^{\beta}(\mathbf{r}, t) = \sum_{\mu} c_{\mu k}^{\beta}(t)\chi_\mu(\mathbf{r}) \tag{32}$$

The first example of *ab initio* noncollinear real-time electronic dynamics was reported in 2014.[68] In that work, Ding et al. derived and utilized a density-matrix-based two-component Liouville−von Neumann equation in the orthonormal basis:[68,70]

$$i\frac{\partial}{\partial t}\begin{pmatrix} \mathbf{P}'^{\alpha\alpha}(t) & \mathbf{P}'^{\alpha\beta}(t) \\ \mathbf{P}'^{\beta\alpha}(t) & \mathbf{P}'^{\beta\beta}(t) \end{pmatrix} = \left[\begin{pmatrix} \mathbf{F}'^{\alpha\alpha}(t) & \mathbf{F}'^{\alpha\beta}(t) \\ \mathbf{F}'^{\beta\alpha}(t) & \mathbf{F}'^{\beta\beta}(t) \end{pmatrix}, \begin{pmatrix} \mathbf{P}'^{\alpha\alpha}(t) & \mathbf{P}'^{\alpha\beta}(t) \\ \mathbf{P}'^{\beta\alpha}(t) & \mathbf{P}'^{\beta\beta}(t) \end{pmatrix}\right] \tag{33}$$

where $\mathbf{P}'^{\alpha\alpha}(t)$ and $\mathbf{F}'^{\alpha\beta}(t)$ are the density and Fock/Kohn−Sham matrices in an orthonormal basis, which are transformed from AO-basis quantities in with a spin-blocked structure,

$$P_{\mu\nu}^{\sigma\tau}(t) = \sum_{i}^{N} c_{\mu i}^{\sigma}(t)\cdot c_{\nu i}^{\tau *}(t), \ \ \sigma, \tau \in \{\alpha, \beta\} \tag{34}$$

$$\mathbf{F}^{\sigma\tau}(t) = \mathbf{h}^{\sigma\tau}(t) + \delta_{\sigma\tau}[\mathbf{J}^{\alpha\alpha}(t) + \mathbf{J}^{\beta\beta}(t)] - (1-\zeta)\mathbf{V}_{xc}^{\sigma\tau} + \zeta\mathbf{K}^{\sigma\tau}(t) \tag{35}$$

The magnetization densities $\mathbf{P}'^{\alpha\beta}$ and $\mathbf{P}'^{\beta\alpha}$ give rise to the noncollinear spin projection on the x and y rotational axes. The off-diagonal Fock/Kohn−Sham matrices, $\mathbf{F}'^{\alpha\beta}$ and $\mathbf{F}'^{\beta\alpha}$, arise from the spin coupling with external (e.g., magnetic field) and internal (e.g., spin−orbit coupling) perturbations. For hybrid DFT, the HF exchange integral $\mathbf{K}$ takes on a fractional value scaled by a nonzero scaling factor ζ, whereas $\zeta = 0$ for pure DFT kernels.

The nonrelativistic Hamiltonian ignores interactions explicitly associated with the spin degrees of freedom, such as the spin−spin interactions, spin−orbit couplings, and spin-magnetic field interactions. Although it seems the extension of the nonrelativistic time-dependent many-electron methods to the relativistic case is straightforward, incorporation of special relativity introduces new conceptual difficulties. First, the theory of special relativity assumes the equivalence of all inertial reference frames under Lorentz transformation of the space-time coordinates. A relativistic quantum mechanical description of a molecular system requires a definition of a Lorentz invariant molecular Hamiltonian, which is not readily established. As a result, separation of the space-time coordinates must be performed in a particular reference frame and will only be valid in this reference frame. For molecular systems, the most convenient reference frame is the Born−Oppenheimer frame where the nuclei are at rest, and the electromagnetic potential created by the nuclei is simply a scalar potential.

The time-dependent two-component framework (eq 33) is well-suited for the inclusion of scalar relativistic or spin-coupling effects, subject to an appropriate transformation from the bispinor or four-component representation of the Dirac equation, such as the Douglas−Kroll−Hess,[451−453] the normalized elimination of the small components[454,455] or the zeroth order regular approximation (ZORA)[456,457] and the exact two-component (X2C) method.[98,417−431] Because relativistic methods are not the focus of this Review, we refer readers to refs.[458,459,430] for a more thorough review of the subject matter. Applications of the relativistic real-time four-component method were first reported by Repisky et al.[69] and more recently by De Santis et al.[460] for computing absorption spectra. In 2016, a real-time relativistic two-component method was developed by Goings et al.[70] to study spin-forbidden excitations; this approach was then extended to the description of nonlinear optical properties by Repisky et al.[100]

https://dx.doi.org/10.1021/acs.chemrev.0c00223
Chem. Rev. XXXX, XXX, XXX−XXX

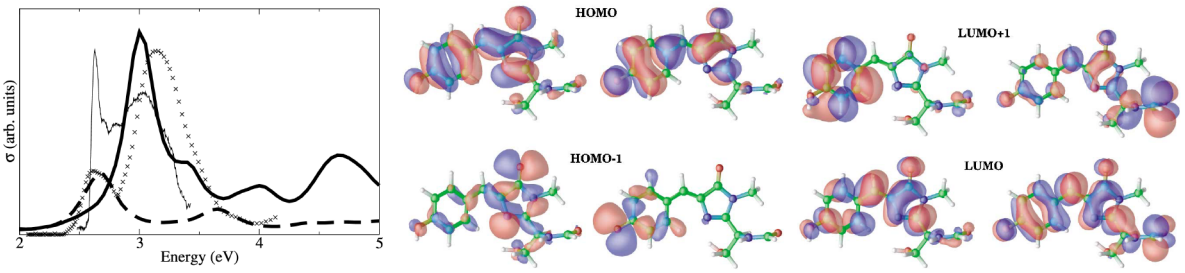

Figure 7. (Left Panel) Computed absorption spectra of the neutral (thick solid line) and anionic (thick dashed line) GFP chromophores, compared with two separate experiments (thin solid line and crosses). The anionic spectrum was divided by a factor of 4 for comparative purposes. (Middle and Right Panels) Kohn–Sham orbitals of the neutral (left) and anionic (right) GFP chromophores, corresponding to the most important orbital transitions involved in the main excitations. Adapted with permission from ref 74. Copyright (2003) American Physical Society.

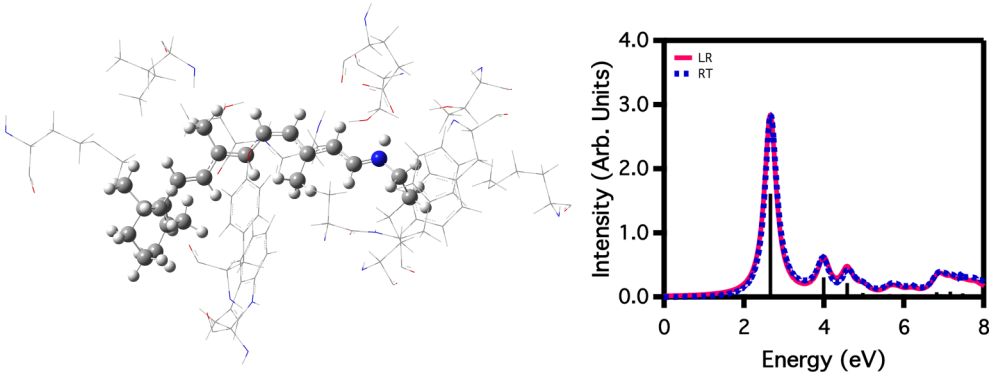

Figure 8. (Left) 11-*cis* retinal protonated Schiff base (RPSB) in a shell of residues from bovine rhodopsin. The chromophore is covalently bonded to the Lys296 residue. The free valency created on C_δ by the division of the QM (shown in a ball and stick representation) and MM (shown in a line representation) regions was capped with a hydrogen link atom. See ref 494 for details in the partitioning scheme. (Right) LR- and RT-TDDFT/MMPol computed absorption spectrum of RPSB in bovine rhodopsin. Adapted with permission from ref 152. Copyright (2017) American Chemical Society.

2.6. Real-Time Methods in Complex and Nonequilibrium Environments

Chemical properties, including nuclear conformation, spectroscopy, and chemical reactivity, can often be dramatically modified by interaction with the surrounding medium (e.g., through solvation).[461−464] These environmental interactions could be steric[465,466] or specific electronic perturbations such as hydrogen bonding, dipole−dipole, or noncovalent interactions.[467−469] Unfortunately, treating the system and its surrounding environment with high levels of theory is computationally intractable.

Instead, practical theoretical models focus on capturing the most important aspects of the system-environment interaction. One of the most computationally tractable approaches is the polarizable continuum model (PCM) that replaces the explicit atomistic environment with an implicit solvent model.[470−478] The real-time time-dependent formalism of the equilibrium PCM (TDPCM) has been developed into the RT-TDHF/RT-TDDFT framework.[138,139,154] In the initial approach, the environment was kept in equilibrium with respect to the polarization of the system by relaxing the solvent dielectric constant from the dynamic, high frequency (optical) value to the static, zero-frequency value according to an empirical relaxation model. Later, a nonequilibrium TDPCM approach was introduced to explicitly treat the evolution of the dielectric medium as it responds to the time-dependent system polarization.[155,156]

Although continuum models can provide an accurate description for systems with weak interaction with the environment,[474,479−481] an atomistic description of the environment becomes necessary for strong specific system-environment interactions (e.g., solute−solvent hydrogen bonding or protein active sites).[482] Hybrid time-dependent models treat the high-level time-dependent electronic dynamics quantum mechanically (QM), while the environmental response is described at a classical molecular mechanics (MM) level.[483−485] The most common example of these hybrid QM/MM models electrostatically embeds the QM system on effective point charges to represent the environment atoms. Morzan et al. employed an electrostatic embedding model in a real-time QM/MM method to capture the solvatochromic shift of formamide in water.[486] Marques et al. used an electrostatic embedding model to investigate the spectra of the green fluorescent protein (GFP) before and after protonation by its protein environment.[74] These results showed reasonably good agreement with experiment, as seen in Figure 7, demonstrating the utility of QM/MM models for simulating absorption spectra in complex environments.

The electrostatic embedding QM/MM approach can reproduce some solvent induced spectral shifts, but it does not capture time-dependent mutual polarization between the system and its environment. Recently, many approaches for including the system-environment mutual polarization have been explored, including "fluctuating charges",[487−490] "effective fragment potentials",[491,492] "induced dipoles",[493−497] and Drude oscillator-based models.[498] Li and Mennucci extended the polarizable molecular mechanics (MMPol) based on the induced dipole formalism[493,494] to the real-time regime coupled with RT-TDHF/RT-TDDFT[152,499] and TD-CASSCF.[32] In

https://dx.doi.org/10.1021/acs.chemrev.0c00223
Chem. Rev. XXXX, XXX, XXX−XXX

these approaches, the electronic degrees of freedom of the environment, modeled by the induced dipoles with frequency independent polarizabilities in the MMPol regime, respond instantaneously to the electric field at each polarizable site. This approximation is reasonable and useful for cases where the electric field generated by the QM region is oscillating much more slowly than the response in the MM region.[499,500]

Studies coupling the polarizable embedding approach with real time electron dynamics have been successful at predicting spectroscopic properties, such as solvatochromic shifts, as well as providing unique insight into the responsive dynamics of the electronic degrees of freedom in a classical environment. Wu et al. captured the solvatochromic effects of water on the absorption spectrum of coumarin, a common solvatochromic dye; this study also investigated the physical extent of the mutual polarization between dye and solvent after perturbation, demonstrating the diminishing effects of polarizable solvent on the dynamics of the quantum subsystem as a function of distance.[501] Donati et al. explored spectroscopic properties of a similar chromophore, coumarin-153, in methanol and in a covalently bound environment that cannot be modeled with continuum embedding approaches.[152] The calculated absorption spectrum of retinal protonated Schiff base (RPSB) in rhodopsin (Figure 8) demonstrated the mutual polarization of electronic degrees of freedom in environments tightly coupled to the quantum system.[152]

3. NUMERICAL TECHNIQUES

3.1. Basis Set Representations

Over the years, real-time time-dependent electronic structure approaches have been developed in a number of widely used electronic structure programs, with wave function or density matrix representations ranging from Gaussian-type functions,[15,17−23,33,502] numerical atomic orbitals,[14,503−505] real-space grids,[27,506−508] planewaves,[24,122,127,509−514] and mixed Gaussian-type functions and planewaves.[26] Other promising representations include Lagrange functions,[515−517] finite elements[518,519] and maximally localized Wannier functions.[520]

Of the various real-time electronic structure approaches, RT-TDDFT has been explored with all the above-mentioned basis sets, while post-Hartree−Fock theories have only been implemented with Gaussian orbitals, taking full advantage of their analytical properties.[521] This has allowed the development of ground-state, excited-state, and higher-order response properties based on electronic structure theories of increasing complexity over many decades. It is also the mostly widely used basis set representation in quantum chemistry. Each of these representations have their strengths and weaknesses and the specific choice depends on the system and phenomena being investigated, accuracy, and algorithm requirements.

3.2. Time Propagation Methods

A key component in real-time schemes involves the time propagation of the wave function or the density matrix. The correspondence between quantum Hamiltonians and unitary time propagators (Stone's theorem[522]) imposes strict requirements on time-propagation algorithms. As a result, general purpose integrators like the Runge−Kutta method[523] are not necessarily appropriate for evolving the TDSE as they can become unstable with increasing system size, and stable propagation often necessitates the use of small time steps. On the other hand, algorithms based on the Magnus expansion,[15,259,524−527] which are unitary by construction, and other symplectic integrators[405,528−539] can be useful in this context. Beyond this Review, we refer the reader to the reviews of Kosloff[540] and Castro and workers[259,541] for a more general overview of time propagation schemes.

The goal of any time-propagation method is to find a numerical solution of the time-dependent Schrödinger or Dirac equation [eq 1] or associated approximations. The Magnus expansion achieves this via an exponential form of the propagator $U(t, t_0)$ that relates wave functions or density matrices at different times as follows,

$$\Psi(t) = U(t, t_0)\Psi(t_0) \tag{36}$$

$$U(t, t_0) = \exp(\Omega(t, t_0)); \quad U(t_0, t_0) = I \tag{37}$$

Given this propagator, eq 1 can be cast as,

$$\frac{\partial}{\partial t}U(t, t_0)\Psi(t_0) = \tilde{H}(t)U(t, t_0)\Psi(t_0) \tag{38}$$

where $\tilde{H}(t) \equiv \frac{-i}{\hbar}H(t)$. In the Magnus expansion, $\Omega(t, t_0)$ is written as a power-series,

$$\begin{aligned}\Omega(t, t_0) = &\int_{t_0}^{t} \tilde{H}_1 \mathrm{d}t_1 \\ &+ \frac{1}{2}\int_{t_0}^{t} \mathrm{d}t_1 \int_{t_0}^{t_1} \mathrm{d}t_2 [\tilde{H}_1, \tilde{H}_2] \\ &+ \frac{1}{6}\int_{t_0}^{t} \mathrm{d}t_1 \int_{t_0}^{t_1} \mathrm{d}t_2 \int_{t_0}^{t_2} \mathrm{d}t_3 ([\tilde{H}_1, [\tilde{H}_2, \tilde{H}_3]] + [\tilde{H}_3, [\tilde{H}_2, \tilde{H}_1]]) + \ldots\end{aligned} \tag{39}$$

where $\tilde{H}_k = \tilde{H}(t_k)$. One can think of each order in this series as a correction accounting for the proper time-ordering of the Hamiltonian. A higher order expansion allows for larger time steps, but this benefit must be weighed against the subsequent requirement that more Hamiltonian evaluations be carried out at every time step. One complication with the Magnus propagation approach arises from requiring the knowledge of the Hamiltonian at a future time, which, in the case of single-particle theories like RT-TDHF and RT-TDDFT, is unknown.[18] As a result, different predictor schemes have to be used, which also have to conserve time-reversibility.

The simplest propagator based on the Magnus expansion just uses the first term in eq 39,

$$\Omega(t, t_0) \approx \int_{t_0}^{t} \tilde{H}_1 \mathrm{d}t_1 \tag{40}$$

Equation 40 can be numerically integrated with a forward-Euler-like time integrator but more accurate approaches are based on second-order methods.

A popular second-order method approximates the first term in eq 39 by the midpoint rule, leading to an $O(\Delta t^2)$ time integrator[132,542]

$$\psi(t_{k+1}) = \exp(\Delta t \tilde{H}(t_{k+1/2}))\psi(t_k) \tag{41}$$

where Δt is the time step and subscript k is the time index. Modifying the time index to eliminate the need to evaluate the Hamiltonian at fractional time steps, by changing the time step to $2\Delta t$, leads to the modified midpoint unitary transformation (MMUT) method[15,95,526]

$$\psi(t_{k+1}) = \exp(2\Delta t \tilde{H}(t_k))\psi(t_{k-1}) \tag{42}$$

https://dx.doi.org/10.1021/acs.chemrev.0c00223
Chem. Rev. XXXX, XXX, XXX−XXX

The MMUT method is a leapfrog-type unitary integrator that assumes $\tilde{H}$ is linear over the time interval and that higher-order terms go to zero when this approximation is applied to eq 39. Other integrators based on the Magnus expansion have also been developed.[259,527] These integrators are all symplectic and consequently practically energy conserving. The Runge−Kutta class of methods, on the other hand, are nonsymplectic and are thus subject to energy drifts over the course of a long-time simulation. Real-time methods using Magnus integrators require the evaluation of a matrix exponential, which is nontrivial and often the most time-consuming step. In matrix form, eq 42 can be rewritten as

$$\mathbf{P}'(t_{k+1}) = \mathbf{U}(t_k)\cdot\mathbf{P}'(t_{k-1})\cdot\mathbf{U}^{\dagger}(t_k) \tag{43}$$

$$\mathbf{U}(t_k) = \exp[-i2\Delta t\mathbf{H}(t_k)] \tag{44}$$

The time-evolution matrix $\mathbf{U}(t_k)$ can be constructed using various methods such as direct diagonalization or power-series- or Lanczos-based approximations. For small Hamiltonian matrices (i.e., those for which direct diagonalization at every time step does not create a bottleneck), the time-evolution matrix can be constructed using the eigenvectors $\mathbf{C}(t_k)$ and eigenvalues $\boldsymbol{\epsilon}(t_k)$ of the matrix representation of the Hamiltonian at time t_k

$$\mathbf{C}^{\dagger}(t_k)\cdot\mathbf{H}'(t_k)\cdot\mathbf{C}(t_k) = \boldsymbol{\epsilon}(t_k) \tag{45}$$

$$\mathbf{U}(t_k) = \mathbf{C}(t_k)\cdot\exp[-i2\Delta t\boldsymbol{\epsilon}(t_k)]\cdot\mathbf{C}^{\dagger}(t_k) \tag{46}$$

The Baker−Campbell−Hausdorff (BCH)[543] and other polynomial expansions offer an attractive alternative to matrix diagonalization as they only involve general matrix multiplication operations, which are more straightforward to parallelize.[18] Defining $\mathbf{W} = -i2\Delta t\mathbf{H}(t_k)$ and writing eq 42 in matrix form,

$$P'(t_{k+1}) = e^{\mathbf{W}_k}P'(t_{k-1})(t)e^{-\mathbf{W}_k} \tag{47}$$

we can use the BCH expansion to evolve the density matrix as,

$$\begin{aligned}\mathbf{P}'(t_{k+1}) = \mathbf{P}'(t_{k-1}) &+ \frac{1}{1!}[\mathbf{W}_k, \mathbf{P}'(t_{k-1})] \\ &+ \frac{1}{2!}[\mathbf{W}_k, [\mathbf{W}_k, \mathbf{P}'(t_{k-1})]] \\ &+ \frac{1}{3!}[\mathbf{W}_k, [\mathbf{W}_k, [\mathbf{W}_k, \mathbf{P}'(t_{k-1})]]] + \ldots\end{aligned} \tag{48}$$

The BCH expansion has been shown to have superior convergence properties as compared to a simple power series expansion.[18]

The Chebyshev expansion approach[259,544−546] has also been explored as an alternative to diagonalization in the construction of the time-evolution operator given by eq 44.[544,545,547−551] Because the Chebyshev expansion requires matrix eigenvalues within the spectral range of $[-1, 1]$, an approximate estimate of the upper and lower bounds of the eigenspectrum is used to achieve this mapping of the Hamiltonian matrix.[387,551]

Propagation schemes for correlated wave functions (i.e., at the CI, CC, or ADC levels of theory) are oftentimes based on simple procedures, such as the fourth-order Runge−Kutta (RK4) integrator[22,47,49,50] (or RK4 augmented by a variational splitting[552] scheme[404]). However, the utility of more sophisticated integrators has also been explored in this context. For example, for linear and Hermitian expansions of the wave function, the real and imaginary parts of the wave function form a pair of conjugate variables that obey classical equations of motion, a fact that has inspired the development of high-order explicit symplectic integrators for general wave packet dynamics;[536,538,539] explicit symplectic integrators of this form have been applied to electron dynamics at the truncated CI level of theory.[36] Pedersen and Kvaal have noted that the t- and λ-amplitudes of CC theory form a pair of conjugate variables that obey complex classical equations of motion and have developed an implicit symplectic integrator tailored to that problem.[405] In addition, many applications[40,43−46] of time-dependent ADC theory employ the short iterative Lanczos (SIL) scheme.[553] In SIL, a tridiagonal subspace approximation to the Hamiltonian is constructed according to the Lanczos procedure, and the system is evolved according to dynamical equations associated with this approximate Hamiltonian. This approximation is only valid for short time intervals, after which the Lanczos procedure must be repeated to construct an updated approximation to the Hamiltonian. This SIL procedure has been extended to imaginary-time dynamics at the ADC level of theory,[432] where it has been demonstrated that imaginary time TD-ADC with SIL becomes competitive, in terms of computational effort, with frequency-domain ADC calculations.

3.3. Signal Processing

Real-time methods can be very efficient for computing spectra in molecules and materials with a high density of states as, in principle, an entire absorption spectrum can be computed from a single real-time simulation (see Section 4.1). In a nutshell, this requires computing the frequency-dependent response of the system via Fourier transform (FT) of the dipole moment following interaction with a laser pulse with sufficient bandwidth to cover a spectral region of interest. In practice, a narrow-in-time pulse (or delta function) is typically used. Real-time methods, however, suffer from two main drawbacks: first, the spectra generated from the dipole moment do not contain any information about the molecular orbitals or excited states involved in each transition, which is typically how spectra are interpreted. Second, long simulation times are typically required to resolve the spectra via FTs, with denser spectra requiring longer simulations.

Many approaches exist for interpreting spectra generated via real-time methods. The simplest approach is to visualize each transition by exciting a particular mode with a narrow-band quasi-monochromatic field and plotting the deviation of the charge density (or other observable) from the ground state.[18,95] This process, however, involves a separate simulation for each resonant peak, each of which requires a very long simulation times in order to selectively excite a particular mode. This makes it unsuitable for spectra with multiple nearby peaks. Alternatively, the FT of the deviation of the 3D time-dependent density from the ground state can be used to characterize each peak,[554] but this requires a FT at each point in space and involves either 4D data ($x, y, z, t \rightarrow x, y, z, \omega$) or reduction via integration over particular directions. Another method to extract orbital-resolved information involves projecting the wave function onto the ground-state molecular orbitals (MOs) in order to deconvolute the dipole moment into a sum of transitions between MO pairs.[69,555] In a density matrix TDHF/TDDFT framework, this procedure requires the projection of the density matrix and dipole operator onto the ground state MO basis:

$$\mathbf{P}^{\mathrm{MO}}(t) = \mathbf{C}^{\dagger}\mathbf{P}(t)\mathbf{C} \tag{49}$$

https://dx.doi.org/10.1021/acs.chemrev.0c00223
Chem. Rev. XXXX, XXX, XXX−XXX

$$\mathbf{D}^{\mathrm{MO}} = \mathbf{C}^{\dagger}\mathbf{D}\mathbf{C} \tag{50}$$

where $\mathbf{C}$ is the eigenvector matrix for the ground state Fock/Kohn−Sham matrix in the AO basis. Using these quantities, the time-dependent MO dipole contributions can be defined as

$$\mu_{ia,d}(t) = \mathbf{D}^{\mathrm{MO}}_{ia,d}\mathbf{P}^{\mathrm{MO}}_{ai,d}(t) + \mathbf{D}^{\mathrm{MO}}_{ai,d}\mathbf{P}^{\mathrm{MO}}_{ia,d}(t) \tag{51}$$

where $d = x, y, z$, and i, a are indices for the molecular orbitals, generally occupied and virtual, respectively. The total dipole given by

$$\mu_d(t) = \mu_{d,0} + \sum_{i=1}^{N_t}\sum_{a=i+1}^{N_t}\mu_{ia,d}(t) \tag{52}$$

where N_t is the number of steps in the simulation. The static contribution to the dipole is given by

$$\mu_{d,0} = \sum_{i=1}^{N_t}\mathbf{P}^{\mathrm{MO}}_{ii}\mathbf{D}^{\mathrm{MO}}_{ii,d} \tag{53}$$

Note that here the matrices are assumed to be unitary (i.e., no complex absorbing potential) and square (i.e., no linear dependencies in the overlap matrix). For the more general case involving linear dependencies, see ref 555.

Because the FT is a linear operator, the total spectrum is simply the sum of the spectra for each of these transition dipoles, i.e., in TDHF/TDDFT the spectrum is a sum of the contributions from all combinations of occupied → virtual MO pairs. Accordingly, the spectrum can be decomposed into orbital contributions, much like in linear response calculations (see Figure 9). Note that $\mu_{ia}(\omega)$, which are not physical observables, can contain negative peaks but the total dipole spectrum is guaranteed to be positive. The magnitudes of these features can be used to construct numerical weights of each MO pair to the peak by integrating over each peak (or via peak-fitting). These weights give a qualitative interpretation similar to linear response coefficients, which makes RT methods an essentially complete replacement to linear-response methods, albeit with more complicated and time-consuming data analysis. There are two important caveats, however. First, only optically active excitations can be analyzed, where as LR methods can capture selection or spin forbidden transitions. Second, this MO decomposition techniques are not valid for the case of strong-fields, where Stark shifting of the orbitals makes the projection onto the ground state in eq 51 invalid.

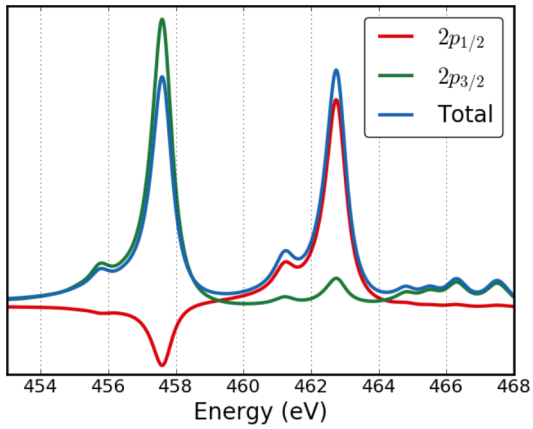

Figure 9. $L_{2,3}$ absorption edges for $TiCl_4$ modeled with B3LYP and the aug-cc-pVTZ basis set. The time evolving dipole was split into different spinor pairs, and only contributions from the 2p orbitals are included. Adapted with permission from ref 98. Copyright (2018) American Chemical Society.

The main drawback of real-time approaches over frequency-domain (eigenspectrum-based) methods is the long simulation times are often required to adequately converge a spectrum via a Fourier transform, i.e., the Fourier "uncertainty principle". This issue can be especially problematic for high energy spectra with high spectral densities, such as those relevant to X-ray absorption. The simplest trick to improve spectral resolution is to preprocess the signal by damping and padding with zeros:

$$\tilde{\mu}(\omega) = \int_0^{\infty} \mathrm{d}t m(t) e^{i\omega t} \tag{54}$$

$$m(t) = \begin{cases} [\mu(t) - \langle\mu\rangle]\mathrm{e}^{-t/\tau}, & t \le t_{\max} \\ 0, & t > t_{\max} \end{cases} \tag{55}$$

where $\langle\mu\rangle$ is either the dipole moment at $t = 0$ or the average dipole moment, and τ is a damping parameter that corresponds to a phenomenological lifetime (line width) in the spectrum. This lifetime must be chosen to be small enough such that the discontinuity in eq 55 does not introduce ringing artifacts in the spectrum, which in practice can blur nearby peaks in a dense spectrum.

Fortunately, there are numerous alternatives to Fourier analysis that can be used to accelerate spectral convergence of time signals without resorting to broadending. Such harmonic inversion methods[556] include Prony's method, filter diagonalization,[557−559] Padé approximants,[560−562] and linear predictors.[563,564] These methods have applications in virtually all types of time-domain simulations ranging from classical electrodynamics,[561,562] to molecular dynamics,[564] to quantum dynamics.[555,557,559,565] There are advantages and disadvantages to each. As an example, filter diagonalization fits the time signal to a sum of damped oscillations. This can rapidly converge spectra containing only a few dominant modes, but may have convergence issues for highly dense spectra. Padé approximants (discussed below) assume nothing about the line shape but require a matrix inversion and can introduce artifacts into the spectrum if the time signal is too short. These techniques are especially effective when used in conjunction with a dipole decomposition scheme, where each $\mu_{ia}(\omega)$ is computed separately using an accelerated transform, and the total spectrum is computed from the sum of these contributions. This strategy exploits the fact that each transition dipole is spectrally sparser than the total, which facilitates convergence of the accelerated transforms.

A good general purpose transform is the Padé approximant to the FT, which in a diagonal form consists of writing the discrete FT as a ratio of power series expansions:

$$\mu(z) = \sum_{k=0}^{M} c_k(z_k)^k = \frac{\sum_{k=0}^{M} a_k z^k}{\sum_{k=0}^{M} b_k z^k} \tag{56}$$

where $M = N_t/2$, $z_k = e^{-i\omega\Delta t}$, and the coefficients $\{c_k\} = \mu(t_k)$ are the discrete values of the input time signal. Thus, we have a linear system for the coefficients

$$\sum_{k=0}^{M} c_k z^k \sum_{m=0}^{M} b_m z^m = \sum_{k=0}^{M} a_k z^k \tag{57}$$

https://dx.doi.org/10.1021/acs.chemrev.0c00223
Chem. Rev. XXXX, XXX, XXX−XXX

with $a_0 = c_0$ and $b_0 = 1$ chosen by convention. The unknown coefficients $\{a_k\}$ and $\{b_k\}$ are determined by solving the matrix equation:

$$\mathbf{Gb} = \mathbf{d} \tag{58}$$

where $\mathbf{G}$ is a $N_t \times N_t$ matrix with elements $G_{km} = c_{N_t-m+k}$, $\mathbf{d}$ is a column vector of length N_t with elements given by $d_k = -c_{N_t+k}$, and $\mathbf{b}$ is a vector of length N_t. The elements of $\mathbf{b}$ can be found via inversion of the $\mathbf{G}$ matrix, which has Toeplitz symmetry:

$$\mathbf{b} = \mathbf{G}^{-1}\mathbf{d} \tag{59}$$

The coefficients $\{a_k\}$ are then given by

$$a_k = \sum_{m=0}^{k} b_m c_{k-m}, \qquad k = 1, \ldots N_t \tag{60}$$

Once these coefficients have been determined, the FT can be computed using eq 56. Critically, because these coefficients are independent of frequency, the spectrum can be generated for an arbitrary spectral density. This is analogous to extrapolating the input signal to an arbitrarily long time. Although this procedure requires the solution of a linear equation [eq 57] for each $\mu_{ia}(t)$, the cost of this procedure is modest, and, in practice, one can often compute a fully converged spectrum with 1/5 or less of a simulation time compared to a traditional FT (see Figure 10).

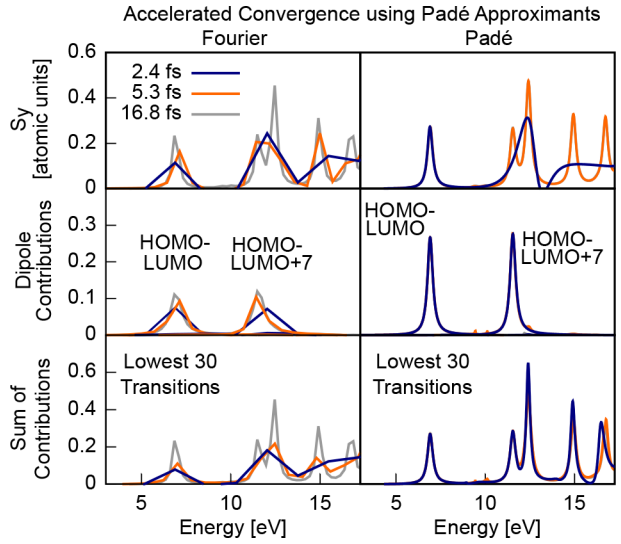

Figure 10. Convergence of the valence absorption spectrum for water using a conventional FT (left) and Padé accelerated transition dipole scheme (PT; right) for various simulation times. PT of the total dipole converges roughly 3 times faster than the FT, and PT of the dipole contributions 7 times faster. Adapted with permission from ref 555. Copyright (2016) American Chemical Society.

This approach is especially well-suited to X-ray absorption, because one needs only consider transitions from a limited set of occupied orbitals, much like orbital windowed linear response.[566]

4. APPLICATION OF REAL-TIME TIME-DEPENDENT ELECTRONIC STRUCTURE METHODS

4.1. UV/Vis Spectroscopy

One of the biggest advantages of real-time electronic structure theory over solving for the lowest energy eigenstates is the ability to simulate the linear (UV−vis) absorption spectrum of a system with a dense manifold of states. Using real-time electronic propagation, the entire energy spectrum is obtained after Fourier transform of the dipole moment (Section 3.3), providing the response of all electronic states that the system accesses via the applied perturbation. Real-time methods may be preferable over matrix eigenstate methods, and are particularly advantageous for metallic systems and clusters, where collective oscillations of the electrons are important for capturing plasmonic excitations.[144,145,151,567] However, for real-time propagation of the electron density with TDHF or TDDFT, the time-evolution of the electron density may be more cost efficient than solving for hundreds of excited states via a linear response matrix formulation that requires generating a matrix-vector product for all occupied-virtual orbital combinations, see Figure 11.[85] The crossover point in computational cost will

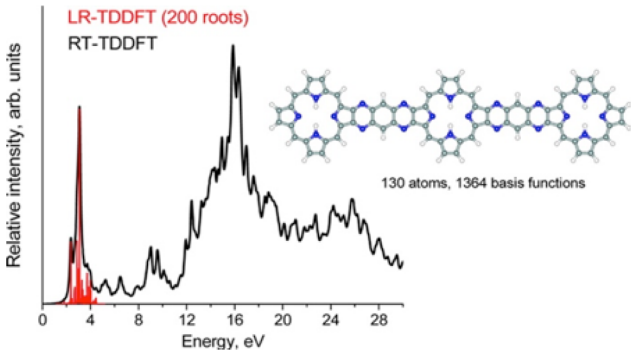

Figure 11. Absorption spectrum of $C_{72}H_{38}N_{20}$ (inset) calculated using the B3LYP functional in combination with the 6-31G(d) basis set. The linear response TDDFT spectrum contains 200 roots compared to the RT-TDDFT absorption spectrum from Fourier transform of the dipole moment. Adapted with permission from ref 85. Copyright (2015) American Chemical Society.

depend on the implementation, the requested number of states, the desired resolution of the spectrum, and time-step for numerical propagation.

The UV−vis linear absorption spectrum can be obtained from a real-time simulation by Fourier transforming the field-free time-dependent dipole moment after perturbation by a weak, off-resonant perturbation (often an electric field applied as a delta function). To obtain oscillator strength values that are proportional to the linear response values, the dipole strength function $S(\omega)$ should be used

$$S(\omega) = \frac{1}{3}\mathrm{Tr}[\sigma(\omega)] \tag{61}$$

where $\sigma(\omega)$ is the absorption cross section tensor with diagonal elements that can be computed from the polarizability by

$$\sigma_{ii}(\omega) = \frac{4\pi\omega}{c}\mathrm{Im}[\alpha_{ii}(\omega)] \tag{62}$$

and

$$\alpha_{ii}(\omega) = \frac{\mu_i(\omega)}{E_i(\omega)} \tag{63}$$

Here, $\mu_i(\omega)$ and $E_i(\omega)$ are the Fourier transforms of the dipole moment and electric field for $i = x, y, z$, respectively.

Early applications of the real-time TDDFT method by Yabana and Bertsch computed the optical spectra for the benzene molecule[10] and for metallic lithium clusters.[8] A few years later,

https://dx.doi.org/10.1021/acs.chemrev.0c00223
Chem. Rev. XXXX, XXX, XXX−XXX

Ullrich and coworkers simulated the spectra and collision properties of sodium clusters,[230] with QM/MM UV−vis spectral simulations of biological chromophores performed by Rubio and coworkers following closely after these early studies.[74,75] Real-time methods are now widely used for simulations of UV−vis spectra for a variety of complex systems.[15,18,34,69,70,76−80,82,84−88,568,569]

4.2. X-ray Absorption Spectroscopy

Recent advances in synchrotron technology have greatly improved the temporal and energy resolution of X-ray photons, making X-ray absorption spectroscopy (XAS) an indispensable experimental technique in materials and chemical sciences. Excitation of core electrons to unoccupied bound orbitals or to the continuum allows XAS to probe element specific chemical processes that provide insights into the local electronic and binding environment.[570,571]

XAS K-, L-, and M-edge spectra are generated from photoexcitations of electrons in $n = 1$, $n = 2$, and $n = 3$ orbitals, respectively, where n is the principal quantum number. Because core electrons move close to the speed of light, relativistic effects play an important role in XAS. Scalar relativistic effects lead to contraction of core orbitals, which blue-shifts the entire XAS spectrum relative to a spectrum calculated with a nonrelativistic Hamiltonian.[95,338,339,566,572−574] Spin−orbit coupling splits the degenerate $2p$ orbitals into $2p_{1/2}$ and $2p_{3/2}$ manifolds, giving rise to unique features in L-edge XAS spectra and a more complicated spectra at the M-edge. Therefore, electronic structure methods that include relativistic effects are needed to accurately describe XAS spectra, especially at the L- and M-edges. A uniform energy shift to spectra derived from nonrelativistic calculations is often sufficient for describing the K-edge.

Many *ab initio* methods have been developed to model core excitations, and the majority of these approaches operate within the frequency domain. K-edge spectra have been obtained with linear response TDDFT (LR-TDDFT),[95,338,566,574−577] algebraic-diagrammatic construction,[578−580] linear-response density cumulant theory,[581] coupled-cluster theory using both the complex polarization propagator[582,583] and the EOM-CC formalisms,[574] and restricted active space (RAS) multiconfigurational methods.[584,585] L-edge XAS spectra can be computed using RAS with perturbative spin−orbit coupling[586,587] and the more recently developed relativistic two-component LR-TDDFT.[340]

In the time-domain, nonrelativistic RT-TDDFT[96] and time-dependent EOM-CC[49] have been applied to compute molecular K-edge XAS. Recently, time-dependent variational four- and two-component relativistic TDDFT methods were developed to model the XAS L-edge spectra.[97,98] Two-component variational relativistic real-time methods are an attractive alternative to their four-component analogues due to the balance of the computational cost and theoretical accuracy offered by the former. For example, in work by Kasper et al. the $L_{2,3}$ spectra of $SiCl_4$, obtained using the real-time X2C method, were in excellent agreement with experimentally obtained spectra (Figure 12) and similar in quality to those calculated at the four-component level.[98]

Finally, simulations of X-ray absorption can be challenging for systems with a high density of states, as finite basis set effects can introduce unphysical "intruder peaks" into XAS spectra. These features arise from transitions from valence orbitals to very high lying virtual orbitals, which should have zero lifetime because they reside within the continuum. Such peaks are unlikely to occur for smaller molecules, but are unavoidable for larger systems. This issue is avoided if using a large simulation box with a grid or planewave basis, provided an appropriate boundary condition is used (e.g., complex absorbing potential). For more details regarding open TDDFT systems, see review by Rubio and coworkers.[589] For atom-centered basis set methods, however, it is usually more efficient to instead give the virtual states a phenomenological lifetime[109] to filter the intruder peaks from the spectrum. This technique has been successfully applied to resolve the K-edge XAS spectrum of α-quartz (Figure 13).[96]

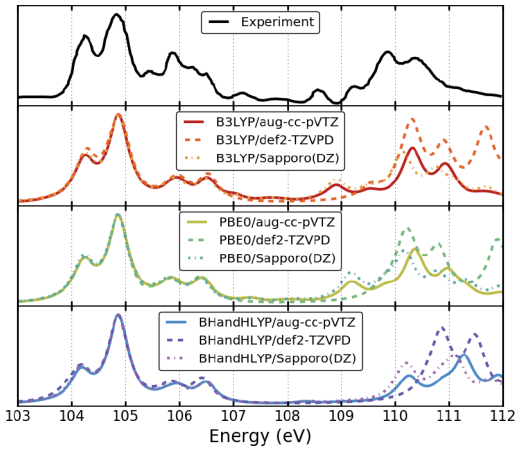

Figure 12. Two-component relativistic RT-TDDFT modeled $L_{2,3}$ absorption edges for $SiCl_4$, compared to experimental spectrum.[588] Adapted with permission from ref 98. Copyright (2018) American Chemical Society.

4.3. Excited State Absorption and Emission

There are numerous methods for probing excited state dynamics, such as transient absorption spectroscopy, where modulations in the absorption as a function of time delay between a pump and a probe laser pulse encode the dynamics in the system.[590] Although conceptually simple, one of the main challenges with time-resolved experiments is the ability to characterize overlapping transient spectral features within an energy range. This problem grows with increases in system size and complexity of the electronic structure. From the standpoint of theory, the ability to simulate the excited-state dynamics and extract the corresponding excited-state absorption (ESA) spectrum is of great value, allowing one to interpret and predict experiments. The success of such a procedure obviously hinges on the accuracy of the theoretical approach.

Currently, the primary approach to compute ESA is via response theory.[591,592] Within linear response (LR) theory, the poles of the response function yield the excitation energies of the system, and transition moments between excited states can be obtained from the second-order residues of the quadratic response function. Together, these quantities can be used to evaluate the ESA of a molecular system. The first-order residues of the quadratic response function can also be used to obtain the two-photon absorption. In spite of these advantages, quadratic response theory is a numerically prohibitive approach for the computation of ESA in large molecular systems with high densities of states as the excited states have to be treated individually, which can become computationally infeasible when seeking the full spectrum of the system. An alternative approach is to reformulate the problem by calculating the linear response from an excited state reference. Formally, this approach is

https://dx.doi.org/10.1021/acs.chemrev.0c00223
Chem. Rev. XXXX, XXX, XXX−XXX

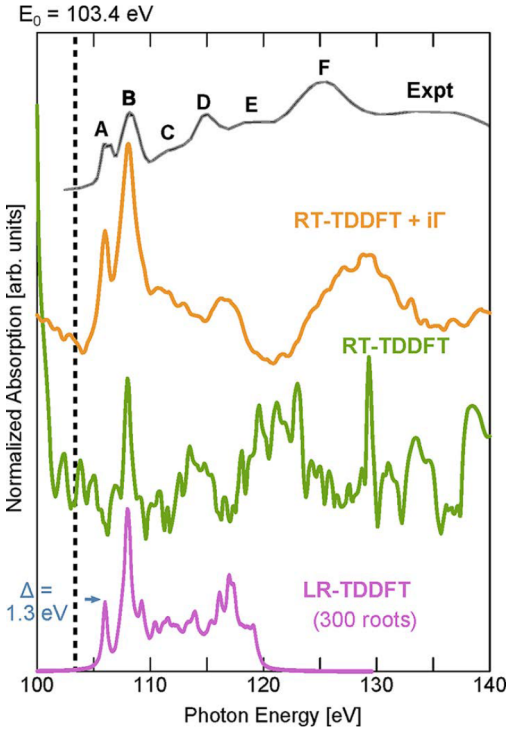

Figure 13. Computed real-time TDDFT K-edge XAS of α-quartz with (orange) and without (green) a complex absorbing potential, along with corresponding linear response TDDFT (purple) and experimental data. Adapted with permission from ref 96. Copyright (2015) American Chemical Society.

equivalent to the quadratic response with respect to the ground state. However, this relationship only holds within an exact treatment (namely, full CI[591]) and not for approximate theories.

RT-TDDFT has been shown to be an efficient and appealing method for computing spectra of systems with high densities of states.[83,85] It has also been intuitively used in the context of pump−probe experiments by De Giovannini and coworkers,[82] where an electric field is first applied to pump the system to a target excited state and a second electric field is used to probe the response of that excited state. The outstanding question with this approach, however, is whether the probe pulse is actually interacting with the intended target excited state, because resonant excitations are problematic and challenging to achieve with RT-TDDFT.[82,84,246,261−263,267,593,594]

Fischer and coworkers[86] have proposed an alternate approach that circumvents the RT-TDDFT-specific challenges associated with resonant excitations but that still relies upon RT-TDDFT to probe the response of the target excited state. One first performs a LR-TDDFT gradient[595,596] calculation to compute the density matrix of the excited state of interest. This serves as the initial superposition state for a subsequent RT-TDDFT calculation, which then effectively yields the response of the excited state of interest. In order to preserve the exact structure of this approach, an exact exchange-correlation kernel, which is a functional of the initial state and complete history of the density, would be needed.[597] However, in practice, approximate exchange-correlation functionals within the adiabatic approximation have to be used. Maitra and coworkers have formally analyzed the errors in the propagation of initial states that derive from these two key approximations.[297]

Despite the use of exchange-correlation approximations that are, in general, designed for the ground state, this strategy of seeding RT-TDDFT simulations with LR-TDDFT densities has been shown to reproduce the ESA features in a number of molecular systems, including zinc phthalocyanine[87] and tetrapyridyl porphyrins.[299] Li and coworkers have also combined RT-TDDFT with Ehrenfest dynamics simulations in order to investigate excited-state lifetimes.[134,135] Parkhill and coworkers[93] also developed a combined RT-TDDFT/non-adiabatic-relaxation model[20] to simulate the transient absorption spectra of pyrazole and a GFP-chromophore derivative. Lopata and coworkers alternatively used a constrained DFT initial state to compute transient X-ray absorption for pumped molecules, which showed a decreased in absorption and a blue shift in the frequency with increasing electron density around the absorbing atom.[598] Recently, Ghosh and coworkers[599] have also reported simulations of ESA with the semiempirical RT-INDO/S approach (see Section 2.2) that compares well with RT-TDDFT.

4.4. Charge Transfer, Plasmon Excitations, and Exciton Dynamics

Charge transfer, which we here consider as a process wherein electrons transfer between states or between regions of space, has central importance in biochemistry, in photosynthesis, in the generation and storage of electricity, as well as in electro-optic activity (i.e., photovoltaic cells, fuel cells, organic chromophores for use in optical fibers and light-emission diodes, etc.). Real-time electronic structure methods can explicitly model time-resolved, nonperturbative charge-transfer and exciton dynamics in donor−acceptor or dye molecules applicable to the development of solar cells,[18,81,136,142,148,390,391,600,601] molecular conductance,[121] energy transfer between chromophores,[568] and plasmon behavior in noble metal nanowires and nanoparticles.[144,145,388] Here, we first focus on simulations of charge transfer with fixed nuclei, then highlight some applications where the nuclear motion is key to driving the charge-transfer dynamics.

Within the RT-TDDFT method, inaccuracies in charge transfer can be traced both to the approximate exchange-correlation functional and the adiabatic approximation. Errors due to the approximate exchange-correlation functional affect excitation energies and charge transfer rates. Local and semilocal density functionals yield a very poor description of charge-transfer excitations, but improved excitation energies are often predicted with long-range correction to the exchange functional.[325,602,603] However, errors in charge transfer due to the adiabatic approximation are much more challenging to remedy. When a resonant field is applied to the ground state to induce charge transfer to the resonant excited state for a model double-well potential for two electrons, RT-TDDFT within the adiabatic approximation qualitatively fails,[140] see Figure 14. However, another study suggests that the charge transfer from an excited state to the ground state might be more accurately captured by the adiabatic approximation.[265] For a detailed explanation of the impact of the adiabatic approximation on the charge-transfer dynamics of model systems, see work by Maitra[140,265] and ref 252.

Despite the poor behavior of RT-TDDFT within the adiabatic approximation simulating the charge transfer of model systems, it is widely used for simulating the charge transfer of more complex systems such as organic materials and metal nanoparticles. In 2011, Chapman et al. simulated RT-TDDFT ultrafast charge-transfer dynamics in a photoexcited fullerene complex.[136] A charge-transfer event was observed following the

https://dx.doi.org/10.1021/acs.chemrev.0c00223
Chem. Rev. XXXX, XXX, XXX−XXX

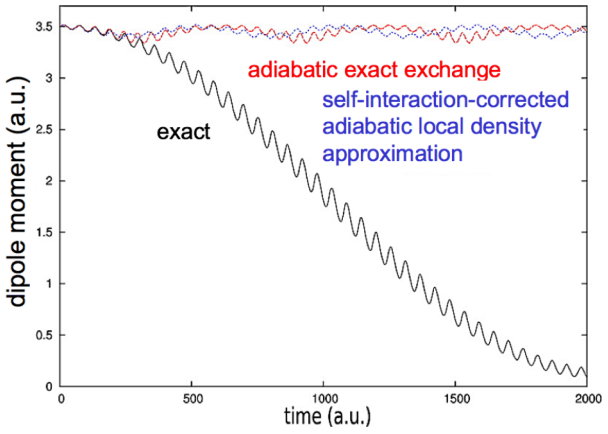

Figure 14. Absolute values of dipole moments for the charge transfer from the ground state between closed-shell fragments for exact propagation (solid black line), RT-TDDFT with adiabatic exact exchange (dashed red line), and RT-TDDFT with the self-interaction-corrected adiabatic local density approximation (dotted blue line). The calculations were performed in the presence of a resonant field for a model double well potential with two electrons in one dimension. Adapted with permission from ref 140. Copyright (2013) American Chemical Society.

photoexcitation of C_{60}:DMA (DMA = *N*,*N*-diethylamine) where the initial electron−hole pair is localized in fullerene (Figure 15). This charge transfer can potentially give rise to a

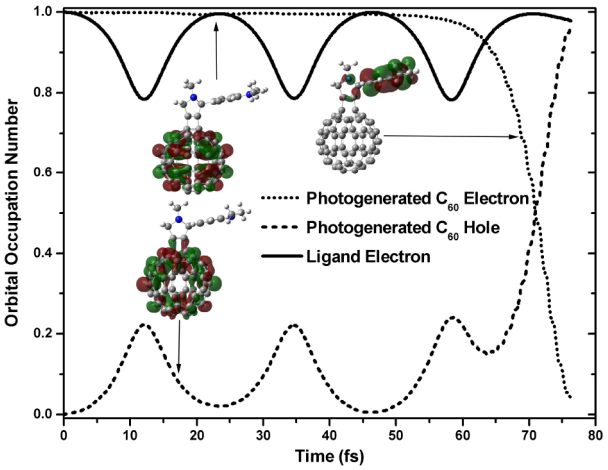

Figure 15. Time evolution of photogenerated electron (dotted line) and hole (dashed line) localized on C_{60} and an electron localized on the DMA ligand (solid line) following a fullerene-localized excitation. Adapted with permission from ref 136. Copyright (2011) American Chemical Society.

long-lived photogenerated electron−hole pair. A subsequent study, using RT-TDDFT with a time-dependent polarizable model,[138] has shown that solvated ligand-to-fullerene charge transfer is enhanced relative to vacuum due to solvent reorganization of excited electronic states and solvent−solute coupling.[139] A follow up real-time time-dependent DFTB study was performed by Oviedo and Wong on the same system using explicit toluene and water solvent molecules but different system conditions.[148]

Using real-time time-dependent DFTB, Sanchez and coworkers have studied the nonequilibrium charge injection mechanism from both catchetol and cresol dye molecules to a TiO_2 nanoparticle (Figure 16).[390,391] The simulations of a Type II photoinjection mechanism showed direct promotion of an

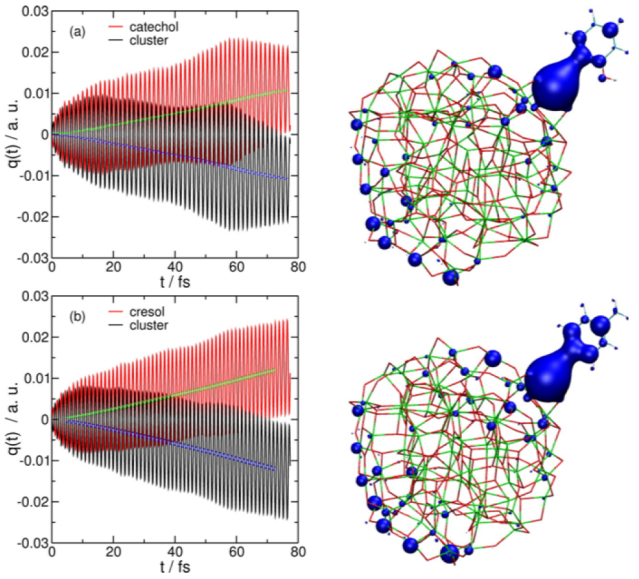

Figure 16. Changes in Mulliken charges with respect to their ground state values as a function of time for a dye chromophore and TiO_2 nanoparticle together with the plots of the spatial distribution of electrons involved in the optical excitation during the application of resonant electric field. Adapted with permission from ref 391. Copyright (2012) American Chemical Society.)

electron from the dye to the first unoccupied level of the conduction band of the nanoparticle during the application of the resonant field. The evolution of the molecular orbital populations showed an exchange from the highest occupied molecular orbital of the dye to a manifold of high-energy orbitals from the conduction band of the nanoparticle.

RT-TDDFT electronic dynamics has also been applied to study excitonic and plasmonic dynamics in metal nanowires and metal nanoparticles. Ding et al. illustrated the electronic dynamic characteristics of a molecular plasmon in silver nanowires from the perspective of a coherent multielectron oscillation.[144] This work was later extended to the investigation of the exciton transfer rate and diffusion length driven by the pure dephasing mechanism in a silver nanowire array (Figure 17).[145] The team of Ilawe, Oviedo, and Wong demonstrated that highly long-range electronic couplings in a multiparticle plasmonic nanoantenna system were responsible for electronic excitation transfer(Figure 18),[388] finding that the common nearest-neighbor Förster resonance energy transfer model is inadequate for accurately characterizing electronic excitation transfer. Real-time TDCI calculations have also been used to model rapid dephasing of plasmon-like excitations in model systems[36] that could be interpreted as electron thermalization.[604]

Using RT-TDDFT with Ehrenfest dynamics, Meng and Kaxiras investigated electron and hole dynamics upon photoexcitation in dye-sensitized solar cells made from three model dyes interfaced with a TiO_2 semiconductor surface.[600] The amount of charge transfer was determined by the integral of excited electron (hole) density projected onto the TiO_2 orbitals. They found that after excitation, the electron gradually delocalizes and is injected into the semiconductor TiO_2 region, on a time scale of 125−175 fs, whereas the hole does not

https://dx.doi.org/10.1021/acs.chemrev.0c00223
Chem. Rev. XXXX, XXX, XXX−XXX

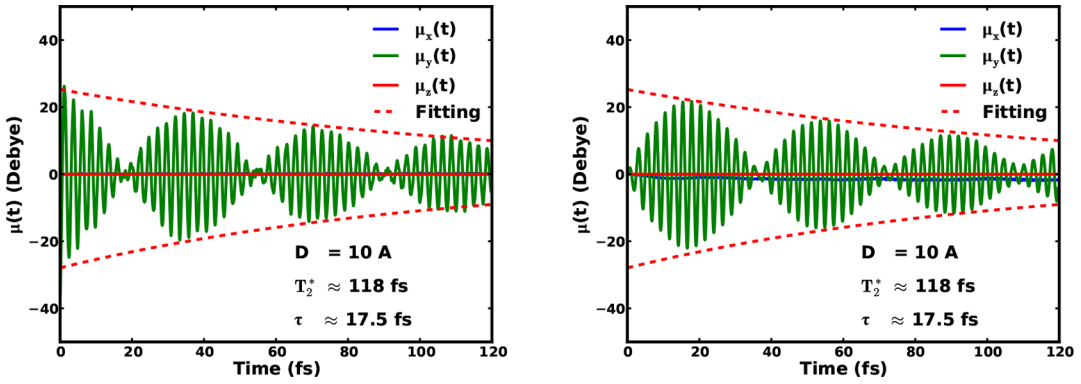

Figure 17. Time evolving dipole moments (Cartesian components) in the first (left) and second (right) silver nanowire at an interchain separation distance of 10.0 Å. Adapted with permission from ref 145. Copyright (2015) American Chemical Society.

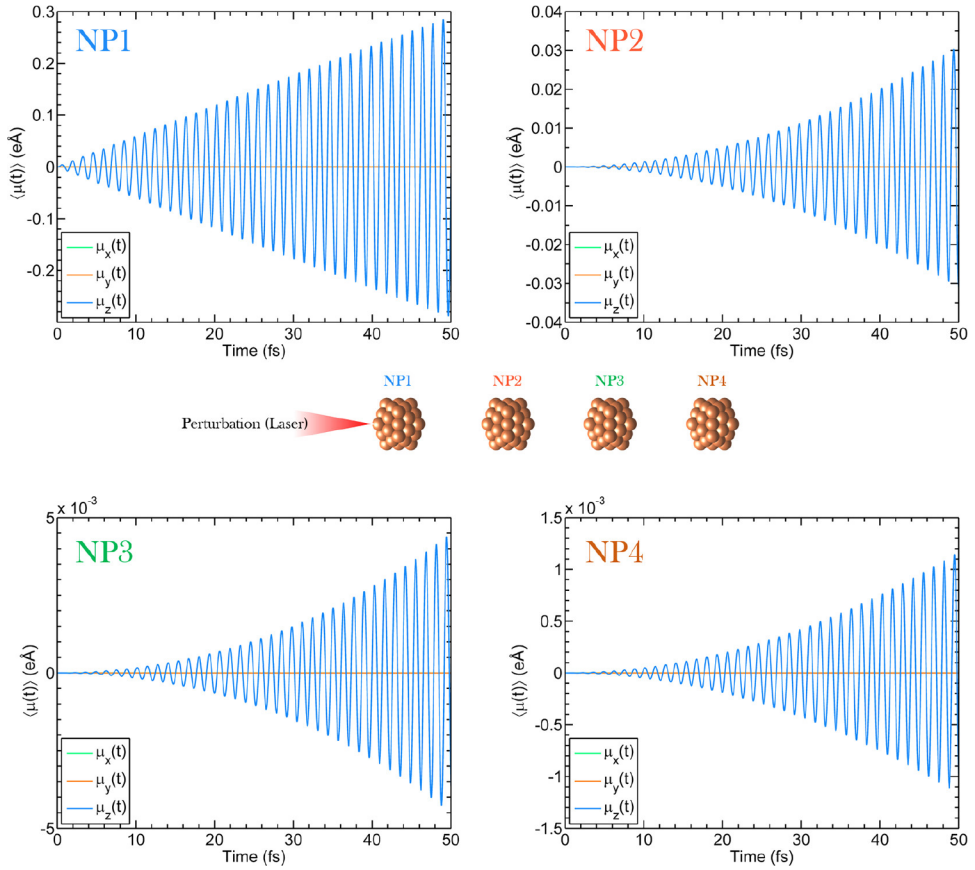

Figure 18. Time-dependent dipole moments induced in the four nanoparticles of a plasmonic nanoantenna system upon optical excitation of nanoparticle 1 (NP1) with a sinusoidal electric field perturbation. The induced dipole moments in the nanoparticles are indicative of the electronic excitation transfer in the multiparticle plasmonic nanosystem. Adapted with permission from ref 388. Copyright (2017) American Chemical Society.

penetrate through the interface region. The hole injection time is much longer than the time for electron injection, and hole injection only starts after the excited electron has been completely injected into the TiO_2(Figure 19).[600] Ehrenfest dynamics on the RT-TDDFT surface has been used to simulate the charge transfer in a light-harvesting molecular triad with good comparison with experimental time scales,[141] as well as charge delocalization and transfer in an organic polymer−fullerene photovoltaic system,[143] with both studies showing that vibronic motion is key to driving the charge transfer dynamics. When exciton−phonon coupling is considered in RT-TDDFT Ehrenfest dynamics, molecular vibrations have been shown to induce molecular plasmon decay and transfer.[149,567] Petrone and coworkers have applied RT-TDDFT to study the dynamics of photoexcited charge carriers in ladder-type donor−acceptor block copolymers.[142] Shortly after the formation of the exciton, the electron and hole densities dissociate to yield a pseudo charge-separated state. Based on the observed orbital pathways involved in the short-time dynamics, *p* and *n* type conductivity have been identified in different block copolymers. When the charge carrier dynamics is coupled to molecular vibrations, the dynamical evolution of the polaron pair can be observed. Donati and coworkers have applied RT-TDDFT Ehrenfest dynamics and wavelet analysis to investigate the formation of polaron pairs

https://dx.doi.org/10.1021/acs.chemrev.0c00223
Chem. Rev. XXXX, XXX, XXX−XXX

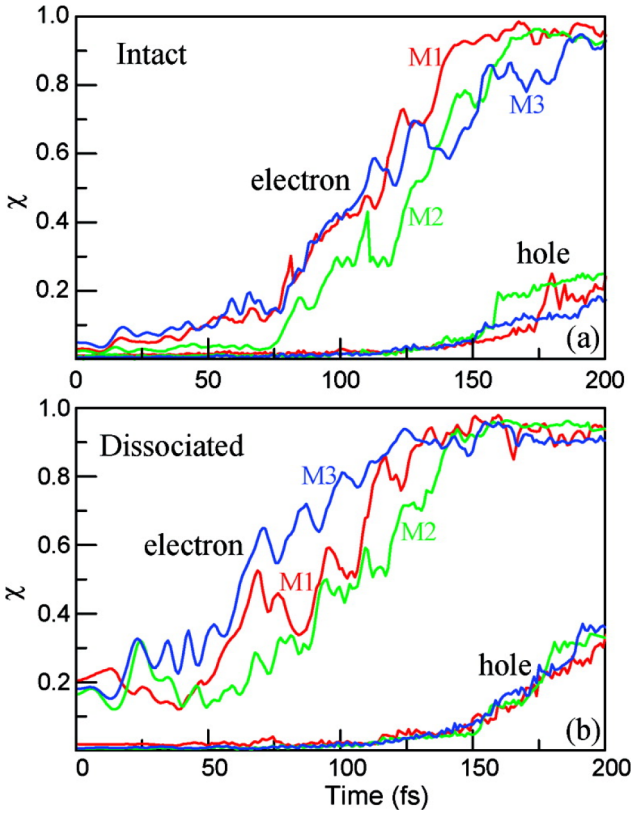

Figure 19. Comparison of electron and hole dynamics of three model dyes of increasing size, in intact and dissociated forms, representing the injection probability from the dye to the TiO_2 nanocrystal surface. Adapted with permission from ref 600. Copyright (2010) American Chemical Society.

in a thiophene oligomer.[605] The formation of a polaron pair is modulated by the out-of-plane motion of the polymer backbone dynamics with an observed lifetimes of ~10 fs.

4.5. Nonlinear Properties and Multidimensional Spectroscopy

One of the great advantages of real-time approaches is their ability to model the nonlinear response of a system to electromagnetic radiation. These techniques allow one to consider pulse shapes and field strengths representative of those applied in experimental settings. Simulations thus go beyond the perturbative regime, capturing all orders of response simultaneously. As a result, real-time time-dependent approaches have emerged as the a key method for describing highly nonlinear processes and properties.

High harmonic generation (HHG), arising from the interaction between molecular (hyper)polarizabilities and an external field, occurs at integer multiple frequencies of the driving frequency of the laser that illuminates the medium.[606,607] As such, HHG can supply high-energy attosecond pulses for ultrafast spectroscopy experiments.[606−609] From the computational point of view, the HHG power spectrum can, in principle, be extracted from the time-evolution of the dipole moment,[610] after the system is perturbed by a monochromatic external field. One challenge in extracting such nonlinear response properties from real-time electronic structure simulations is that all orders of response are combined in one time signal, which is apparent from the expansion of the dipole moment interacting with an external monochromatic field, $\mathbf{E}(t) = \mathbf{A}\cos(\omega t)$,

$$\mu_i(t) = \mu_i^0 + \sum_j \mu_{ij}^{(1)}(t)A_j + \sum_{jk} \mu_{ijk}^{(2)}(t)A_jA_k + \sum_{jkl} \mu_{ijkl}^{(3)}(t)A_jA_kA_l + \cdots \quad (64)$$

$$\mu_{ij}^{(1)}(t) = \alpha_{ij}(-\omega;\ \omega)\cos(\omega t) \quad (65)$$

$$\mu_{ijk}^{(2)}(t) = \frac{1}{4}[\beta_{ijk}(-2\omega;\ \omega,\ \omega)\cos(2\omega t) + \beta_{ijk}(0;\ \omega,\ -\omega)] \quad (66)$$

$$\mu_{ijkl}^{(3)}(t) = \frac{1}{24}[\gamma_{ijkl}(-3\omega;\ \omega,\ \omega,\ \omega)\cos(3\omega t) + 3\overline{\gamma}_{ijkl}(-\omega;\ \omega,\ \omega,\ -\omega)\cos(\omega t)] \quad (67)$$

Here, ω and $\mathbf{A}$ are the frequency and the amplitude vector of the field, respectively, and $\alpha(-\omega;\ \omega)$, $\beta(-2\omega;\ \omega,\ \omega)$, and $\gamma(-3\omega;\ \omega,\ \omega,\ \omega)$ are the frequency-dependent (hyper)-polarizabilities, which give rise to the linear response and second- and third-harmonic generations. $\beta(0;\ \omega,\ -\omega)$ and $\gamma(-\omega;\ \omega,\ \omega,\ -\omega)$ also appear in the dipole expansion; these terms are related to optical rectification and degenerate four-wave mixing, respectively. Eq 62 suggests that one can use some signal processing techniques to extract frequency-dependent (hyper)polarizabilities from the time-evolving dipole moment.

When the field strength is small, one can obtain linear and nonlinear molecular response properties by ignoring the higher order contributions. Chen et al.[611] used the filter diagonalization approach to extract the first hyperpolarizability tensor. Rehr et al.[14] obtained second-order response properties by applying the finite-field method in conjunction with a quasimonochromatic approximation to RT-TDDFT, driven by a Gaussian-enveloped external field. Bandrauk et al. resolved the high-order harmonic spectra of atomic hydrogen by numerical solving the time-dependent Schrödinger equation, with a Hamiltonian augmented by a linearly polarized laser pulse.[612] TD-CI has also been applied to compute the (non)linear properties of small molecules, and it has been shown that TD-CI-based techniques outperform RT-TDDFT in the prediction of HHG spectra if higher order excitation operators are included in the TD-CI expansion.[29,30,37,38,392,393]

The most general approach for computing frequency-dependent polarizabilities and hyperpolarizabilities via real-time simulations was developed by Ding et al.[99] Individual orders are separated into independent expressions which are free from higher order contributions up to the fourth order. Using time-evolving dipole moments from just a few short simulations, one can determine polarizabilities, and first and second hyperpolarizabilities in good agreement with those calculated using response theory. For example, Figure 20 shows the time-evolutions of the linear and nonlinear properties of the paramagnetic BeH molecule computed using TD-CI. The first- and second-order dipole responses show excellent agreement between the real-time signals and analytical expressions, and there are noticeable deviations, arising from the absence of higher-order corrections, of the real-time simulations from the truncated analytical expression for the third-order dipole response.

The accuracy of calculated (hyper)polarizability tensors is sensitive to the approximate field-matter interaction and the quality of basis set.[393,613] The field-matter interaction is usually treated within the electric-dipole approximation in the length

https://dx.doi.org/10.1021/acs.chemrev.0c00223
Chem. Rev. XXXX, XXX, XXX−XXX

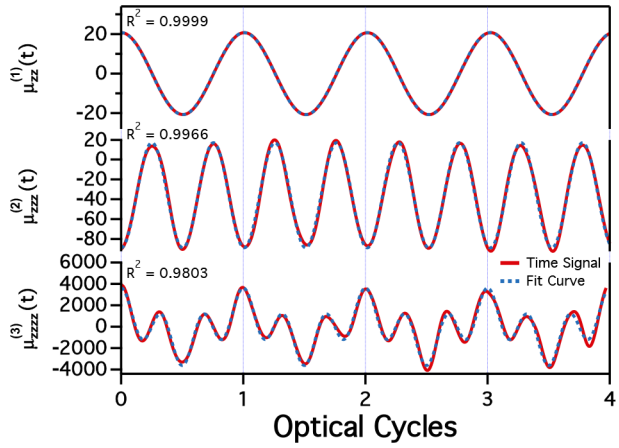

Figure 20. Time-evolutions of the first-, second-, and third-order responses of BeH modeled with the TD-CIS/6-31+G(d) level of theory. The fit curves and their R^2 values overlay the simulation data. Adapted with permission from ref 38. Copyright (2018) Elsevier.

gauge form. Some have suggested the use of alternative gauges (*i.e*, the velocity or acceleration gauge) to improve the description of the power spectrum in finite basis sets.[614−616] Simple $\cos^2$ or $\sin^2$ pulse envelopes are often used to "dress" the perturbing field,[37,393] but even the field envelope can be tailored to enhance or damp specific harmonics.[617] Additional diffuse functions have been shown to improve the quality of (hyper)polarizabilities extracted from the time-domain approach.[99] For TD-CI, recent work by Lestrange et al. suggests that accurate nonlinear properties may require CI expansions that span most of the full CI configuration space. Specifically, as much as 2/3 of the full CI space is needed to obtain nonlinear properties accurate to within 5% of the exact (full CI) values.[38]

Work by Konecny et al.[100] has shown that nonlinear properties can be significantly affected by relativistic effects. In calculations on a $W(CO)_5py$ complex, it was found that the dominant component of the second harmonic generation tensor was shifted by about 35% compared to that obtained from a nonrelativistic method. Importantly, this work also demonstrated that these higher-order properties can still be captured using approximate relativistic methods such X2C, with almost no loss of accuracy compared to fully relativistic 4-component Dirac calculations.

Multidimensional nonlinear spectroscopy[618−621] has become an indispensable tool for probing molecular structure, structural/electronic dynamics, energy transfer, and chemical reactions and the nature of excited state correlations. Useful information on the couplings between molecular degrees of freedom (spin, vibrational, or electronic) can be obtained by disentangling a congested one-dimensional spectrum into n-dimensions by scanning the interpulse delays. Spreading the linear absorption spectrum in multidimensions allows one to monitor and unravel the dynamics of, e.g., intermolecular energy transfer processes in molecular aggregates. Intense ultrashort pulses are needed to monitor subfemtosecond electronic processes. These signals are commonly simulated by the sum-over-states (SOS) technique, in which the signal is calculated from electronic eigenstates and the coupling to electric fields, which is treated perturbatively under the dipole approximation. Nonlinear signals are calculated from corresponding transition dipoles, transition energies, and dephasing rates. An alternative approach for computing multidimensional signals is to simulate the electronic dynamics by propagating the one-electron reduced density matrix, driven by multiple electric fields. In this way, one avoids having to explicitly calculate many electronic eigenstates. Nonlinear effects induced by intense external fields are automatically accounted for because the incoming fields are treated in a nonperturbative way. These effects can, in principle, be calculated with the wide range of real-time electronic structure methods discussed in this Review.

In a novel application of real-time electronic structure methods, Mukamel and coworkers have recently used RT-TDDFT to implement a phase cycling[622] scheme to extract desired nonlinear signals from a finite set of RT-TDDFT simulations for multiple incoming fields with variable phases. The scheme was implemented for four-wave mixing signals. RT-TDDFT simulations were performed to compute XUV and X-ray nonlinear signals for the CO molecule and were found to be in qualitative agreement with CASSCF sum-over-states (SOS) calculations.

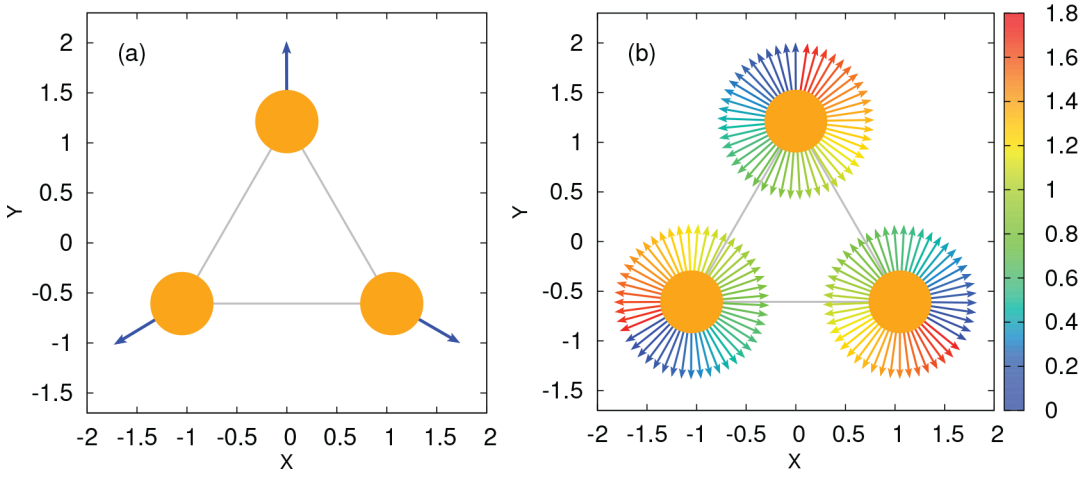

Figure 21. (a) The initial spin magnetization of an equilateral triangle formed by three Li atoms, Li_3, with an Li−Li bond length of 2.10 Å and (b) the time evolution of the spin magnetization in a uniform magnetic field that is applied perpendicular to the plane of the trimer ($B_z = 8.5 \times 10^{-5}$ au [~20 T]). The time-evolution is represented as the progression of coloration in units of picoseconds, and the magnetization vector is represented in units of Bohr magneton. Adapted with permission from ref 68. Copyright (2014) American Institute of Physics.

https://dx.doi.org/10.1021/acs.chemrev.0c00223
Chem. Rev. XXXX, XXX, XXX−XXX

In other recent nonlinear studies that have demonstrated the robustness of RT-TDDFT, Bruner and coworkers[298] reported a study of charge migration dynamics following nitrogen 1*s* ionization of nitrosobenzene comparable to that of post-Hartree−Fock wave-function-based methods, Cho and coworkers[623] simulated the electronic dynamics after a valence or core ionization in the glycine-phenylalanine dipeptide and calculated the resulting time-resolved X-ray diffraction signals, Bruner and coworkers[624] computed the resonant X-ray sum-frequency generation (SFG) signals of the oxygen and fluorine K-edges in acetyl fluoride and, more recently, Nascimento and coworkers have explored how subtle changes can be probed in nearly indistinguishable intramolecular chemical environments.[625]

In a nutshell, real-time propagation of the reduced single-particle density matrix, driven by external fields, allows for the simulation of multidimensional nonlinear signals in a non-perturbative manner, beyond perturbative response-based SOS methods. In addition, complex ultrafast nonlinear dynamics can also be simulated sufficiently accurately.

4.6. Spin and Magnetization Dynamics

Model Hamiltonians parametrized by experimental or empirical data have historically been the method of choice for modeling spin dynamics. These methods have succeeded in describing fundamental spin physics, but they are incapable of simulating the time-evolution of the spin-dependent wave function or density matrix. A fully time-dependent first-principles electronic structure description is needed to simulate spin dynamics driven by strong spin noncollinearity, spin−orbit coupling, or by interactions with intense external electromagnetic fields. In 2014, Ding et al. reported the first fully *ab initio* real-time treatment of spin dynamics driven by an external magnetic field using a noncollinear two-component method.[68] The one-electron Pauli Hamiltonian including magnetic field effects can be expressed as

$$h^{\text{Pauli}} = \hat{h}_0(\mathbf{r}) + \frac{1}{2}(\boldsymbol{\sigma} - i\mathbf{r}\times\nabla)\cdot\mathbf{B} + \frac{1}{8}(\mathbf{B}\times\mathbf{r})^2 \tag{68}$$

where $\hat{h}_0(\mathbf{r})$ is the one-electron Hamiltonian in the absence of the external field. The second term accounts for spin and orbital Zeeman interactions, and the third term, which is quadratic in the strength of magnetic field, is the diamagnetic contribution. Figure 21 shows that, with this treatment, the magnetization of each spin precesses about the magnetic field at each lattice point.

Although the orbital Zeeman and the diamagnetic terms are relatively small and do not directly affect the spin dynamics, they play an important role in diamagnetism, especially in the presence of a strong magnetic field.[68,626−630] In the initial work by Ding, only the spin Zeeman term was considered in the spin-blocked core Hamiltonian in a real-time nonrelativistic two-component framework,

$$h' = \begin{pmatrix} h'^{\alpha\alpha} & h'^{\alpha\beta} \\ h'^{\beta\alpha} & h'^{\beta\beta} \end{pmatrix} = \begin{pmatrix} h'_0 + \frac{1}{2}B_z\mathbf{S} & \frac{1}{2}(B_x - iB_y)\mathbf{S} \\ \frac{1}{2}(B_x + iB_y)\mathbf{S} & h'_0 - \frac{1}{2}B_z\mathbf{S} \end{pmatrix} \tag{69}$$

The orbital Zeeman and the diamagnetic contribution were later included by Sun et al. in the two-component Hartree−Fock approach using the Pauli matrix representation.[631]

The nonrelativistic spin-field coupling developed in refs 68 and 631 relaxes the standard spin constraints, allowing electrons to respond to external magnetic fields. However, the extension of real-time methods to the relativistic Dirac equation is critical for accurate treatment of spin and magnetization dynamics of transition metal and heavy element complexes. Spin−spin and spin−orbit couplings, which can connect different spin states, cause spin-forbidden processes to become weakly allowed, leading to features in electronic absorption spectra that are absent in nonrelativistic treatments. For example, the ns^2 to ns^1np^1 transitions of group 12 atoms have been studied using relativistic RT-TDDFT at both the four-component and two-component levels of theory.[70,100] The $^3P_1$ state is weakly allowed by the presence of the spin−orbit coupling operator and a nonzero transition moment is observed. This effect becomes more important moving down the periodic table from Zn to Cd to Hg, as the magnitude of the relativistic corrections grows more prominent.

4.7. Electronic Circular Dichroism and Magnetic Circular Dichroism

Electronic circular dichroism (ECD) models the differential absorption of left- and right-handed circularly polarized light, providing a useful tool for determining the absolute configuration of chiral enantiomers.[632] RT-TDDFT has been developed for computing ECD spectra of molecules using grid-based[89,90] and atomic-orbital-based[92] simulation protocols. The ECD signal is determined by the isotropic rotatory strength for the transition between states $|\psi_n\rangle$ and $|\psi_j\rangle$, which is given by[632]

$$R_{jn} \equiv \text{Tr}[\text{Im}(\langle\psi_n|\boldsymbol{\mu}|\psi_j\rangle\langle\psi_j|\mathbf{m}|\psi_n\rangle)] \tag{70}$$

where $\boldsymbol{\mu} = \mathbf{r}$ and $\mathbf{m} = \frac{-i}{2c}(\mathbf{r}\times\nabla)$ are the electric dipole and magnetic dipole operators, respectively (in the length gauge), and c is the speed of light.

The most common methods for computing the ECD spectrum are based on the response formalism,[633−642] or the complex polarization propagator technique.[643,644] In the time domain, if an electric dipole field is applied as a perturbation, the time-dependent magnetic dipole obtained from the electronic dynamics is required for simulating ECD. The Fourier transform of the time-dependent magnetic dipole gives the rotatory strength (eq 70)[89,92] as

$$R(\omega) = \sum_{j\neq n}\delta(\omega - \omega_{jn})R_{jn} = \text{Tr}\left[\frac{1}{\pi}\text{Re}\frac{m_\alpha(\omega)}{\kappa_\beta}\right] \tag{71}$$

where κ is the magnitude of the electric field, and the labels α and β denote Cartesian coordinates. LR and RT-TDDFT methods have been shown to give essentially the same results in the weak field limit (e.g., Figure 22), though RT-TDDFT is able to compute the whole ECD band spectrum with only three simulations of the electron dynamics.

The moment-based TD-EOM-CC approach[22,49] described in Section 2.4 is applicable to any type of linear electronic spectroscopy, including ECD.[52] In this formalism, the ECD spectrum can be extracted from the Fourier transform of the electric-dipole−magnetic-dipole and magnetic-dipole−electric-dipole correlation functions (for specific expressions, the reader is referred to ref 52.). One important distinction between the evaluation of linear absorption and ECD spectra at the TD-EOM-CC level of theory is that, in the latter case, the computational effort is doubled, as both the electric-dipole−magnetic-dipole and magnetic-dipole−electric-dipole correlation functions must be evaluated. This complication arises

https://dx.doi.org/10.1021/acs.chemrev.0c00223
Chem. Rev. XXXX, XXX, XXX−XXX

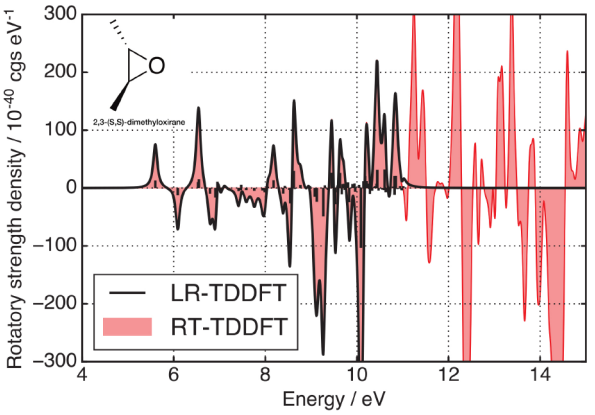

Figure 22. ECD spectra of 2,3-(*S*,*S*)-dimethyloxirane (DMO) computed at the PBEPBE/6-311+G** level of theory. Adapted with permission from ref 92. Copyright (2016) American Institute of Physics.

because the similarity-transformation of the Hamiltonian and other operators destroys their hermiticity. For spectroscopies like ECD that are defined by multiple operators (i.e., the electric and magnetic dipole operators), it is common[645] to restore symmetry properties of the transition amplitudes through an average. In this way, the rotatory strengths defined by eq 70 would become

$$R_{jn} \equiv \frac{1}{2}(\mathrm{Tr}[\mathrm{Im}(\langle\psi_n|\boldsymbol{\mu}|\psi_j\rangle\langle\psi_j|\boldsymbol{m}|\psi_n\rangle)] + \mathrm{Tr}[\mathrm{Im}(\langle\psi_n|\boldsymbol{m}|\psi_j\rangle\langle\psi_j|\boldsymbol{\mu}|\psi_n\rangle)]) \tag{72}$$

As in the case of linear absorption spectra, ECD spectra generated via TD-EOM-CC are numerically indistinguishable from those generated by conventional EOM-CC approaches, in the limit that all roots are computed in the conventional calculation. Further, because real-time simulations yield broad-band spectra, one can easily quantify the degree to which TD-EOM-CC violates the Condon sum rule,[646] which states that the sum of all rotatory strengths from a given initial state should equal zero. In other words, the integrated area under a TD-EOM-CC-derived ECD spectrum should vanish. The analysis presented in ref 52. suggests that deviations from this rule are gauge dependent and are significantly more severe in the velocity-gauge than in the length-gauge.

In magnetic circular dichroism (MCD) experiments, an external static magnetic field is applied in addition to the circularly polarized probing light. The magnetic field breaks the spin and orbital degeneracies through the couplings of spin and orbital angular momenta to the field. As a result, the optical selection rules are modified, giving rise to additional spectroscopic features that are otherwise inaccessible at zero field.[647] Although the simulation of an ECD spectrum only needs to treat electric field perturbations, both static magnetic and probing electric fields are necessary for simulating MCD. Various perturbative approaches to simulate magnetic field effects have been used with electronic structure methods for computing MCD spectra,[648−664] however they are not applicable to the real-time formalism, which requires a variational treatment of all external perturbations. This is particularly challenging for time-dependent electronic structure simulations using atomic orbitals; in the presence of electromagnetic fields, physical observables depend on the origin of the electromagnetic field.[615,665−671]

The MCD strength of excited state $|\psi_j\rangle$ can be defined as

$$R_j = -\frac{1}{3\mu_B|\mathbf{B}|}\sum_{\alpha\beta\gamma}\epsilon_{\alpha\beta\gamma}\mathrm{Im}[\langle\psi_0|\mu_\alpha|\psi_j\rangle^\gamma\langle\psi_j|\mu_\beta|\psi_0\rangle^\gamma] \tag{73}$$

where **B** is the external magnetic field, μ_B is Bohr magneton, and $\epsilon_{\alpha\beta\gamma}$ is Levi−Civita symbol ($\epsilon_{xyz} = \epsilon_{yzx} = \epsilon_{zxy} = 1$, $\epsilon_{yxz} = \epsilon_{xzy} = \epsilon_{zyx} = -1$, otherwise 0). The superscript γ explicitly denotes the direction of the applied magnetic field. The MCD strength function eq 73 requires the computation of the imaginary component of the quantity $\langle\psi_0|\mu_\alpha|\psi_j\rangle^\gamma\langle\psi_j|\mu_\beta|\psi_0\rangle^\gamma$ from time-dependent electronic structure methods. However, this quantity cannot be easily extracted from Fourier transformation of time-dependent observables. Bertsch et al.[91] expanded eq 73 in the power of electric field perturbation and obtained the following working expression for computing MCD spectra using real-time methods

$$R_j = \frac{1}{6\pi|\mathbf{B}|}\sum_{\alpha\beta\gamma}\varepsilon_{\alpha\beta\gamma}\mathrm{Re}\left(\frac{\mu_\alpha^\gamma}{\kappa^\beta} - \frac{\mu_\beta^\gamma}{\kappa^\alpha}\right) \tag{74}$$

Li and coworkers later derived the same expression based on a close connection between the real-time signal and the response function formalism, which leads to a more generalized approach to compute any type of spectrum.[94]

Bertsch and coworkers included the orbital Zeeman term in the electronic Hamiltonian using a real-space local density approximation (LDA) to simulate effective A and B terms of MCD spectra.[91] More recently, Li and coworkers developed a RT-TDDFT approach to MCD that was generalized to hybrid GGA and included a variational treatment of the static magnetic perturbation.[94] That work demonstrated that, when simulating MCD, the most satisfactory solution to the gauge-origin problem arising from the use of an incomplete Gaussian-type basis[615,665−671] is to variationally include the effects of a uniform magnetic field with London orbitals.[631,640,664,672−678]

4.8. Electron Dynamics in Strong Fields

Interactions of molecules with intense laser pulses can result in a number of nonperturbative electronic phenomena involving ionization of electron(s).[679] These can be loosely categorized by the Keldysh adiabaticity parameter $\gamma = \frac{\omega\sqrt{2E_i}}{F}$, where E_i is the ionization potential of the molecule, and ω and F are the field frequencies and amplitudes, respectively. In the limit of high photon energy and low intensity (Keldysh $\gamma \gg 1$), multiphoton ionization dominates where multiple photons are absorbed. High intensity and low frequency fields ($\gamma \ll 1$) result in tunnel barrier-suppression, and above-threshold ionization where the electron escape through or above the Coulomb potential confining the electron to the parent molecule. Molecular strong-field ionization can depend strongly on the geometry of the molecule (e.g., charge resonance enhance ionization), as well as the light polarization with respect to the molecule. Because strong laser pulses produce electric fields comparable to those experienced by valence electrons in a molecule, simulating these phenomena requires a description of time-dependent electronic structure beyond the perturbation limit. In the strong-field regime, real-time techniques are particularly advantageous as they can explicitly simulate the nonperturbative electronic response to strong electric fields, such charge redistribution, multiphoton absorption, high-harmonic generation, strong-field ionization, photoelectron spectroscopy, and shape and Feshbach resonances.[34,76,101,109,112,113,384,612,680−683]

https://dx.doi.org/10.1021/acs.chemrev.0c00223
Chem. Rev. XXXX, XXX, XXX−XXX

Simulations of strong-field dynamics can be challenging for real-time methods, as these require a description of the wave function or density far from the molecule. Typically this is achieved with grid-based methods using a combination of a large simulation box along with some way of reducing spurious reflections from the edges of the box. These include: complex absorbing potentials (CAPs) to remove outgoing electron flux,[41,120,589,684−686] exterior complex scaling,[687−689] or masks that link an inner region (e.g., TDDFT) to an outer region solved using known basis states (e.g., free electron in field).[690,691] Although less commonly done, strong-field ionization can also be described using atomic-centered basis sets, which have the advantage of allowing wave function methods and hybrid TDDFT, but require either additional bases for the continuum (e.g., B-splines[692,693]) or careful choice of CAPs. Because it is most relevant to real-time electronic structure methods discussed in this Review, we now focus on the case of atom-centered basis sets with CAPs.

A typical CAP consists of an imaginary, position-dependent potential, which is added to the time-dependent Hamiltonian:

$$\hat{H}(\mathbf{r}, t) = \hat{H}_0(\mathbf{r}, t) - i\Gamma(\mathbf{r}) \tag{75}$$

Here, $\hat{H}_0$ $(\mathbf{r},t)$ is the Hamiltonian without the CAP and Γ (t) is a spatial potential that is zero around the molecule and smoothly increases at the boundary of the simulation. For the purposes of strong-field ionization (SFI), the results should not depend on the specific functional form of the CAP, nor its magnitude or location from the molecule, provided reflections are minimized. In most cases, smoothly increasing functions (e.g., sigmoidal) are used.[112,589,682,685] Formally, this Hamiltonian is non-Hermitian which requires propagating the left $\langle\psi_L(t)|$ and right $|\psi_R(t)\rangle$ eigenvectors independently, with C-products used to compute the expectation values: $\langle A(t)\rangle = \langle\psi_L(t)|\hat{A}|\psi_R(t)\rangle$.[694] Generally, however, the standard equations of motion (eq 43) and expectation values can be used, as well as the (Hermitian) ground state computed via an SCF without the CAP. This approximation is valid when the CAP has negligible effect on the bound states.

Construction of a CAP in a grid or planewave basis is straightforward, as Γ $(\mathbf{r})$ is simply a local one-body potential. When using atom-centered basis sets, however, this requires projection onto the atomic orbitals,

$$\Gamma_{\mu\nu} = \langle\mu|\Gamma(\mathbf{r})|\nu\rangle = \int d\mathbf{r}\phi_\mu^*(\mathbf{r})\Gamma(\mathbf{r})\phi_\nu(\mathbf{r}) \tag{76}$$

These integrals can be performed either over the Cartesian or atom-centered grids. Using CAPs with atom-centered basis sets requires highly diffuse functions to describe the wave function far from the molecule.[112,113,681,682] The limited spatial extent of these bases also limits the range of the valid CAP positions, as a CAP too close to the molecule will affect the bound states, while too far results in an insufficient overlap of the basis with the CAP. If chosen correctly, simulations with a CAP will not affect the electron density near the molecule yet outgoing flux will be removed completely. Put another way, the eigenvalues for the bound states (occupied and virtual) should be unaffected by the CAP, whereas the unbound states acquire lifetimes. A CAP that is too "weak" or misplaced might not remove all outgoing charge, causing artificial reflections from the simulation box, whereas, conversely, a sharply shaped CAP might cause reflections from the potential itself. The protocol to choose the CAP location and strength is to determine a range of parameters where the results are insensitive. See Figure 23 for an example.

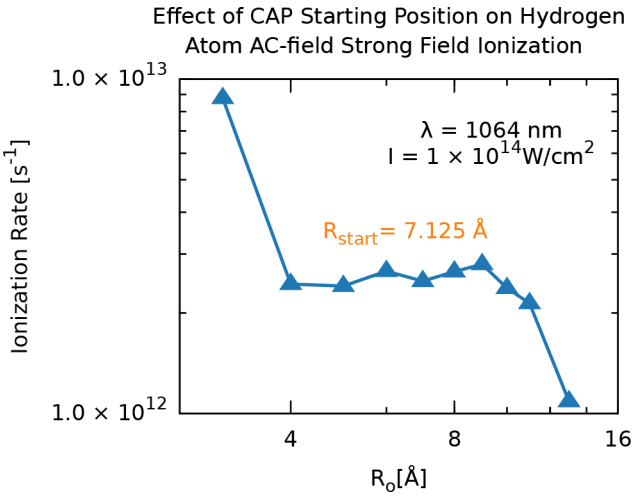

Figure 23. Strong-field ionization rates computed using an atomic orbital basis as a function of CAP starting distance R_0 for a hydrogen atom under 1064 nm light with intensity 1×10^{14} W/cm^2. The rates are overestimated for smaller R_0 values due to the CAP affecting the ground state. The rates are underestimated at large R_0 due to insufficient overlap with the basis. The rates are insensitive between 4.0 and 9.0 Å, giving results in quantitative agreement with grid-based methods. Adapted with permission from ref 682. Copyright (2016) American Institute of Physics.

Once a CAP has been chosen, experimental observables such as the SFI yield for a particular laser polarization and intensity can be computed from the change in the electronic norm. Weaker intensities can also be challenging for atom-centered basis sets, as they require CAPs far from the molecule to capture the tunnelling correctly. Additionally, basis set CAP calculations are "leaky" due to small amounts of norm being lost due to nonzero overlap with the ground state. This must be corrected for by subtracting this linear leakage rate from the computed time-dependent norm.[682,683] Using TDCIS with CAPs, Schlegel and coworkers successfully mapped out the angular dependence of the ionization rates for small molecules in strong fields (see Figure 24).[112,113,681] These simulations shed light on the orbitals involved in strong-field ionization as well as the localization of the hole in the molecule.[683,695] When using TDDFT, the use of range-separated functionals has been shown to give significant improvements over traditional TDDFT, due to their correct long-range asymptotic potential and reduced self-interaction.[682]

5. OUTLOOK

Real-time electronic structure methods provide an unprecedented view of electron dynamics on the atto- and femtosecond time scales with vast potential to yield new insights into the electronic behavior of molecules and materials. With recent development of accurate real-time post-SCF methods, advanced DFT functional forms,[696−698] and full quantum descriptions of the electrons and nuclei,[514,699,700] real-time simulations have become more accurate and have the capability of simulating ultrafast multidimensional spectroscopies and quantum dynamics in the presence of a strong electromagnetic field, in the relativistic regime, and in the quantum electrodynamics formalism.

https://dx.doi.org/10.1021/acs.chemrev.0c00223
Chem. Rev. XXXX, XXX, XXX−XXX

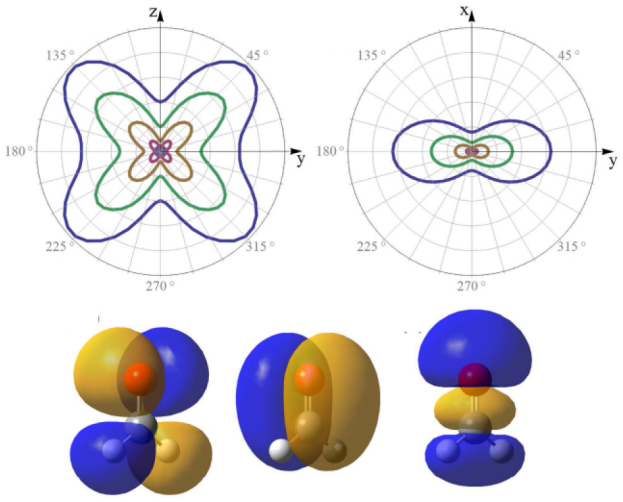

Figure 24. Angle dependence of the ionization yield for CH_2O calculated with the TDCIS-CAP approach: (Top Panel) polar plots, in plane with and perpendicular to the molecular axis, for field strengths of 0.04, 0.05, 0.06, 0.07, and 0.08 E_h/ea_0. (Bottom Panel) Dyson orbitals for the $^2B_2$, $^2B_1$, and $^2A_1$ states. Adapted with permission from ref 113. Copyright (2015) American Chemical Society.

The current prospect of universal quantum computing[701,702] provides an exciting new tool for the simulation of quantum dynamics because quantum computers obey the time-dependent Schrödinger equation by nature. Modeling time-dependent electronic dynamics in molecules and extracting information for the purpose of applications such as spectroscopy is relatively unexplored with regard to quantum algorithms. The next generation of real-time methods will encompass innovations in applied mathematics bolstered by high-performance software and/or quantum computing algorithms. The ever-improving computational efficiency of real-time methods will allow the simulation of the electron dynamics of larger scale and more complex systems, bringing chemical insight into dynamical processes with experimentally relevant spatial and time resolutions.

AUTHOR INFORMATION

Corresponding Authors

Xiaosong Li − *Department of Chemistry, University of Washington, Seattle, Washington 98195-1700, United States;* orcid.org/0000-0001-7341-6240; Email: xsli@uw.edu

Niranjan Govind − *Physical and Computational Sciences Directorate, Pacific Northwest National Laboratory, Richland, Washington 99354, United States;* orcid.org/0000-0003-3625-366X; Email: niri.govind@pnnl.gov

Christine Isborn − *Department of Chemistry and Chemical Biology, University of California, Merced, California 95343, United States;* orcid.org/0000-0002-4905-9113; Email: cisborn@ucmerced.edu

A. Eugene DePrince, III − *Department of Chemistry and Biochemistry, Florida State University, Tallahassee, Florida 32306-4390, United States;* orcid.org/0000-0003-1061-2521; Email: deprince@chem.fsu.edu

Kenneth Lopata − *Department of Chemistry, Louisiana State University, Baton Rouge, Louisiana 70803, United States;* orcid.org/0000-0002-9141-684X; Email: klopata@lsu.edu

Complete contact information is available at: https://pubs.acs.org/10.1021/acs.chemrev.0c00223

Notes

The authors declare no competing financial interest.

Biographies

Xiaosong Li earned a B.S. Chemistry from the University of Science and Technology of China in 1999 and a Ph.D. in Theoretical Chemistry from Wayne State University in 2003. Following a postdoctoral training at Yale University, he joined the University of Washington as Assistant Professor in the fall of 2005. He was promoted to Associate Professor in 2011 and to Full Professor in 2015. Currently, he is the Harry and Catherine Jaynne Boand Endowed Professor and Associate Chair of Chemistry at the University of Washington. His research focuses on developing and applying time-dependent relativistic and nonrelativistic electronic structure theories for studying excited state chemical processes that underpin energy conversion, photocatalysis, and ultrafast spectroscopies. In addition to his work at University of Washington, he is an Associate Editor of Chemical Physics Reviews, American Institute of Physics.

Niranjan Govind earned a Ph.D. in Physics from McGill University, followed by a postdoc from 1997−2000 at the Department of Chemistry at the University of California, Los Angeles. From 2000−2007, he was a staff scientist at Accelrys, Inc. in San Diego. He joined the Pacific Northwest National Laboratory (PNNL) in 2007 and has been a Chief Scientist since 2015. His research interests focus on the development and application of time-dependent electronic structure methods for molecules and materials, relativistic electronic structure methods, X-ray spectroscopies, and ultrafast dynamics. In addition to his position at PNNL, he serves on the Editorial Board of Electronic Structure, IOPScience, UK.

Christine Isborn earned her B.S. in Chemistry and Physics at the University of San Francisco and her Ph.D. in Chemistry at the University of Washington, Seattle. After postdoctoral training at Stanford University, she started as an Assistant Professor at the University of California in Merced in 2012 and was promoted to Associate Professor in 2019. Her research interests involve developing methods for optical spectroscopy, understanding how molecules interact with light, and how molecular environments, such as solvent, ions, or interfaces, tune this light−matter interaction.

Eugene DePrince received his B.S. in Chemistry from the University of Tennessee at Knoxville (2005), followed by his Ph.D. from the University of Chicago (2009). He held postdoctoral appointments at Argonne National Laboratory (2010−2011) and Georgia Institute of Technology (2011−2013) and began his independent research career as an Assistant Professor in the Department of Chemistry & Biochemistry at Florida State University in 2013. He was promoted to Associate Professor in 2018. His research interests include the development application of reduced-density-matrix-based electronic structure methods for describing strongly correlated molecular systems as well as the development of time-dependent many-body methods.

Kenneth Lopata earned a B.S. in Chemical Physics from the University of Toronto in 2004 and a Ph.D. in Chemistry from the University of California, Los Angeles in 2010. Between 2010 and 2013, he held the Wiley Postdoctoral Fellowship at Pacific Northwest National Laboratory. He subsequently joined Louisiana State University as an Assistant Professor in 2013 and was promoted to Associate Professor in 2019. His research interests focus on developing and applying time-dependent quantum chemistry methods to simulate the attosecond motion of electrons in molecules and materials during and immediately following interaction with intense and/or high energy laser pulses.

https://dx.doi.org/10.1021/acs.chemrev.0c00223
Chem. Rev. XXXX, XXX, XXX−XXX

ACKNOWLEDGMENTS

X.L. acknowledges support from the U.S. Department of Energy, Office of Science, Basic Energy Sciences, in the Computational and Theoretical Chemistry program under Award DE-SC0006863 for the development of the first-principles electronic dynamics and relativistic TDDFT. The development of linear response TDDFT method for computational spectroscopy was supported by the National Science Foundation (CHE-1856210 to X.L.). The development of the open source software package is supported by the National Science Foundation (OAC-1663636 to X.L. and A.E.D.). The computational study of interfacial charge transfer was supported by IDREAM (Interfacial Dynamics in Radioactive Environments and Materials), an Energy Frontier Research Center funded by the U.S. Department of Energy (DOE), Office of Science, Basic Energy Sciences (BES). Computational L-edge spectroscopy is partially supported by the U.S. Department of Energy, Office of Science, Office of Basic Energy Sciences, Division of Chemical Sciences, Geosciences and Biosciences, through Argonne National Laboratory under Contract DE-AC02-06CH11357. N.G. and X.L. acknowledge support from the Computational Chemical Sciences (CCS) Program of the U.S. Department of Energy, Office of Science, Basic Energy Sciences, Chemical Sciences, Geosciences and Biosciences Division in the Center for Scalable and Predictive methods for Excitations and Correlated phenomena (SPEC) at the Pacific Northwest National Laboratory. N.G. also acknowledges support by the U.S. Department of Energy, Office of Science, Office of Advanced Scientific Computing Research, Scientific Discovery through Advanced Computing (SciDAC) program (2013-2017) under Award KC-030102062653 (Charge Transfer and Charge Transport in Photoactivated Systems), a University of Minnesota/LBNL/PNNL partnership, under which portions of the research were initiated. C.I. is supported by the U.S. Department of Energy, Office of Science, Basic Energy Sciences, in the Computational and Theoretical Chemistry (CTC) and Condensed Phase and Interfacial Molecular Science (CPIMS) programs, under Award DE-SC0019053, for improved methods for modeling functional transition metal compounds in complex environments: ground states, excited states, and spectroscopies and in the CTC program, under Award DE-SC0020203, for developing new models of charge transfer, nonadiabatic dynamics, and nonlinear spectroscopy. A.E.D. acknowledges support from the National Science Foundation under Grant CHE-1554354 for the development of time-dependent equation of motion coupled-cluster methods for X-ray absorption spectroscopy. K.L. acknowledges support from the U.S. Department of Energy, Office of Science, Basic Energy Sciences, Atomic, Molecular and Optical Sciences program under Award DE-SC0017868 for simulations of X-ray absorption spectroscopy, and the U.S. Department of Energy, Office of Science, Basic Energy Sciences, under Award DE-SC0012462 for charge migration and strong-field electron dynamics. This work benefited from computational resources provided by EMSL, a Department of Energy, Office of Science User Facility sponsored by the Office of Biological and Environmental Research and located at the Pacific Northwest National Laboratory (PNNL) and PNNL Institutional Computing (PIC). PNNL is operated by Battelle Memorial Institute for the United States Department of Energy under DOE Contract DE-AC05-76RL1830. Portions of this research were conducted with HPC resources provided by Louisiana State University, the Louisiana Optical Network, and the MERCED computational resources supported by the NSF MRI Program (Grant ACI-1429783). The research also benefited from resources provided by the National Energy Research Scientific Computing Center (NERSC), a Department of Energy, Office of Science User Facility supported by the Office of Science of the U.S. Department of Energy under Contract DE-AC02-05CH11231.

REFERENCES

(1) Koonin, S. E.; Davies, K. T. R.; Maruhn-Rezwani, V.; Feldmeier, H.; Krieger, S. J.; Negele, J. W. Time-dependent Hartree-Fock Calculations for $^{16}O + ^{16}O$ and $^{40}Ca + ^{40}Ca$ reactions. *Phys. Rev. C: Nucl. Phys.* **1977**, *15*, 1359−1374.

(2) Flocard, H.; Koonin, S. E.; Weiss, M. S. Three-dimensional Time-dependent Hartree-Fock Calculations: Application to $^{16}O + ^{16}O$ collisions. *Phys. Rev. C: Nucl. Phys.* **1978**, *17*, 1682−1699.

(3) Davies, K. T. R.; Devi, K. R. S.; Strayer, M. R. Time-Dependent Hartree-Fock Fusion Calculations for $^{86}Kr + ^{139}La$ and $^{84}Kr + ^{209}Bi$ Collisions. *Phys. Rev. Lett.* **1980**, *44*, 23−26.

(4) Devi, K. R. S.; Koonin, S. E. Mean-Field Approximation to p + He Scattering. *Phys. Rev. Lett.* **1981**, *47*, 27−30.

(5) Kulander, K. C.; Devi, K. R. S.; Koonin, S. E. Time-dependent Hartree-Fock Theory of Charge Exchange: Application to He^{2+} + He. *Phys. Rev. A: At., Mol., Opt. Phys.* **1982**, *25*, 2968−2975.

(6) Meyer, H.-D.; Manthe, U.; Cederbaum, L. S. The Multi-configurational Time-dependent Hartree Approach. *Chem. Phys. Lett.* **1990**, *165*, 73−78.

(7) Micha, D. A.; Runge, K. Time-dependent Many-electron Approach to Slow Ion-atom Collisions: The Coupling of Electronic and Nuclear Motions. *Phys. Rev. A: At., Mol., Opt. Phys.* **1994**, *50*, 322−336.

(8) Yabana, K.; Bertsch, G. F. Time-dependent Local-density Approximation in Real Time. *Phys. Rev. B: Condens. Matter Mater. Phys.* **1996**, *54*, 4484−4487.

(9) Yabana, K.; Bertsch, G. Optical Response of Small Carbon Clusters. *Z. Phys. D: At., Mol. Clusters* **1997**, *42*, 219−225.

(10) Yabana, K.; Bertsch, G. F. Time-dependent Local-density Approximation in Real Time: Application to Conjugated Molecules. *Int. J. Quantum Chem.* **1999**, *75*, 55−66.

(11) Bertsch, G. F.; Iwata, J.-I.; Rubio, A.; Yabana, K. Real-space, Real-time Method for the Dielectric Function. *Phys. Rev. B: Condens. Matter Mater. Phys.* **2000**, *62*, 7998−8002.

(12) Marques, M. A.; Castro, A.; Bertsch, G. F.; Rubio, A. Octopus: a First-principles Tool for Excited Electron-ion Dynamics. *Comput. Phys. Commun.* **2003**, *151*, 60−78.

(13) Castro, A.; Appel, H.; Oliveira, M.; Rozzi, C. A.; Andrade, X.; Lorenzen, F.; Marques, M. A. L.; Gross, E. K. U.; Rubio, A. Octopus: a Tool for the Application of Time-dependent Density Functional Theory. *Phys. Status Solidi B* **2006**, *243*, 2465−2488.

(14) Takimoto, Y.; Vila, F.; Rehr, J. Real-time Time-dependent Density Functional Theory Approach for Frequency-dependent Nonlinear Optical Response in Photonic Molecules. *J. Chem. Phys.* **2007**, *127*, 154114.

(15) Li, X.; Smith, S. M.; Markevitch, A. N.; Romanov, D. A.; Levis, R. J.; Schlegel, H. B. A Time-Dependent Hartree-Fock Approach for Studying the Electronic Optical Response of Molecules in Intense Fields. *Phys. Chem. Chem. Phys.* **2005**, *7*, 233−239.

(16) Isborn, C. M.; Li, X.; Tully, J. C. TDDFT Ehrenfest Dynamics: Collisions between Atomic Oxygen and Graphite Clusters. *J. Chem. Phys.* **2007**, *126*, 134307.

(17) Eshuis, H.; Balint-Kurti, G. G.; Manby, F. R. Dynamics of Molecules in Strong Oscillating Electric Fields using Time-Dependent Hartree−Fock Theory. *J. Chem. Phys.* **2008**, *128*, 114113.

(18) Lopata, K.; Govind, N. Modeling Fast Electron Dynamics with Real-time Time-dependent Density Functional Theory: Application to Small Molecules and Chromophores. *J. Chem. Theory Comput.* **2011**, *7*, 1344−1355.

https://dx.doi.org/10.1021/acs.chemrev.0c00223
Chem. Rev. XXXX, XXX, XXX−XXX

(19) Gao, B.; Ruud, K.; Luo, Y. Plasmon Resonances in Linear Noble-Metal Chains. *J. Chem. Phys.* **2012**, *137*, 194307.
(20) Nguyen, T. S.; Parkhill, J. Nonadiabatic Dynamics for Electrons at Second-Order: Real-Time TDDFT and OSCF2. *J. Chem. Theory Comput.* **2015**, *11*, 2918−2924.
(21) Zhu, Y.; Herbert, J. M. Self-consistent Predictor/Corrector Algorithms for Stable and Efficient Integration of the Time-Dependent Kohn-Sham Equation. *J. Chem. Phys.* **2018**, *148*, 044117.
(22) Nascimento, D. R.; DePrince, A. E., III Linear Absorption Spectra from Explicitly Time-Dependent Equation-of-Motion Coupled-Cluster Theory. *J. Chem. Theory Comput.* **2016**, *12*, 5834−5840.
(23) Maliyov, I.; Crocombette, J.-P.; Bruneval, F. Electronic Stopping Power from Time-Dependent Density-Functional Theory in Gaussian Basis. *Eur. Phys. J. B* **2018**, *91*, 172.
(24) Schleife, A.; Draeger, E. W.; Kanai, Y.; Correa, A. A. Plane-wave Pseudopotential Implementation of Explicit Integrators for Time-dependent Kohn-Sham Equations in Large-scale Simulations. *J. Chem. Phys.* **2012**, *137*, 22A546.
(25) Andrade, X.; Alberdi-Rodriguez, J.; Strubbe, D. A.; Oliveira, M. J. T.; Nogueira, F.; Castro, A.; Muguerza, J.; Arruabarrena, A.; Louie, S. G.; Aspuru-Guzik, A.; Rubio, A.; Marques, M. A. L. Time-dependent Density-functional Theory in Massively Parallel Computer Architectures: the Octopus Project. *J. Phys.: Condens. Matter* **2012**, *24*, 233202.
(26) Andermatt, S.; Cha, J.; Schiffmann, F.; VandeVondele, J. Combining Linear-Scaling DFT with Subsystem DFT in Born−Oppenheimer and Ehrenfest Molecular Dynamics Simulations: from Molecules to a Virus in Solution. *J. Chem. Theory Comput.* **2016**, *12*, 3214−3227.
(27) Walter, M.; Häkkinen, H.; Lehtovaara, L.; Puska, M.; Enkovaara, J.; Rostgaard, C.; Mortensen, J. J. Time-Dependent Density-Functional Theory in the Projector Augmented-Wave Method. *J. Chem. Phys.* **2008**, *128*, 244101.
(28) Sato, T.; Ishikawa, K. L. Time-dependent Complete-active-space Self-consistent-field Method for Multielectron Dynamics in Intense Laser Fields. *Phys. Rev. A: At., Mol., Opt. Phys.* **2013**, *88*, 023402.
(29) Miyagi, H.; Madsen, L. B. Time-dependent Restricted-active-space Self-consistent-field Theory for Laser-driven Many-electron Dynamics. *Phys. Rev. A: At., Mol., Opt. Phys.* **2013**, *87*, 062511.
(30) Miyagi, H.; Madsen, L. B. Time-dependent Restricted-active-space Self-consistent-field Theory for Laser-driven Many-electron Dynamics. II. Extended Formulation and Numerical Analysis. *Phys. Rev. A: At., Mol., Opt. Phys.* **2014**, *89*, 063416.
(31) Sato, T.; Ishikawa, K. L. Time-dependent Multiconfiguration Self-consistent-field Method Based on the Occupation-restricted Multiple-active-space Model for Multielectron Dynamics in Intense Laser Fields. *Phys. Rev. A: At., Mol., Opt. Phys.* **2015**, *91*, 023417.
(32) Liu, H.; Jenkins, A. J.; Wildman, A.; Frisch, M. J.; Lipparini, F.; Mennucci, B.; Li, X. Time-Dependent Complete Active Space Embedded in a Polarizable Force Field. *J. Chem. Theory Comput.* **2019**, *15*, 1633−1641.
(33) Krause, P.; Klamroth, T.; Saalfrank, P. Time-dependent Configuration-interaction Calculations of Laser-pulse-driven Many-electron Dynamics: Controlled Dipole Switching in Lithium Cyanide. *J. Chem. Phys.* **2005**, *123*, 074105.
(34) Schlegel, H. B.; Smith, S. M.; Li, X. Electronic Optical Response of Molecules in Intense Fields: Comparison of TD-HF, TD-CIS, and TD-CIS(D) Approaches. *J. Chem. Phys.* **2007**, *126*, 244110.
(35) Sonk, J. A.; Caricato, M.; Schlegel, H. B. TD-CI Simulation of the Electronic Optical Response of Molecules in Intense Fields: Comparison of RPA, CIS, CIS(D), and EOM-CCSD. *J. Phys. Chem. A* **2011**, *115*, 4678−4690.
(36) DePrince, A. E.; Pelton, M.; Guest, J. R.; Gray, S. K. Emergence of Excited-State Plasmon Modes in Linear Hydrogen Chains from Time-Dependent Quantum Mechanical Methods. *Phys. Rev. Lett.* **2011**, *107*, 196806.
(37) Luppi, E.; Head-Gordon, M. Computation of High-harmonic Generation Spectra of H_2 and N_2 in Intense Laser Pulses using Quantum Chemistry Methods and Time-dependent Density Functional Theory. *Mol. Phys.* **2012**, *110*, 909−923.
(38) Lestrange, P. J.; Hoffmann, M. R.; Li, X. Time-Dependent Configuration Interaction using the Graphical Unitary Group Approach: Nonlinear Electric Properties. *Adv. Quantum Chem.* **2018**, *76*, 295−313.
(39) Ulusoy, I. S.; Stewart, Z.; Wilson, A. K. The Role of the CI Expansion Length in Time-Dependent Studies. *J. Chem. Phys.* **2018**, *148*, 014107.
(40) Cederbaum, L. S.; Zobeley, J. Ultrafast Charge Migration by Electron Correlation. *Chem. Phys. Lett.* **1999**, *307*, 205−210.
(41) Santra, R.; Cederbaum, L. S. Complex Absorbing Potentials in the Framework of Electron Propagator Theory. I. General Formalism. *J. Chem. Phys.* **2002**, *117*, 5511−5521.
(42) Feuerbacher, S.; Sommerfeld, T.; Santra, R.; Cederbaum, L. S. Complex Absorbing Potentials in the Framework of Electron Propagator Theory. II. Application to Temporary Anions. *J. Chem. Phys.* **2003**, *118*, 6188−6199.
(43) Kuleff, A. I.; Cederbaum, L. S. Tracing Ultrafast Interatomic Electronic Decay Processes in Real Time and Space. *Phys. Rev. Lett.* **2007**, *98*, 083201.
(44) Dutoi, A. D.; Cederbaum, L. S.; Wormit, M.; Starcke, J. H.; Dreuw, A. Tracing Molecular Electronic Excitation Dynamics in Real Time and Space. *J. Chem. Phys.* **2010**, *132*, 144302.
(45) Kuleff, A. I.; Cederbaum, L. S. Ultrafast Correlation-driven Electron Dynamics. *J. Phys. B: At., Mol. Opt. Phys.* **2014**, *47*, 124002.
(46) Neville, S. P.; Schuurman, M. S. A General Approach for the Calculation and Characterization of X-ray Absorption Spectra. *J. Chem. Phys.* **2018**, *149*, 154111.
(47) Huber, C.; Klamroth, T. Explicitly Time-dependent Coupled Cluster Singles Doubles Calculations of Laser-driven Many-electron Dynamics. *J. Chem. Phys.* **2011**, *134*, 054113.
(48) Pigg, D. A.; Hagen, G.; Nam, H.; Papenbrock, T. Time-dependent Coupled-cluster Method for Atomic Nuclei. *Phys. Rev. C: Nucl. Phys.* **2012**, *86*, 014308.
(49) Nascimento, D. R.; DePrince, A. E., III Simulation of Near-edge X-ray Absorption Fine Structure with Time-dependent Equation-of-motion Coupled-cluster Theory. *J. Phys. Chem. Lett.* **2017**, *8*, 2951−2957.
(50) Sato, T.; Pathak, H.; Orimo, Y.; Ishikawa, K. L. Communication: Time-dependent Optimized Coupled-cluster Method for Multielectron dynamics. *J. Chem. Phys.* **2018**, *148*, 051101.
(51) Kristiansen, H. E.; Schoyen, O. S.; Kvaal, S.; Pedersen, T. B. Numerical Stability of Time-Dependent Coupled-Cluster Methods for Many-Electron Dynamics in Intense Laser Pulses. *J. Chem. Phys.* **2020**, *152*, 071102.
(52) Nascimento, D. R.; DePrince, A. E. A General Time-Domain Formulation of Equation-of-Motion Coupled-Cluster Theory for Linear Spectroscopy. *J. Chem. Phys.* **2019**, *151*, 204107.
(53) Koulias, L. N.; Williams-Young, D. B.; Nascimento, D. R.; DePrince, A. E.; Li, X. Relativistic Time-Dependent Equation-of-Motion Coupled-Cluster. *J. Chem. Theory Comput.* **2019**, *15*, 6617−6624.
(54) Folkestad, S. D.; et al. e^T 1.0: An Open Source Electronic Structure Program with Emphasis on Coupled Cluster and Multilevel Methods. *J. Chem. Phys.* **2020**, *152*, 184103.
(55) Skeidsvoll, A. S.; Balbi, A.; Koch, H. Time-Dependent Coupled Cluster Theory for Ultrafast Transient Absorption Spectroscopy. 2020, arXiv:2005.12749.
(56) Requist, R.; Pankratov, O. Adiabatic Approximation in Time-Dependent Reduced-Density-Matrix Functional Theory. *Phys. Rev. A: At., Mol., Opt. Phys.* **2010**, *81*, 042519.
(57) Requist, R.; Pankratov, O. Time-Dependent Occupation Numbers in Reduced-Density-Matrix-Functional Theory: Application to an Interacting Landau-Zener Model. *Phys. Rev. A: At., Mol., Opt. Phys.* **2011**, *83*, 052510.
(58) Appel, H.; Gross, E. K. U. Time-Dependent Natural Orbitals and Occupation Numbers. *Europhys. Lett.* **2010**, *92*, 23001.

https://dx.doi.org/10.1021/acs.chemrev.0c00223
Chem. Rev. XXXX, XXX, XXX−XXX

(59) Jeffcoat, D. B.; DePrince, A. E. N-Representability-Driven Reconstruction of the Two-Electron Reduced-Density Matrix for a Real-Time Time-Dependent Electronic Structure Method. *J. Chem. Phys.* **2014**, *141*, 214104.
(60) Elliott, P.; Maitra, N. T. Density-Matrix Propagation Driven by Semiclassical Correlation. *Int. J. Quantum Chem.* **2016**, *116*, 772−783.
(61) Akbari, A.; Hashemi, M. J.; Rubio, A.; Nieminen, R. M.; van Leeuwen, R. Challenges in Truncating the Hierarchy of Time-Dependent Reduced Density Matrices Equations. *Phys. Rev. B: Condens. Matter Mater. Phys.* **2012**, *85*, 235121.
(62) Lackner, F.; Březinová, I.; Sato, T.; Ishikawa, K. L.; Burgdörfer, J. Propagating Two-Particle Reduced Density Matrices without Wave Functions. *Phys. Rev. A: At., Mol., Opt. Phys.* **2015**, *91*, 023412.
(63) Coleman, A. J. Structure of Fermion Density Matrices. *Rev. Mod. Phys.* **1963**, *35*, 668−686.
(64) Born, M.; Green, H. S. A General Kinetic Theory of Liquids. I. The Molecular Distribution Functions. *Proc. R. Soc. (London)* **1946**, *188*, 10−18.
(65) Kirkwood, J. G. The Statistical Mechanical Theory of Transport Processes I. General Theory. *J. Chem. Phys.* **1946**, *14*, 180−201.
(66) Yvon, J. Une Methode d'etude des Correlations dans les Fluides Quantiques en Equilibre. *Nucl. Phys.* **1957**, *4*, 1−20.
(67) Bogoliubov, N. N. *The Dynamical Theory in Statistical Physics*;Hindustan: Delhi, 1965.
(68) Ding, F.; Goings, J. J.; Frisch, M. J.; Li, X. Ab Initio Non-Relativistic Spin Dynamics. *J. Chem. Phys.* **2014**, *141*, 214111.
(69) Repisky, M.; Konecny, L.; Kadek, M.; Komorovsky, S.; Malkin, O. L.; Malkin, V. G.; Ruud, K. Excitation Energies from Real-time Propagation of the Four-component Dirac-Kohn-Sham Equation. *J. Chem. Theory Comput.* **2015**, *11*, 980−991.
(70) Goings, J. J.; Kasper, J. M.; Egidi, F.; Sun, S.; Li, X. Real Time Propagation of the Exact Two Component Time-Dependent Density Functional Theory. *J. Chem. Phys.* **2016**, *145*, 104107.
(71) Ullrich, C.; Reinhard, P.; Suraud, E. Electron Dynamics in Strongly Excited Sodium Clusters: A Density-functional Study with Self-interaction Correction. *J. Phys. B: At., Mol. Opt. Phys.* **1998**, *31*, 1871−1885.
(72) Yabana, K.; Bertsch, G. F. Optical Response of Small Silver Clusters. *Phys. Rev. A: At., Mol., Opt. Phys.* **1999**, *60*, 3809−3814.
(73) Castro, A.; Marques, M. A. L.; Alonso, J. A.; Bertsch, G. F.; Yabana, K.; Rubio, A. Can Optical Spectroscopy Directly Elucidate the Ground State of C20? *J. Chem. Phys.* **2002**, *116*, 1930−1933.
(74) Marques, M. A.; López, X.; Varsano, D.; Castro, A.; Rubio, A. Time-Dependent Density-Functional Approach for Biological Chromophores: The Case of the Green Fluorescent Protein. *Phys. Rev. Lett.* **2003**, *90*, 258101.
(75) Lopez, X.; Marques, M. A. L.; Castro, A.; Rubio, A. Optical Absorption of the Blue Fluorescent Protein: A First-Principles Study. *J. Am. Chem. Soc.* **2005**, *127*, 12329−12337.
(76) Smith, S. M.; Li, X.; Markevitch, A. N.; Romanov, D. A.; Levis, R. J.; Schlegel, H. B. A Numerical Simulation of Nonadiabatic Electron Excitation in the Strong Field Regime: Linear Polyenes. *J. Phys. Chem. A* **2005**, *109*, 5176−5185.
(77) Isborn, C. M.; Li, X. Modeling the Doubly Excited State with Time-Dependent Hartree−Fock and Density Functional Theories. *J. Chem. Phys.* **2008**, *129*, 204107.
(78) Isborn, C. M.; Li, X. Singlet-Triplet Transitions in Real-Time Time-Dependent Hartree-Fock/Density Functional Theory. *J. Chem. Theory Comput.* **2009**, *5*, 2415−2419.
(79) Kawashita, Y.; Yabana, K.; Noda, M.; Nobusada, K.; Nakatsukasa, T. Oscillator Strength Distribution of C_{60} in the Time-dependent Density Functional Theory. *J. Mol. Struct.: THEOCHEM* **2009**, *914*, 130−135.
(80) Chiodo, L.; Salazar, M.; Romero, A. H.; Laricchia, S.; Sala, F. D.; Rubio, A. Structure, Electronic, and Optical Properties of TiO_2 Atomic Clusters: An Ab Initio Study. *J. Chem. Phys.* **2011**, *135*, 244704.
(81) Govind, N.; Lopata, K.; Rousseau, R.; Andersen, A.; Kowalski, K. Visible Light Absorption of n-Doped TiO_2 Rutile using (LR/RT)-TDDFT and Active Space EOMCCSD Calculations. *J. Phys. Chem. Lett.* **2011**, *2*, 2696−2701.
(82) De Giovannini, U.; Brunetto, G.; Castro, A.; Walkenhorst, J.; Rubio, A. Simulating Pump-probe Photoelectron and Absorption Spectroscopy on the Attosecond Timescale with Time-dependent Density Functional Theory. *ChemPhysChem* **2013**, *14*, 1363−1376.
(83) Wang, Y.; Lopata, K.; Chambers, S. A.; Govind, N.; Sushko, P. V. Optical Absorption and Band Gap Reduction in $(Fe_{1-x}Cr_x)_2O_3$ Solid Solutions: A First-Principles Study. *J. Phys. Chem. C* **2013**, *117*, 25504−25512.
(84) Habenicht, B. F.; Tani, N. P.; Provorse, M. R.; Isborn, C. M. Two-electron Rabi Oscillations in Real-Time Time-Dependent Density-Functional Theory. *J. Chem. Phys.* **2014**, *141*, 184112.
(85) Tussupbayev, S.; Govind, N.; Lopata, K.; Cramer, C. J. Comparison of Real-time and Linear-response Time-dependent Density Functional Theories for Molecular Chromophores Ranging from Sparse to High Densities of States. *J. Chem. Theory Comput.* **2015**, *11*, 1102−1109.
(86) Fischer, S. A.; Cramer, C. J.; Govind, N. Excited State Absorption from Real-Time Time-Dependent Density Functional Theory. *J. Chem. Theory Comput.* **2015**, *11*, 4294−4303.
(87) Fischer, S. A.; Cramer, C. J.; Govind, N. Excited-State Absorption from Real-Time Time-eependent Density Functional Theory: Optical Limiting in Zinc Phthalocyanine. *J. Phys. Chem. Lett.* **2016**, *7*, 1387−1391.
(88) De Giovannini, U.; Hübener, H.; Rubio, A. A First-principles Time-dependent Density Functional Theory Framework for Spin and Time-resolved Angular-resolved Photoelectron Spectroscopy in Periodic Systems. *J. Chem. Theory Comput.* **2017**, *13*, 265−273.
(89) Yabana, K.; Bertsch, G. F. Application of the Time-dependent Local Density Approximation to Optical Activity. *Phys. Rev. A: At., Mol., Opt. Phys.* **1999**, *60*, 1271−1279.
(90) Varsano, D.; Espinosa-Leal, L. A.; Andrade, X.; Marques, M. A. L.; di Felice, R.; Rubio, A. Towards a Gauge Invariant Method for Molecular Chiroptical Properties in TDDFT. *Phys. Chem. Chem. Phys.* **2009**, *11*, 4481−4489.
(91) Lee, K.-M.; Yabana, K.; Bertsch, G. F. Magnetic Circular Dichroism in Real-time Time-dependent Density Functional Theory. *J. Chem. Phys.* **2011**, *134*, 144106.
(92) Goings, J. J.; Li, X. An Atomic Orbital Based Real-Time Time-Dependent Density Functional Theory for Computing Electronic Circular Dichroism Band Spectra. *J. Chem. Phys.* **2016**, *144*, 234102.
(93) Nguyen, T. S.; Koh, J. H.; Lefelhocz, S.; Parkhill, J. Black-Box, Real-Time Simulations of Transient Absorption Spectroscopy. *J. Phys. Chem. Lett.* **2016**, *7*, 1590−1595.
(94) Sun, S.; Beck, R.; Williams-Young, D. B.; Li, X. Simulating Magnetic Circular Dichroism Spectra with Real-Time Time-Dependent Density Functional Theory in Gauge Including Atomic Orbitals. *J. Chem. Theory Comput.* **2019**, *15*, 6824−6831.
(95) Lopata, K.; Van Kuiken, B. E.; Khalil, M.; Govind, N. Linear-response and Real-time Time-dependent Density Functional Theory Studies of Core-level Near-edge X-ray Absorption. *J. Chem. Theory Comput.* **2012**, *8*, 3284−3292.
(96) Fernando, R. G.; Balhoff, M. C.; Lopata, K. X-ray Absorption in Insulators with Non-Hermitian Real-time Time-dependent Density Functional Theory. *J. Chem. Theory Comput.* **2015**, *11*, 646−654.
(97) Kadek, M.; Konecny, L.; Gao, B.; Repisky, M.; Ruud, K. X-ray Absorption Resonances Near $L_{2,3}$-edges from Real-time Propagation of the Dirac−Kohn−Sham density matrix. *Phys. Chem. Chem. Phys.* **2015**, *17*, 22566−22570.
(98) Kasper, J. M.; Lestrange, P. J.; Stetina, T. F.; Li, X. Modeling $L_{2,3}$-Edge X-ray Absorption Spectroscopy with Real-Time Exact Two-Component Relativistic Time-Dependent Density Functional Theory. *J. Chem. Theory Comput.* **2018**, *14*, 1998−2006.
(99) Ding, F.; Van Kuiken, B. E.; Eichinger, B. E.; Li, X. An Efficient Method for Calculating Dynamical Hyperpolarizabilities Using Real-Time Time-Dependent Density Functional Theory. *J. Chem. Phys.* **2013**, *138*, 064104.

https://dx.doi.org/10.1021/acs.chemrev.0c00223
Chem. Rev. XXXX, XXX, XXX−XXX

(100) Konecny, L.; Kadek, M.; Komorovsky, S.; Malkina, O. L.; Ruud, K.; Repisky, M. Acceleration of Relativistic Electron Dynamics by Means of X2C Transformation: Application to the Calculation of Nonlinear Optical Properties. *J. Chem. Theory Comput.* **2016**, *12*, 5823−5833.
(101) Harumiya, K.; Kono, H.; Fujimura, Y.; Kawata, I.; Bandrauk, A. D. Intense Laser-field Ionization of H_2 Enhanced by Two-electron Dynamics. *Phys. Rev. A: At., Mol., Opt. Phys.* **2002**, *66*, 043403.
(102) Lein, M.; Kreibich, T.; Gross, E.; Engel, V. Strong-field Ionization Dynamics of a Model H_2 Molecule. *Phys. Rev. A: At., Mol., Opt. Phys.* **2002**, *65*, 033403.
(103) Baer, R.; Neuhauser, D.; Ždánská, P. R.; Moiseyev, N. Ionization and High-order Harmonic Generation in Aligned Benzene by a Short Intense Circularly Polarized Laser Pulse. *Phys. Rev. A: At., Mol., Opt. Phys.* **2003**, *68*, 043406.
(104) Chu, X.; Chu, S.-I. Role of the Electronic Structure and Multielectron Responses in Ionization Mechanisms of Diatomic Molecules in Intense Short-pulse Lasers: An All-electron Ab Initio Study. *Phys. Rev. A: At., Mol., Opt. Phys.* **2004**, *70*, 061402.
(105) De Wijn, A.; Lein, M.; Kümmel, S. Strong-field Ionization in Time-dependent density functional theory. *Europhys. Lett.* **2008**, *84*, 43001.
(106) Klinkusch, S.; Saalfrank, P.; Klamroth, T. Laser-induced Electron Dynamics Including Photoionization: A Heuristic Model within Time-dependent Configuration Interaction Theory. *J. Chem. Phys.* **2009**, *131*, 114304.
(107) Hochstuhl, D.; Bonitz, M. Two-photon Ionization of Helium Studied with the Multiconfigurational Time-dependent Hartree-Fock Method. *J. Chem. Phys.* **2011**, *134*, 084106.
(108) Hochstuhl, D.; Bonitz, M. Time-dependent Restricted-active-space Configuration-interaction Method for the Photoionization of Many-electron Atoms. *Phys. Rev. A: At., Mol., Opt. Phys.* **2012**, *86*, 053424.
(109) Lopata, K.; Govind, N. Near and Above Ionization Electronic Excitations with Non-Hermitian Real-time Time-dependent Density Functional Theory. *J. Chem. Theory Comput.* **2013**, *9*, 4939−4946.
(110) Bauch, S.; Sørensen, L. K.; Madsen, L. B. Time-dependent Generalized-active-space Configuration-interaction Approach to Photoionization Dynamics of Atoms and Molecules. *Phys. Rev. A: At., Mol., Opt. Phys.* **2014**, *90*, 062508.
(111) Crawford-Uranga, A.; De Giovannini, U.; Räsänen, E.; Oliveira, M. J.; Mowbray, D. J.; Nikolopoulos, G. M.; Karamatskos, E. T.; Markellos, D.; Lambropoulos, P.; Kurth, S.; Rubio, A. Time-dependent Density-functional Theory of Strong-field Ionization of Atoms by Soft X-rays. *Phys. Rev. A: At., Mol., Opt. Phys.* **2014**, *90*, 033412.
(112) Krause, P.; Sonk, J. A.; Schlegel, H. B. Strong Field Ionization Rates Simulated with Time-dependent Configuration Interaction and an Absorbing Potential. *J. Chem. Phys.* **2014**, *140*, 174113.
(113) Krause, P.; Schlegel, H. B. Angle-dependent Ionization of Small Molecules by Time-dependent Configuration Interaction and an Absorbing Potential. *J. Phys. Chem. Lett.* **2015**, *6*, 2140−2146.
(114) Hoerner, P.; Schlegel, H. B. Angular Dependence of Ionization by Circularly Polarized Light Calculated with Time-Dependent Configuration Interaction with an Absorbing Potential. *J. Phys. Chem. A* **2017**, *121*, 1336−1343.
(115) Hoerner, P.; Schlegel, H. B. Angular Dependence of Strong Field Ionization of Haloacetylenes HCCX (X = F, Cl, Br, I), Using Time-dependent Configuration Interaction with an Absorbing Potential. *J. Phys. Chem. C* **2018**, *122*, 13751−13757.
(116) Peralta, J. E.; Hod, O.; Scuseria, G. E. Magnetization Dynamics from Time-Dependent Noncollinear Spin Density Functional Theory Calculations. *J. Chem. Theory Comput.* **2015**, *11*, 3661−3668.
(117) Elliott, P.; Krieger, K.; Dewhurst, J.; Sharma, S.; Gross, E. Optimal Control of Laser-induced Spin-orbit Mediated Ultrafast Demagnetization. *New J. Phys.* **2016**, *18*, 013014.
(118) Baer, R.; Gould, R. A Method for Ab Initio Nonlinear Electron-density Evolution. *J. Chem. Phys.* **2001**, *114*, 3385−3392.
(119) Baer, R.; Neuhauser, D. Ab Initio Electrical Conductance of a Molecular Wire. *Int. J. Quantum Chem.* **2003**, *91*, 524−532.
(120) Baer, R.; Seideman, T.; Ilani, S.; Neuhauser, D. Ab Initio Study of the Alternating Current Impedance of a Molecular Junction. *J. Chem. Phys.* **2004**, *120*, 3387−3396.
(121) Cheng, C.-L.; Evans, J. S.; Van Voorhis, T. Simulating Molecular Conductance using Real-time Density Functional Theory. *Phys. Rev. B: Condens. Matter Mater. Phys.* **2006**, *74*, 155112.
(122) Qian, X.; Li, J.; Lin, X.; Yip, S. Time-dependent Density Functional Theory with Ultrasoft Pseudopotentials: Real-time Electron Propagation across a Molecular Junction. *Phys. Rev. B: Condens. Matter Mater. Phys.* **2006**, *73*, 035408.
(123) Sánchez, C. G.; Stamenova, M.; Sanvito, S.; Bowler, D. R.; Horsfield, A. P.; Todorov, T. N. Molecular Conduction: Do Time-dependent Simulations Tell You More than the Landauer Approach? *J. Chem. Phys.* **2006**, *124*, 214708.
(124) Zelovich, T.; Kronik, L.; Hod, O. State Representation Approach for Atomistic Time-dependent Transport Calculations in Molecular Junctions. *J. Chem. Theory Comput.* **2014**, *10*, 2927−2941.
(125) Zelovich, T.; Kronik, L.; Hod, O. Driven Liouville von Neumann Approach for Time-dependent Electronic Transport Calculations in a Nonorthogonal Basis-set Representation. *J. Phys. Chem. C* **2016**, *120*, 15052−15062.
(126) Hod, O.; Rodríguez-Rosario, C. A.; Zelovich, T.; Frauenheim, T. Driven Liouville von Neumann Equation in Lindblad Form. *J. Phys. Chem. A* **2016**, *120*, 3278−3285.
(127) Lian, C.; Ali, Z. A.; Kwon, H.; Wong, B. M. Indirect but Efficient: Laser-Excited Electrons Can Drive Ultrafast Polarization Switching in Ferroelectric Materials. *J. Phys. Chem. Lett.* **2019**, *10*, 3402−3407.
(128) Liang, W.; Isborn, C. M.; Li, X. Laser-Controlled Dissociation of $C_2H_2^{2+}$: Ehrenfest Dynamics Using Time-Dependent Density Functional Theory. *J. Phys. Chem. A* **2009**, *113*, 3463−3469.
(129) Liang, W.; Isborn, C. M.; Lindsay, A.; Li, X.; Smith, S. M.; Levis, R. J. Time-Dependent Density Functional Theory Calculations of Ehrenfest Dynamics of Laser Controlled Dissociation of NO^+: Pulse Length and Sequential Multiple Single-Photon Processes. *J. Phys. Chem. A* **2010**, *114*, 6201−6206.
(130) Krieger, K.; Castro, A.; Gross, E. Optimization Schemes for Selective Molecular Cleavage with Tailored Ultrashort Laser Pulses. *Chem. Phys.* **2011**, *391*, 50−61.
(131) Castro, A.; Werschnik, J.; Gross, E. K. Controlling the Dynamics of Many-electron Systems from First Principles: A Combination of Optimal Control and Time-dependent Density-functional Theory. *Phys. Rev. Lett.* **2012**, *109*, 153603.
(132) Micha, D. A. Time-Dependent Many-Electron Treatment of Electronic Energy and Charge Transfer in Atomic Collisions. *J. Phys. Chem. A* **1999**, *103*, 7562−7574.
(133) Micha, D. A. *Adv. Quantum Chem.*, 1999; Vol. 35; pp 317−337.
(134) Li, X.; Tully, J. C. Ab Initio Time-Resolved Density Functional Theory for Lifetimes of Excited Adsorbate States at Metal Surfaces. *Chem. Phys. Lett.* **2007**, *439*, 199−203.
(135) Moss, C. L.; Isborn, C. M.; Li, X. Ehrenfest Dynamics with a Time-Dependent Density-Functional-Theory Calculation of Lifetimes and Resonant Widths of Charge-Transfer States of Li^+ Near an Aluminum Cluster Surface. *Phys. Rev. A: At., Mol., Opt. Phys.* **2009**, *80*, 024503.
(136) Chapman, C. T.; Liang, W.; Li, X. Ultrafast Coherent Electron-Hole Separation Dynamics in a Fullerene Derivative. *J. Phys. Chem. Lett.* **2011**, *2*, 1189−1192.
(137) Ding, F.; Chapman, C. T.; Liang, W.; Li, X. Mechanisms of Bridge-Mediated Electron Transfer: A TDDFT Electronic Dynamics Study. *J. Chem. Phys.* **2012**, *137*, 22A512.
(138) Nguyen, P.; Ding, F.; Fischer, S. A.; Liang, W.; Li, X. Solvated First-Principles Excited State Charge Transfer Dynamics with Time-Dependent Polarizable Continuum Model and Solvent Dielectric Relaxation. *J. Phys. Chem. Lett.* **2012**, *3*, 2898−2904.
(139) Chapman, C. T.; Liang, W.; Li, X. Solvent Effects on Intramolecular Charge Transfer Dynamics in a Fullerene Derivative. *J. Phys. Chem. A* **2013**, *117*, 2687−2691.

https://dx.doi.org/10.1021/acs.chemrev.0c00223
Chem. Rev. XXXX, XXX, XXX−XXX

(140) Fuks, J. I.; Elliott, P.; Rubio, A.; Maitra, N. T. Dynamics of Charge-transfer Processes with Time-dependent Density Functional Theory. *J. Phys. Chem. Lett.* **2013**, *4*, 735−739.
(141) Rozzi, C. A.; Falke, S. M.; Spallanzani, N.; Rubio, A.; Molinari, E.; Brida, D.; Maiuri, M.; Cerullo, G.; Schramm, H.; Christoffers, J.; Lienau, C. Quantum Coherence Controls the Charge Separation in a Prototypical Artificial Light-harvesting System. *Nat. Commun.* **2013**, *4*, 1602.
(142) Petrone, A.; Lingerfelt, D. B.; Rega, N.; Li, X. From Charge-Transfer to a Charge-Separated State: A Perspective from the Real-Time TDDFT Excitonic Dynamics. *Phys. Chem. Chem. Phys.* **2014**, *16*, 24457−24465.
(143) Falke, S. M.; Rozzi, C. A.; Brida, D.; Maiuri, M.; Amato, M.; Sommer, E.; De Sio, A.; Rubio, A.; Cerullo, G.; Molinari, E.; Lienau, C. Coherent Ultrafast Charge Transfer in an Organic Photovoltaic Blend. *Science* **2014**, *344*, 1001−1005.
(144) Ding, F.; Guidez, E. B.; Aikens, C. M.; Li, X. Quantum Coherent Plasmon in Silver Nanowires: A Real-Time TDDFT Study. *J. Chem. Phys.* **2014**, *140*, 244705.
(145) Peng, B.; Lingerfelt, D. B.; Ding, F.; Aikens, C. M.; Li, X. Real-Time TDDFT Studies of Exciton Decay and Transfer in Silver Nanowire Arrays. *J. Phys. Chem. C* **2015**, *119*, 6421−6427.
(146) Provorse, M. R.; Isborn, C. M. Electron Dynamics with Real-time Time-dependent Density Functional Theory. *Int. J. Quantum Chem.* **2016**, *116*, 739−749.
(147) Schaffhauser, P.; Kümmel, S. Using Time-dependent Density Functional Theory in Real Time for Calculating Electronic Transport. *Phys. Rev. B: Condens. Matter Mater. Phys.* **2016**, *93*, 035115.
(148) Oviedo, M. B.; Wong, B. M. Real-time Quantum Dynamics Reveals Complex, Many-body Interactions in Solvated Nanodroplets. *J. Chem. Theory Comput.* **2016**, *12*, 1862−1871.
(149) Donati, G.; Lingerfelt, D. B.; Aikens, C. M.; Li, X. Molecular Vibration Induced Plasmon Decay. *J. Phys. Chem. C* **2017**, *121*, 15368−15374.
(150) Zelovich, T.; Hansen, T.; Liu, Z.-F.; Neaton, J. B.; Kronik, L.; Hod, O. Parameter-free Driven Liouville-von Neumann Approach for Time-dependent Electronic Transport Simulations in Open Quantum Systems. *J. Chem. Phys.* **2017**, *146*, 092331.
(151) Senanayake, R. D.; Lingerfelt, D. B.; Kuda-Singappulige, G. U.; Li, X.; Aikens, C. M. Real-Time TDDFT Investigation of Optical Absorption in Gold Nanowires. *J. Phys. Chem. C* **2019**, *123*, 14734−14745.
(152) Donati, G.; Wildman, A.; Caprasecca, S.; Lingerfelt, D. B.; Lipparini, F.; Mennucci, B.; Li, X. Coupling Real-Time Time-Dependent Density Functional Theory with Polarizable Force Field. *J. Phys. Chem. Lett.* **2017**, *8*, 5283−5289.
(153) Morzan, U. N.; Ramírez, F. F.; Oviedo, M. B.; Sánchez, C. G.; Scherlis, D. A.; Lebrero, M. C. G. Electron Dynamics in Complex Environments with Real-time Time Dependent Density Functional Theory in a QM-MM Framework. *J. Chem. Phys.* **2014**, *140*, 164105.
(154) Liang, W.; Chapman, C. T.; Ding, F.; Li, X. Modeling Ultrafast Solvated Electronic Dynamics Using Time-Dependent Density Functional Theory and Polarizable Continuum Model. *J. Phys. Chem. A* **2012**, *116*, 1884−1890.
(155) Corni, S.; Pipolo, S.; Cammi, R. Equation of Motion for the Solvent Polarization Apparent Charges in the Polarizable Continuum Model: Application to Real-time TDDFT. *J. Phys. Chem. A* **2015**, *119*, 5405−5416.
(156) Ding, F.; Lingerfelt, D. B.; Mennucci, B.; Li, X. Time-Dependent Non-Equilibrium Dielectric Response in QM/Continuum Approaches. *J. Chem. Phys.* **2015**, *142*, 034120.
(157) Pipolo, S.; Corni, S.; Cammi, R. Equation of Motion for the Solvent Polarization Apparent Charges in the Polarizable Continuum Model: Application to Time-dependent CI. *J. Chem. Phys.* **2017**, *146*, 064116.
(158) Koh, K. J.; Nguyen-Beck, T. S.; Parkhill, J. Accelerating Realtime TDDFT with Block-orthogonalized Manby-Miller Embedding Theory. *J. Chem. Theory Comput.* **2017**, *13*, 4173−4178.
(159) Zheng, X.; Wang, F.; Yam, C. Y.; Mo, Y.; Chen, G. Time-dependent Density Functional Theory for Open Systems. *Phys. Rev. B: Condens. Matter Mater. Phys.* **2007**, *75*, 195127.
(160) Chapman, C. T.; Liang, W.; Li, X. Open-System Electronic Dynamics and Thermalized Electronic Structure. *J. Chem. Phys.* **2011**, *134*, 024118.
(161) Koo, S. K.; Yam, C. Y.; Zheng, X.; Chen, G. First-principles Liouville−von Neumann Equation for Open Systems and Its Applications. *Phys. Status Solidi B* **2012**, *249*, 270−275.
(162) Tempel, D. G.; Yuen-Zhou, J.; Aspuru-Guzik, A. *Fundamentals of Time-Dependent Density Functional Theory*; Springer, 2012; pp 211−229.
(163) Yuen-Zhou, J.; Aspuru-Guzik, A. Remarks on Time-dependent Current-density Functional Theory for Open Quantum Systems. *Phys. Chem. Chem. Phys.* **2013**, *15*, 12626−12636.
(164) Nguyen, T. S.; Nanguneri, R.; Parkhill, J. How Electronic Dynamics with Pauli Exclusion Produces Fermi−Dirac Statistics. *J. Chem. Phys.* **2015**, *142*, 134113.
(165) Nguyen, T. S.; Parkhill, J. Nonradiative Relaxation in Real-Time Electronic Dynamics OSCF2: Organolead Triiodide Perovskite. *J. Phys. Chem. A* **2016**, *120*, 6880−6887.
(166) Ruggenthaler, M.; Mackenroth, F.; Bauer, D. Time-dependent Kohn-Sham Approach to Quantum Electrodynamics. *Phys. Rev. A: At., Mol., Opt. Phys.* **2011**, *84*, 042107.
(167) Tokatly, I. V. Time-dependent Density Functional Theory for Many-electron Systems Interacting with Cavity Photons. *Phys. Rev. Lett.* **2013**, *110*, 233001.
(168) Ruggenthaler, M.; Flick, J.; Pellegrini, C.; Appel, H.; Tokatly, I. V.; Rubio, A. Quantum-electrodynamical Density-functional Theory: Bridging Quantum Optics and Electronic-structure Theory. *Phys. Rev. A: At., Mol., Opt. Phys.* **2014**, *90*, 012508.
(169) Pellegrini, C.; Flick, J.; Tokatly, I. V.; Appel, H.; Rubio, A. Optimized Effective Potential for Quantum Electrodynamical Time-dependent Density Functional Theory. *Phys. Rev. Lett.* **2015**, *115*, 093001.
(170) Flick, J.; Ruggenthaler, M.; Appel, H.; Rubio, A. Kohn−Sham Approach to Quantum Electrodynamical Density-functional Theory: Exact Time-dependent Effective Potentials in Real Space. *Proc. Natl. Acad. Sci. U. S. A.* **2015**, *112*, 15285−15290.
(171) Flick, J.; Ruggenthaler, M.; Appel, H.; Rubio, A. Atoms and Molecules in Cavities, from Weak to Strong Coupling in Quantum-electrodynamics (QED) Chemistry. *Proc. Natl. Acad. Sci. U. S. A.* **2017**, *114*, 3026−3034.
(172) Nascimento, D. R.; DePrince, A. E., III Modeling Molecule-plasmon Interactions using Quantized Radiation Fields within Time-dependent Electronic Structure Theory. *J. Chem. Phys.* **2015**, *143*, 214104.
(173) Mordovina, U.; Bungey, C.; Appel, H.; Knowles, P. J.; Rubio, A.; Manby, F. R. Polaritonic Coupled-Cluster Theory. *Phys. Rev. Research* **2020**, *2*, 023262.
(174) Haugland, T. S.; Ronca, E.; Kjonstad, E. F.; Rubio, A.; Koch, H. Coupled Cluster Theory for Molecular Polaritons: Changing Ground and Excited States. *arXiv.org* **2020**, 1−18.
(175) Tully, J. C. Mixed Quantum-Classical Dynamics. *Faraday Discuss.* **1998**, *110*, 407−419.
(176) Worth, G.; Robb, M.; Lasorne, B. Solving the Time-Dependent Schrödinger Equation for Nuclear Motion in One Step: Direct Dynamics of Non-adiabatic Systems. *Mol. Phys.* **2008**, *106*, 2077−2091.
(177) Tully, J. C. Perspective: Nonadiabatic Dynamics Theory. *J. Chem. Phys.* **2012**, *137*, 22A301.
(178) Yarkony, D. R. Nonadiabatic Quantum Chemistry − Past, Present, and Future. *Chem. Rev.* **2012**, *112*, 481−498.
(179) Tavernelli, I. Nonadiabatic Molecular Dynamics Simulations: Synergies between Theory and Experiments. *Acc. Chem. Res.* **2015**, *48*, 792−800.
(180) Curchod, B. F. E.; Martinez, T. J. Ab Initio Nonadiabatic Quantum Molecular Dynamics. *Chem. Rev.* **2018**, *118*, 3305−3336.

https://dx.doi.org/10.1021/acs.chemrev.0c00223
Chem. Rev. XXXX, XXX, XXX−XXX

(181) Abedi, A.; Maitra, N. T.; Gross, E. K. U. Correlated Electron-Nuclear Dynamics: Exact Factorization of the Molecular Wavefunction. *J. Chem. Phys.* **2012**, *137*, 22A530.
(182) McLachlan, A. D. A. Variational Solution of the Time-dependent Schrödinger Equation. *Mol. Phys.* **1964**, *8*, 39−44.
(183) Pechukas, P. Time-Dependent Semiclassical Scattering Theory. II. Atomic Collisions. *Phys. Rev.* **1969**, *181*, 174−185.
(184) Tully, J. C.; Preston, R. K. Trajectory Surface Hopping Approach to Nonadiabatic Molecular Collisions: The Reaction of H^+ with D_2. *J. Chem. Phys.* **1971**, *55*, 562−572.
(185) Miller, W. H.; McCurdy, C. W. Classical Trajectory Model for Electronically Non-Adiabatic Collision Phenomena - Classical Analog for Electronic Degrees of Freedom. *J. Chem. Phys.* **1978**, *69*, 5163−5173.
(186) Meyer, H. D.; Miller, W. H. Classical Analog for Electronic Degrees of Freedom in Non-Adiabatic Collision Processes. *J. Chem. Phys.* **1979**, *70*, 3214−3223.
(187) Heller, E. J. Frozen Gaussians - a Very Simple Semi-Classical Approximation. *J. Chem. Phys.* **1981**, *75*, 2923−2931.
(188) Micha, D. A. A Self-Consistent Eikonal Treatment of Electronic-Transitions in Molecular Collisions. *J. Chem. Phys.* **1983**, *78*, 7138−7145.
(189) Tully, J. C. Molecular-Dynamics With Electronic-Transitions. *J. Chem. Phys.* **1990**, *93*, 1061−1071.
(190) Webster, F.; Rossky, P. J.; Friesner, R. A. Nonadiabatic Processes in Condensed Matter - Semiclassical Theory and Implementation. *Comput. Phys. Commun.* **1991**, *63*, 494−522.
(191) Martinez, T. J.; Ben-Nun, M.; Levine, R. D. Multi-Electronic-State Molecular Dynamics: A Wave Function Approach with Applications. *J. Phys. Chem.* **1996**, *100*, 7884−7895.
(192) Martens, C. C.; Fang, J. Y. Semiclassical-limit Molecular Dynamics on Multiple Electronic Surfaces. *J. Chem. Phys.* **1997**, *106*, 4918−4930.
(193) Stock, G.; Thoss, M. Semiclassical Description of Nonadiabatic Quantum Dynamics. *Phys. Rev. Lett.* **1997**, *78*, 578−581.
(194) Ben-Nun, M.; Martinez, T. J. Nonadiabatic Molecular Dynamics: Validation of the Multiple Spawning Method for a Multidimensional Problem. *J. Chem. Phys.* **1998**, *108*, 7244−7257.
(195) Prezhdo, O. V. Mean Field Approximation for the Stochastic Schrodinger Equation. *J. Chem. Phys.* **1999**, *111*, 8366−8377.
(196) Kapral, R.; Ciccotti, G. Mixed Quantum-classical Dynamics. *J. Chem. Phys.* **1999**, *110*, 8919−8929.
(197) Ben-Nun, M.; Quenneville, J.; Martínez, T. J. Ab Initio Multiple Spawning: Photochemistry From First Principles Quantum Molecular Dynamics. *J. Phys. Chem. A* **2000**, *104*, 5161−5175.
(198) Beck, M. H.; Jäckle, A.; Worth, G. A.; Meyer, H.-D. The Multiconfiguration Time-dependent Hartree (MCTDH) Method: A Highly Efficient Algorithm for Propagating Wavepackets. *Phys. Rep.* **2000**, *324*, 1−105.
(199) Ben-Nun, M.; Martinez, T. J. *Advances in Chemical Physics*; John Wiley and Sons, Ltd, 2002; pp 439−512.
(200) Worth, G. A.; Meyer, H.-D.; Cederbaum, L. S. *Conical Intersections*; World Scientific, 2004; pp 583−617.
(201) Li, X.; Tully, J. C.; Schlegel, H. B.; Frisch, M. J. Ab Initio Ehrenfest Dynamics. *J. Chem. Phys.* **2005**, *123*, 084106.
(202) Tao, H.; Levine, B. G.; Martínez, T. J. Ab Initio Multiple Spawning Dynamics Using Multi-State Second-Order Perturbation Theory. *J. Phys. Chem. A* **2009**, *113*, 13656−13662.
(203) Miller, W. H. Electronically Nonadiabatic Dynamics via Semiclassical Initial Value Methods. *J. Phys. Chem. A* **2009**, *113*, 1405−1415.
(204) Coker, D. F.; Xiao, L. Methods for Molecular-Dynamics With Nonadiabatic Transitions. *J. Chem. Phys.* **1995**, *102*, 496−510.
(205) Bittner, E. R.; Rossky, P. J. Quantum Decoherence in Mixed Quantum-Classical Systems - Nonadiabatic Processes. *J. Chem. Phys.* **1995**, *103*, 8130−8143.
(206) Wyatt, R. E.; Bittner, E. R. Quantum Wave Packet Dynamics With Trajectories: Implementation With Adaptive Lagrangian Grids. *J. Chem. Phys.* **2000**, *113*, 8898−8907.
(207) Bedard-Hearn, M. J.; Larsen, R. E.; Schwartz, B. J. Mean-Field Dynamics With Stochastic Decoherence (MF-SD): A New Algorithm for Nonadiabatic Mixed Quantum/Classical Molecular-Dynamics Simulations With Nuclear-Induced Decoherence. *J. Chem. Phys.* **2005**, *123*, 234106.
(208) Shenvi, N.; Subotnik, J. E.; Yang, W. Simultaneous-trajectory Surface Hopping: A Parameter-free Algorithm for Implementing Decoherence in Nonadiabatic Dynamics. *J. Chem. Phys.* **2011**, *134*, 144102.
(209) Subotnik, J. E.; Shenvi, N. A New Approach to Decoherence and Momentum Rescaling in the Surface Hopping Algorithm. *J. Chem. Phys.* **2011**, *134*, 024105.
(210) Fischer, S. A.; Chapman, C. T.; Li, X. Surface Hopping with Ehrenfest Excited Potential. *J. Chem. Phys.* **2011**, *135*, 144102.
(211) Curchod, B. F. E.; Rauer, C.; Marquetand, P.; Gonzalez, L.; Martínez, T. J. Communication: GAIMS − Generalized Ab Initio Multiple Spawning for both Internal Conversion and Intersystem Crossing Processes. *J. Chem. Phys.* **2016**, *144*, 101102.
(212) Space, B.; Coker, D. F. Nonadiabatic Dynamics of Excited Excess Electrons in Simple Fluids. *J. Chem. Phys.* **1991**, *94*, 1976−1984.
(213) Space, B.; Coker, D. F. Dynamics of Trapping and Localization of Excess Electrons in Simple Fluids. *J. Chem. Phys.* **1992**, *96*, 652−663.
(214) Hammes-Schiffer, S.; Tully, J. C. Proton Transfer in Solution: Molecular Dynamics With Quantum Transitions. *J. Chem. Phys.* **1994**, *101*, 4657−4667.
(215) Hammes-Schiffer, S.; Tully, J. C. Vibrationally Enhanced Proton-Transfer. *J. Phys. Chem.* **1995**, *99*, 5793−5797.
(216) Jasper, A. W.; Stechmann, S. N.; Truhlar, D. G. Fewest-Switches with Time Uncertainty: A Modified Trajectory Surface-Hopping Algorithm with Better Accuracy for Classically Forbidden Electronic Transitions. *J. Chem. Phys.* **2002**, *116*, 5424−5431.
(217) Nangia, S.; Jasper, A. W.; Miller, T. F.; Truhlar, D. G. Army Ants Algorithm for Rare Event Sampling of Delocalized Nonadiabatic Transitions by Trajectory Surface Hopping and the Estimation of Sampling Errors by the Bootstrap Method. *J. Chem. Phys.* **2004**, *120*, 3586−3597.
(218) Fabiano, E.; Keal, T.; Thiel, W. Implementation of Surface Hopping Molecular Dynamics using Semiempirical Methods. *Chem. Phys.* **2008**, *349*, 334−347.
(219) Barbatti, M. Nonadiabatic Dynamics with Trajectory Surface Hopping Method. *WIREs Comput. Mol. Sci.* **2011**, *1*, 620−633.
(220) Richter, M.; Marquetand, P.; González-Váquez, J.; Sola, I.; González, L. SHARC: Ab Initio Molecular Dynamics with Surface Hopping in the Adiabatic Representation Including Arbitrary Couplings. *J. Chem. Theory Comput.* **2011**, *7*, 1253−1258.
(221) Cui, G.; Thiel, W. Generalized Trajectory Surface-hopping Method for Internal Conversion and Intersystem Crossing. *J. Chem. Phys.* **2014**, *141*, 124101.
(222) Martens, C. C. Surface Hopping by Consensus. *J. Phys. Chem. Lett.* **2016**, *7*, 2610−2615.
(223) Wang, L.; Akimov, A.; Prezhdo, O. V. Recent Progress in Surface Hopping: 2011−2015. *J. Phys. Chem. Lett.* **2016**, *7*, 2100−2112.
(224) Subotnik, J. E.; Jain, A.; Landry, B.; Petit, A.; Ouyang, W.; Bellonzi, N. Understanding the Surface Hopping View of Electronic Transitions and Decoherence. *Annu. Rev. Phys. Chem.* **2016**, *67*, 387−417.
(225) Nelson, T.; Fernandez-Alberti, S.; Roitberg, A. E.; Tretiak, S. Electronic Delocalization, Vibrational Dynamics, and Energy Transfer in Organic Chromophores. *J. Phys. Chem. Lett.* **2017**, *8*, 3020−3031.
(226) Craig, C. F.; Duncan, W. R.; Prezhdo, O. V. Trajectory Surface Hopping in the Time-Dependent Kohn-Sham Approach for Electron-Nuclear Dynamics. *Phys. Rev. Lett.* **2005**, *95*, 163001.
(227) Prezhdo, O. V.; Duncan, W. R.; Prezhdo, V. V. Photoinduced Electron Dynamics at the Chromophore-Semiconductor Interface: A Time-Domain Ab Initio Perspective. *Prog. Surf. Sci.* **2009**, *84*, 30−68.
(228) Ehrenfest, P. Bemerkung Über Die Angenäherte Gültigkeit Der Klassischen Mechanik Innerhalb Der Quantenmechanik. *Eur. Phys. J. A* **1927**, *45*, 455−457.

https://dx.doi.org/10.1021/acs.chemrev.0c00223
Chem. Rev. XXXX, XXX, XXX−XXX

(229) Gerber, R. B.; Buch, V.; Ratner, M. A. Time-Dependent Self-Consistent Field Approximation for Intramolecular Energy Transfer. I. Formulation and Application to Dissociation of Van Der Waals Molecules. *J. Chem. Phys.* **1982**, *77*, 3022−3030.
(230) Calvayrac, C.; Reinhard, P.-G.; Saraud, E.; Ullrich, C.A. Nonlinear Electron Dynamics in Metal Clusters. *Phys. Rev.* **2000**, *337*, 493−578.
(231) Castro, A.; Marques, M. A. L.; Alonso, J. A.; Bertsch, G. F.; Rubio, A. Excited States Dynamics in Time-Dependent Density Functional Theory. *Eur. Phys. J. D* **2004**, *28*, 211−218.
(232) Miyamoto, Y.; Rubio, A.; Tománek, D. Real-Time Ab Initio Simulations of Excited Carrier Dynamics in Carbon Nanotubes. *Phys. Rev. Lett.* **2006**, *97*, 126104.
(233) Livshits, E.; Baer, R. Time-Dependent Density-Functional Studies of the D_2 Coulomb Explosion. *J. Phys. Chem. A* **2006**, *110*, 8443−8450.
(234) Andrade, X.; Castro, A.; Zueco, D.; Alonso, J. L.; Echenique, P.; Falceto, F.; Rubio, A. Modified Ehrenfest Formalism for Efficient Large-Scale ab initio Molecular Dynamics. *J. Chem. Theory Comput.* **2009**, *5*, 728−742.
(235) Russakoff, A.; Bubin, S.; Xie, X.; Erattupuzha, S.; Kitzler, M.; Varga, K. Time-Dependent Density-Functional Study of the Alignment-Dependent Ionization of Acetylene and Ethylene by Strong Laser Pulses. *Phys. Rev. A: At., Mol., Opt. Phys.* **2015**, *91*, 023422.
(236) Ding, F.; Goings, J. J.; Liu, H.; Lingerfelt, D. B.; Li, X. Ab Initio Two-Component Ehrenfest Dynamics. *J. Chem. Phys.* **2015**, *143*, 114105.
(237) Fedorov, D. A.; Levine, B. G. Nonadiabatic Quantum Molecular Dynamics in Dense Manifolds of Electronic States. *J. Phys. Chem. Lett.* **2019**, *10*, 4542−4548.
(238) Fang, J.-Y.; Hammes-Schiffer, S. Comparison of Surface Hopping and Mean Field Approaches for Model Proton Transfer Reactions. *J. Chem. Phys.* **1999**, *110*, 11166−11175.
(239) Hack, M. D.; Wensmann, A. M.; Truhlar, D. G.; Ben-Nun, M.; Martinez, T. J. Comparison of Full Multiple Spawning, Trajectory Surface Hopping, and Converged Quantum Mechanics for Electronically Nonadiabatic Dynamics. *J. Chem. Phys.* **2001**, *115*, 1172−1186.
(240) Parandekar, P. V.; Tully, J. C. Detailed Balance in Ehrenfest Mixed Quantum-Classical Dynamics. *J. Chem. Theory Comput.* **2006**, *2*, 229−235.
(241) Cheng, S. C.; Zhu, C.; Liang, K. K.; Lin, S. H.; Truhlar, D. G. Algorithmic Decoherence Time for Decay-of-Mixing Non−Born−Oppenheimer Dynamics. *J. Chem. Phys.* **2008**, *129*, 024112.
(242) Akimov, A. V.; Long, R.; Prezhdo, O. V. Coherence Penalty Functional: A Simple Method for Adding Decoherence in Ehrenfest Dynamics. *J. Chem. Phys.* **2014**, *140*, 194107.
(243) Nijjar, P.; Jankowska, J.; Prezhdo, O. V. Ehrenfest and Classical Path Dynamics with Decoherence and Detailed Balance. *J. Chem. Phys.* **2019**, *150*, 204124.
(244) Gross, E. K. U.; Dobson, J. F.; Petersilka, M. In *Density Functional Theory II: Relativistic and Time Dependent Extensions*; Nalewajski, R. F., Ed.; Springer: Berlin, Heidelberg, 1996; pp 81−172.
(245) Dreuw, A.; Head-Gordon, M. Single-Reference Ab Initio Methods for the Calculation of Excited States of Large Molecules. *Chem. Rev.* **2005**, *105*, 4009−4037.
(246) Burke, K.; Werschnik, J.; Gross, E. K. U. Time-Dependent Density Functional Theory: Past, Present, and Future. *J. Chem. Phys.* **2005**, *123*, 062206.
(247) Ullrich, C. A. *Time-Dependent Density-Functional Theory: Concepts and Applications*; Oxford University Press, 2011.
(248) Marques, M. A. L.; Maitra, N. T.; Nogueira, F. M. S.; Gross, E. K. U.; Rubio, A. *Fundamentals of Time-Dependent Density Functional Theory*; Springer-Verlag, 2012.
(249) Casida, M.; Huix-Rotllant, M. Progress in Time-Dependent Density-Functional Theory. *Annu. Rev. Phys. Chem.* **2012**, *63*, 287−323.
(250) Adamo, C.; Jacquemin, D. The Calculations of Excited State Properties with Time-Dependent Density Functional Theory. *Chem. Soc. Rev.* **2013**, *42*, 845−856.
(251) Maitra, N. T. Perspective: Fundamental Aspects of Time-Dependent Density Functional Theory. *J. Chem. Phys.* **2016**, *144*, 220901.
(252) Maitra, N. T. Charge Transfer in Time-dependent Density Functional Theory. *J. Phys.: Condens. Matter* **2017**, *29*, 423001.
(253) Runge, E.; Gross, E. K. U. Density-Functional Theory for Time-Dependent Systems. *Phys. Rev. Lett.* **1984**, *52*, 971−1000.
(254) van Leeuwen, R. Mapping from Densities to Potentials in Time-Dependent Density-Functional Theory. *Phys. Rev. Lett.* **1999**, *82*, 3863−3866.
(255) Casida, M. E. *Recent Advances in Density Functional Methods*; 1995; pp 155−192.
(256) Casida, M. E. In *Recent Developments and Applications of Modern Density Functional Theory*; Seminario, J., Ed.; Theoretical and Computational Chemistry; Elsevier, 1996; Vol. *4*; pp 391 − 439.
(257) Stratmann, R. E.; Scuseria, G. E.; Frisch, M. J. An Efficient Implementation of Time-Dependent Density-Functional Theory for the Calculation of Excitation Energies of Large Molecules. *J. Chem. Phys.* **1998**, *109*, 8218−8224.
(258) Hirata, S.; Head-Gordon, M. Time-dependent Density Functional Theory within the Tamm-Dancoff Approximation. *Chem. Phys. Lett.* **1999**, *314*, 291−299.
(259) Castro, A.; Marques, M. A. L.; Rubio, A. Propagators for the Time-dependent Kohn-Sham Equations. *J. Chem. Phys.* **2004**, *121*, 3425−3433.
(260) Burke, K.; Werschnik, J.; Gross, E. K. U. Time-dependent Density Functional Theory: Past, Present, and Future. *J. Chem. Phys.* **2005**, *123*, 062206.
(261) Raghunathan, S.; Nest, M. Critical Examination of Explicitly Time-dependent Density Functional Theory for Coherent Control of Dipole Switching. *J. Chem. Theory Comput.* **2011**, *7*, 2492−2497.
(262) Raghunathan, S.; Nest, M. The Lack of Resonance Problem in Coherent Control with Real-time Time-dependent Density Functional Theory. *J. Chem. Theory Comput.* **2012**, *8*, 806−809.
(263) Ramakrishnan, R.; Nest, M. Control and Analysis of Single-Determinant Electron Dynamics. *Phys. Rev. A: At., Mol., Opt. Phys.* **2012**, *85*, 054501.
(264) Provorse, M. R.; Habenicht, B. F.; Isborn, C. M. Peak-Shifting in Real-Time Time-Dependent Density Functional Theory. *J. Chem. Theory Comput.* **2015**, *11*, 4791−4802.
(265) Fuks, J. I.; Luo, K.; Sandoval, E. D.; Maitra, N. T. Time-Resolved Spectroscopy in Time-Dependent Density Functional Theory: An Exact Condition. *Phys. Rev. Lett.* **2015**, *114*, 183002.
(266) Luo, K.; Fuks, J. I.; Maitra, N. T. Studies of Spuriously Shifting Resonances in Time-dependent Density Functional Theory. *J. Chem. Phys.* **2016**, *145*, 044101.
(267) Fuks, J.; Helbig, N.; Tokatly, I.; Rubio, A. Nonlinear Phenomena in Time-dependent Density-functional Theory: What Rabi Oscillations Can Teach Us. *Phys. Rev. B: Condens. Matter Mater. Phys.* **2011**, *84*, 075107.
(268) Zang, X.; Schwingenschlögl, U.; Lusk, M. T. Identification and Resolution of Unphysical Multielectron Excitations in the Real-Time Time-Dependent Kohn-Sham Formulation. *Phys. Rev. Lett.* **2020**, *124*, 026402.
(269) Fuks, J. I.; Maitra, N. T. Charge Transfer in Time-dependent Density-functional Theory: Insights from the Asymmetric Hubbard Dimer. *Phys. Rev. A: At., Mol., Opt. Phys.* **2014**, *89*, 062502.
(270) Ullrich, C. A.; Gossmann, U. J.; Gross, E. K. U. Time-Dependent Optimized Effective Potential. *Phys. Rev. Lett.* **1995**, *74*, 872−875.
(271) Liao, S.-L.; Ho, T.-S.; Rabitz, H.; Chu, S.-I. Time-Local Equation for the Exact Optimized Effective Potential in Time-Dependent Density Functional Theory. *Phys. Rev. Lett.* **2017**, *118*, 243001.
(272) Maitra, N. T.; Burke, K. Demonstration of Initial-State Dependence in Time-Dependent Density-Functional Theory. *Phys. Rev. A: At., Mol., Opt. Phys.* **2001**, *63*, 042501.

https://dx.doi.org/10.1021/acs.chemrev.0c00223
Chem. Rev. XXXX, XXX, XXX−XXX

(273) Maitra, N. T.; Burke, K.; Woodward, C. Memory in Time-Dependent Density Functional Theory. *Phys. Rev. Lett.* **2002**, *89*, 023002.
(274) Ruggenthaler, M.; van Leeuwen, R. Global Fixed-Point Proof of Time-Dependent Density-Functional Theory. *Europhys. Lett.* **2011**, *95*, 13001.
(275) Penz, M.; Ruggenthaler, M. Domains of Time-Dependent Density-Potential Mappings. *J. Phys. A: Math. Theor.* **2011**, *44*, 335208.
(276) Ruggenthaler, M.; Giesbertz, K. J. H.; Penz, M.; van Leeuwen, R. Density-Potential Mappings in Quantum Dynamics. *Phys. Rev. A: At., Mol., Opt. Phys.* **2012**, *85*, 052504.
(277) Ruggenthaler, M.; Nielsen, S. E. B.; van Leeuwen, R. Analytic Density Functionals with Initial-State Dependence and Memory. *Phys. Rev. A: At., Mol., Opt. Phys.* **2013**, *88*, 022512.
(278) Nielsen, S. E. B.; Ruggenthaler, M.; van Leeuwen, R. Many-body Quantum Dynamics from the Density. *Europhys. Lett.* **2013**, *101*, 33001.
(279) Ruggenthaler, M.; Penz, M.; van Leeuwen, R. Existence, Uniqueness, and Construction of the Density-Potential Mapping in Time-Dependent Density-Functional Theory. *J. Phys.: Condens. Matter* **2015**, *27*, 203202.
(280) Maitra, N. T.; Zhang, F.; Cave, R. J.; Burke, K. Double Excitations within Time-dependent Density Functional Theory Linear Response. *J. Chem. Phys.* **2004**, *120*, 5932−5937.
(281) Xu, B. X.; Rajagopal, A. K. Current-Density-Functional Theory for Time-Dependent Systems. *Phys. Rev. A: At., Mol., Opt. Phys.* **1985**, *31*, 2682−2684.
(282) Ng, T. K. Transport Properties and a Current-Functional Theory in the Linear-Response regime. *Phys. Rev. Lett.* **1989**, *62*, 2417−2420.
(283) Vignale, G.; Kohn, W. Current-Dependent Exchange-Correlation Potential for Dynamical Linear Response Theory. *Phys. Rev. Lett.* **1996**, *77*, 2037−2040.
(284) Vignale, G.; Ullrich, C. A.; Conti, S. Time-Dependent Density Functional Theory Beyond the Adiabatic Local Density Approximation. *Phys. Rev. Lett.* **1997**, *79*, 4878−4881.
(285) Kurzweil, Y.; Baer, R. Time-Dependent Exchange-Correlation Current Density Functionals with Memory. *J. Chem. Phys.* **2004**, *121*, 8731−8741.
(286) Vignale, G. Mapping from Current Densities to Vector Potentials in Time-Dependent Current Density Functional Theory. *Phys. Rev. B: Condens. Matter Mater. Phys.* **2004**, *70*, 201102.
(287) Ullrich, C. A.; Burke, K. Excitation Energies from Time-Dependent Density-Functional Theory Beyond the Adiabatic Approximation. *J. Chem. Phys.* **2004**, *121*, 28−35.
(288) Tokatly, I. A Unified Approach to the Density-Potential Mapping in a Family of Time-Dependent Density Functional Theories. *Chem. Phys.* **2011**, *391*, 78−82.
(289) Lieb, E. H.; Schrader, R. Current Densities in Density-Functional Theory. *Phys. Rev. A: At., Mol., Opt. Phys.* **2013**, *88*, 032516.
(290) Fuks, J. I.; Lacombe, L.; Nielsen, S. E. B.; Maitra, N. T. Exploring Non-Adiabatic Approximations to the Exchange-Correlation Functional of TDDFT. *Phys. Chem. Chem. Phys.* **2018**, *20*, 26145−26160.
(291) Lacombe, L.; Maitra, N. T. Density-Matrix Coupled Time-Dependent Exchange-Correlation Functional Approximations. *J. Chem. Theory Comput.* **2019**, *15*, 1672−1678.
(292) Fuks, J. I.; Nielsen, S. E. B.; Ruggenthaler, M.; Maitra, N. T. Time-Dependent Density Functional Theory Beyond Kohn-Sham Slater Determinants. *Phys. Chem. Chem. Phys.* **2016**, *18*, 20976−20985.
(293) Almbladh, C.-O.; von Barth, U. Exact Results for the Charge and Spin Densities, Exchange-Correlation Potentials, and Density-Functional Eigenvalues. *Phys. Rev. B: Condens. Matter Mater. Phys.* **1985**, *31*, 3231−3244.
(294) Dobson, J. F. Harmonic-Potential Theorem: Implications for Approximate Many-Body Theories. *Phys. Rev. Lett.* **1994**, *73*, 2244−2247.
(295) Vignale, G. Center of Mass and Relative Motion in Time Dependent Density Functional Theory. *Phys. Rev. Lett.* **1995**, *74*, 3233−3236.
(296) Sun, J.; Ruzsinszky, A.; Perdew, J. P. Strongly Constrained and Appropriately Normed Semilocal Density Functional. *Phys. Rev. Lett.* **2015**, *115*, 036402.
(297) Elliott, P.; Maitra, N. T. Propagation of Initially Excited States in Time-Dependent Density-Functional Theory. *Phys. Rev. A: At., Mol., Opt. Phys.* **2012**, *85*, 052510.
(298) Bruner, A.; Hernandez, S.; Mauger, F.; Abanador, P. M.; LaMaster, D. J.; Gaarde, M. B.; Schafer, K. J.; Lopata, K. Attosecond Charge Migration with TDDFT: Accurate Dynamics from a Well-Defined Initial State. *J. Phys. Chem. Lett.* **2017**, *8*, 3991−3996.
(299) Bowman, D. N.; Asher, J. C.; Fischer, S. A.; Cramer, C. J.; Govind, N. Excited-State Absorption in Tetrapyridyl Porphyrins: Comparing Real-Time and Quadratic-Response Time-Dependent Density Functional Theory. *Phys. Chem. Chem. Phys.* **2017**, *19*, 27452−27462.
(300) Wu, Q.; Van Voorhis, T. Direct Optimization Method to Study Constrained Systems within Density-Functional Theory. *Phys. Rev. A: At., Mol., Opt. Phys.* **2005**, *72*, 024502.
(301) Eshuis, H.; Van Voorhis, T. The Influence of Initial Conditions on Charge Transfer Dynamics. *Phys. Chem. Chem. Phys.* **2009**, *11*, 10293−10298.
(302) Tozer, D. J.; Handy, N. C. On the Determination of Excitation Energies using Density Functional Theory. *Phys. Chem. Chem. Phys.* **2000**, *2*, 2117−2121.
(303) Silva-Junior, M. R.; Schreiber, M.; Sauer, S. P. A.; Thiel, W. Benchmarks for Electronically Excited States: Time-Dependent Density Functional Theory and Density Functional Theory Based Multireference Configuration Interaction. *J. Chem. Phys.* **2008**, *129*, 104103.
(304) Rohrdanz, M. A.; Herbert, J. M. Simultaneous Benchmarking of Ground- and Excited-State Properties with Long-Range-Corrected Density Functional Theory. *J. Chem. Phys.* **2008**, *129*, 034107.
(305) Jacquemin, D.; Wathelet, V.; Perpète, E. A.; Adamo, C. Extensive TD-DFT Benchmark: Singlet-Excited States of Organic Molecules. *J. Chem. Theory Comput.* **2009**, *5*, 2420−2435.
(306) Jacquemin, D.; Perpete, E. A.; Ciofini, I.; Adamo, C.; Valero, R.; Zhao, Y.; Truhlar, D. G. On the Performances of the M06 Family of Density Functionals for Electronic Excitation Energies. *J. Chem. Theory Comput.* **2010**, *6*, 2071−2085.
(307) Plotner, J.; Tozer, D. J.; Dreuw, A. Dependence of Excited State Potential Energy Surfaces on the Spatial Overlap of the Kohn-Sham Orbitals and the Amount of Nonlocal Hartree-Fock Exchange in Time-Dependent Density Functional Theory. *J. Chem. Theory Comput.* **2010**, *6*, 2315−2324.
(308) Caricato, M.; Trucks, G. W.; Frisch, M. J.; Wiberg, K. B. Electronic Transition Energies: A Study of the Performance of a Large Range of Single Reference Density Functional and Wave Function Methods on Valence and Rydberg States Compared to Experiment. *J. Chem. Theory Comput.* **2010**, *6*, 370−383.
(309) Caricato, M.; Trucks, G. W.; Frisch, M. J.; Wiberg, K. B. Oscillator Strength: How Does TDDFT Compare to EOM-CCSD? *J. Chem. Theory Comput.* **2011**, *7*, 456−466.
(310) Leang, S. S.; Zahariev, F.; Gordon, M. S. Benchmarking the Performance of Time-Dependent Density Functional Methods. *J. Chem. Phys.* **2012**, *136*, 104101.
(311) Gonzalez, L.; Escudero, D.; Serrano-Andres, L. Progress and Challenges in the Calculation of Electronic Excited States. *ChemPhysChem* **2012**, *13*, 28−51.
(312) Guido, C. A.; Knecht, S.; Kongsted, J.; Mennucci, B. Benchmarking Time-Dependent Density Functional Theory for Excited State Geometries of Organic Molecules in Gas-Phase and in Solution. *J. Chem. Theory Comput.* **2013**, *9*, 2209−2220.
(313) Prlj, A.; Curchod, B. F. E.; Fabrizio, A.; Floryan, L.; Corminboeuf, C. Qualitatively Incorrect Features in the TDDFT Spectrum of Thiophene-Based Compounds. *J. Phys. Chem. Lett.* **2015**, *6*, 13−21.

https://dx.doi.org/10.1021/acs.chemrev.0c00223
Chem. Rev. XXXX, XXX, XXX−XXX

(314) Tozer, D. J.; Amos, R. D.; Handy, N. C.; Roos, B. O.; Serrano-Andres, L. Does Density Dunctional Theory Contribute to the Understanding of Excited States of Unsaturated Organic Compounds? *Mol. Phys.* **1999**, *97*, 859−868.
(315) Tozer, D. J. Relationship between Long-Range Charge-Transfer Excitation Energy Error and Integer Discontinuity in Kohn-Sham Theory. *J. Chem. Phys.* **2003**, *119*, 12697−12699.
(316) Dreuw, A.; Weisman, J. L.; Head-Gordon, M. Long-Range Charge-Transfer Excited States in Time-Dependent Density Functional Theory Require Non-Local Exchange. *J. Chem. Phys.* **2003**, *119*, 2943−2946.
(317) Bernasconi, L.; Sprik, M.; Hutter, J. Time Dependent Density Functional Theory Study of Charge-Transfer and Intramolecular Electronic Excitations in Acetone-Water Systems. *J. Chem. Phys.* **2003**, *119*, 12417−12431.
(318) Lange, A.; Herbert, J. M. Simple Methods To Reduce Charge-Transfer Contamination in Time-Dependent Density-Functional Calculations of Clusters and Liquids. *J. Chem. Theory Comput.* **2007**, *3*, 1680−1690.
(319) Neugebauer, J.; Louwerse, M. J.; Baerends, E. J.; Wesolowski, T. A. The Merits of the Frozen-Density Embedding Scheme to Model Solvatochromic Shifts. *J. Chem. Phys.* **2005**, *122*, 094115.
(320) Isborn, C. M.; Mar, B. D.; Curchod, B. F. E.; Tavernelli, I.; Martínez, T. J. The Charge Transfer Problem in Density Functional Theory Calculations of Aqueously Solvated Molecules. *J. Phys. Chem. B* **2013**, *117*, 12189−12201.
(321) Tawada, Y.; Tsuneda, T.; Yanagisawa, S.; Yanai, T.; Hirao, K. A Long-Range-Corrected Time-Dependent Density Functional Theory. *J. Chem. Phys.* **2004**, *120*, 8425−8433.
(322) Vydrov, O. A.; Scuseria, G. E. Assessment of a Long-Range Corrected Hybrid Functional. *J. Chem. Phys.* **2006**, *125*, 234109.
(323) Rohrdanz, M. A.; Martins, K. M.; Herbert, J. M. A Long-Range-Corrected Density Functional that Performs Well for both Ground-State Properties and Time-Dependent Density Functional Theory Excitation Energies, including Charge-Transfer Excited States. *J. Chem. Phys.* **2009**, *130*, 054112.
(324) Stein, T.; Kronik, L.; Baer, R. Reliable Prediction of Charge Transfer Excitations in Molecular Complexes Using Time-Dependent Density Functional Theory. *J. Am. Chem. Soc.* **2009**, *131*, 2818−2820.
(325) Autschbach, J. Charge-Transfer Excitations and Time-Dependent Density Functional Theory: Problems and Some Proposed Solutions. *ChemPhysChem* **2009**, *10*, 1757−1760.
(326) Garrett, K.; Sosa Vazquez, X.; Egri, S. B.; Wilmer, J.; Johnson, L. E.; Robinson, B. H.; Isborn, C. M. Optimum Exchange for Calculation of Excitation Energies and Hyperpolarizabilities of Organic Electro-optic Chromophores. *J. Chem. Theory Comput.* **2014**, *10*, 3821−3831.
(327) Casida, M. E.; Jamorski, C.; Casida, K. C.; Salahub, D. R. Molecular Excitation Energies to High-Lying Bound States from Time-Dependent Density-Functional Response Theory: Characterization and Correction of the Time-Dependent Local Density Approximation Ionization Threshold. *J. Chem. Phys.* **1998**, *108*, 4439−4449.
(328) Tozer, D. J.; Handy, N. C. Improving Virtual Kohn-Sham Orbitals and Eigenvalues: Application to Excitation Energies and Static Polarizabilities. *J. Chem. Phys.* **1998**, *109*, 10180−10189.
(329) Hirata, S.; Zhan, C.-G.; Apra, E.; Windus, T. L.; Dixon, D. A. A New, Self-Contained Asymptotic Correction Scheme To Exchange-Correlation Potentials for Time-Dependent Density Functional Theory. *J. Phys. Chem. A* **2003**, *107*, 10154−10158.
(330) van Meer, R.; Gritsenko, O. V.; Baerends, E. J. Physical Meaning of Virtual Kohn-Sham Orbitals and Orbital Energies: An Ideal Basis for the Description of Molecular Excitations. *J. Chem. Theory Comput.* **2014**, *10*, 4432−4441.
(331) Li, S. L.; Truhlar, D. G. Improving Rydberg Excitations within Time-Dependent Density Functional Theory with Generalized Gradient Approximations: The Exchange-Enhancement-for-Large-Gradient Scheme. *J. Chem. Theory Comput.* **2015**, *11*, 3123−3130.
(332) Neugebauer, J.; Baerends, E. J.; Nooijen, M. Vibronic Coupling and Double Excitations in Linear Response Time-Dependent Density Functional Calculations: Dipole-Allowed States of N_2. *J. Chem. Phys.* **2004**, *121*, 6155−6166.
(333) Cave, R. J.; Zhang, F.; Maitra, N. T.; Burke, K. A Dressed TDDFT Treatment of the 2^1Ag States of Butadiene and Hexatriene. *Chem. Phys. Lett.* **2004**, *389*, 39−42.
(334) Levine, B. G.; Ko, C.; Quenneville, J.; Martinez, T. J. Conical Intersections and Double Excitations in Time-Dependent Density Functional Theory. *Mol. Phys.* **2006**, *104*, 1039−1051.
(335) Elliott, P.; Goldson, S.; Canahui, C.; Maitra, N. T. Perspectives on Double-Excitations in TDDFT. *Chem. Phys.* **2011**, *391*, 110−119.
(336) Shu, Y.; Truhlar, D. G. Doubly Excited Character or Static Correlation of the Reference State in the Controversial 2^1A_g State of trans-Butadiene? *J. Am. Chem. Soc.* **2017**, *139*, 13770−13778.
(337) Loos, P.-F.; Boggio-Pasqua, M.; Scemama, A.; Caffarel, M.; Jacquemin, D. Reference Energies for Double Excitations. *J. Chem. Theory Comput.* **2019**, *15*, 1939−1956.
(338) Besley, N. A.; Asmuruf, F. A. Time-dependent Density Functional Theory Calculations of the Spectroscopy of Core Electrons. *Phys. Chem. Chem. Phys.* **2010**, *12*, 12024−12039.
(339) Lestrange, P. J.; Nguyen, P. D.; Li, X. Calibration of Energy-Specific TDDFT for Modeling K-Edge XAS Spectra of Light Elements. *J. Chem. Theory Comput.* **2015**, *11*, 2994−2999.
(340) Stetina, T. F.; Kasper, J. M.; Li, X. Modeling $L_{2,3}$-Edge X-ray Absorption Spectroscopy with Linear Response Exact Two-Component Relativistic Time-Dependent Density Functional Theory. *J. Chem. Phys.* **2019**, *150*, 234103.
(341) Cramer, C. J.; Truhlar, D. G. Density Functional Theory for Transition Metals and Transition Metal Chemistry. *Phys. Chem. Chem. Phys.* **2009**, *11*, 10757−10816.
(342) Zlatar, M.; Gruden-Pavlović, M.; Guell, M.; Swart, M. Computational Study of the Spin-State Energies and UV-Vis Spectra of bis(1,4,7-triazacyclononane) Complexes of Some First-row Transition Metal Cations. *Phys. Chem. Chem. Phys.* **2013**, *15*, 6631−6639.
(343) Vlahović, F.; Perić, M.; Gruden-Pavlović, M.; Zlatar, M. Assessment of TD-DFT and LF-DFT for Study of d-d Transitions in First Row Transition Metal Hexaaqua Complexes. *J. Chem. Phys.* **2015**, *142*, 214111.
(344) Thiel, W. Semiempirical Quantum−Chemical Methods. *Wiley Interdiscip. Rev.: Comput. Mol. Sci.* **2014**, *4*, 145−157.
(345) Hückel, E. Quantentheoretische Beiträge zum Benzolproblem. *Eur. Phys. J. A* **1931**, *70*, 204−286.
(346) Hoffmann, R. An Extended Hückel Theory. I. Hydrocarbons. *J. Chem. Phys.* **1963**, *39*, 1397−1412.
(347) Pople, J. A.; Segal, G. A. Approximate Self-Consistent Molecular Orbital Theory. II. Calculations with Complete Neglect of Differential Overlap. *J. Chem. Phys.* **1965**, *43*, S136−S151.
(348) Pople, J. A.; Segal, G. A. Approximate Self-Consistent Molecular Orbital Theory. III. CNDO Results for AB_2 and AB_3 Systems. *J. Chem. Phys.* **1966**, *44*, 3289−3296.
(349) Pople, J.; Beveridge, D.; Dobosh, P. Approximate Self-Consistent Molecular-Orbital Theory. V. Intermediate Neglect of Differential Overlap. *J. Chem. Phys.* **1967**, *47*, 2026−2033.
(350) Pople, J. A.; Santry, D. P.; Segal, G. A. Approximate Self-Consistent Molecular Orbital Theory. I. Invariant Procedures. *J. Chem. Phys.* **1965**, *43*, S129−S135.
(351) Ridley, J.; Zerner, M. An Intermediate Neglect of Differential Overlap Technique for Spectroscopy: Pyrrole and the Azines. *Theor. Chem. Acc.* **1973**, *32*, 111−134.
(352) Ridley, J. E.; Zerner, M. C. Triplet States via Intermediate Neglect of Differential Overlap: Benzene, Pyridine and the Diazines. *Theor. Chem. Acc.* **1976**, *42*, 223−236.
(353) Baker, J. D.; Zerner, M. C. Characterization of the Random Phase Approximation with the Intermediate Neglect of Differential Overlap Hamiltonian for Electronic Spectroscopy. *J. Phys. Chem.* **1991**, *95*, 8614−8619.
(354) Baker, J. D.; Zerner, M. C. Applications of the Random Phase Approximation with the INDO/S Hamiltonian: UV/VIS Spectra of Free Base Porphin. *Chem. Phys. Lett.* **1990**, *175*, 192−196.

https://dx.doi.org/10.1021/acs.chemrev.0c00223
Chem. Rev. XXXX, XXX, XXX−XXX

(355) Parkinson, W. A.; Zerner, M. C. Calculation of Molecular Polarizabilities for Large Systems within the Random Phase Approximation. *Chem. Phys. Lett.* **1987**, *139*, 563−570.
(356) Tretiak, S.; Mukamel, S. Density Matrix Analysis and Simulation of Electronic Excitations in Conjugated and Aggregated Molecules. *Chem. Rev.* **2002**, *102*, 3171−3212.
(357) Voityuk, A. A. Intermediate Neglect of Differential Overlap for Spectroscopy. *WIREs Comput. Mol. Sci.* **2013**, *3*, 515−527.
(358) Quarti, C.; Fazzi, D.; Del Zoppo, M. A Computational Investigation on Singlet and Triplet Exciton Couplings in Acene Molecular Crystals. *Phys. Chem. Chem. Phys.* **2011**, *13*, 18615−18625.
(359) Nguyen, K. A.; Day, P. N.; Pachter, R.; Tretiak, S.; Chernyak, V.; Mukamel, S. Analysis of Absorption Spectra of Zinc Porphyrin, Zinc m eso-Tetraphenylporphyrin, and Halogenated Derivatives. *J. Phys. Chem. A* **2002**, *106*, 10285−10293.
(360) Rand, B. P.; Cheyns, D.; Vasseur, K.; Giebink, N. C.; Mothy, S.; Yi, Y.; Coropceanu, V.; Beljonne, D.; Cornil, J.; Brédas, J.-L.; Genoe, J. The Impact of Molecular Orientation on the Photovoltaic Properties of a Phthalocyanine/Fullerene Heterojunction. *Adv. Funct. Mater.* **2012**, *22*, 2987−2995.
(361) Hutchison, G. R.; Ratner, M. A.; Marks, T. J. Accurate Prediction of Band Gaps in Neutral Heterocyclic Conjugated Polymers. *J. Phys. Chem. A* **2002**, *106*, 10596−10605.
(362) Beenken, W. J. Photo-Induced Charge Transfer in Fullerene−Oligothiophene Dyads−A Quantum-Chemical Study. *Chem. Phys.* **2009**, *357*, 144−150.
(363) Pourtois, G.; Beljonne, D.; Cornil, J.; Ratner, M. A.; Brédas, J. Photoinduced Electron-Transfer Processes along Molecular Wires based on Phenylenevinylene Oligomers: A Quantum-Chemical Insight. *J. Am. Chem. Soc.* **2002**, *124*, 4436−4447.
(364) Cory, M. G.; Zerner, M. C.; Hu, X.; Schulten, K. Electronic Excitations in Aggregates of Bacteriochlorophylls. *J. Phys. Chem. B* **1998**, *102*, 7640−7650.
(365) Starikov, E.; Cuniberti, G.; Tanaka, S. Conformation Dependence of DNA Exciton Parentage. *J. Phys. Chem. B* **2009**, *113*, 10428−10435.
(366) Lobaugh, J.; Rossky, P. J. Solvent and Intramolecular Effects on the Absorption Spectrum of Betaine-30. *J. Phys. Chem. A* **2000**, *104*, 899−907.
(367) Gieseking, R. L.; Ratner, M. A.; Schatz, G. C. Semiempirical Modeling of Ag Nanoclusters: New Parameters for Optical Property Studies Enable Determination of Double Excitation Contributions to Plasmonic Excitation. *J. Phys. Chem. A* **2016**, *120*, 4542−4549.
(368) Gieseking, R. L.; Ratner, M. A.; Schatz, G. C. Quantum Mechanical Identification of Quadrupolar Plasmonic Excited States in Silver Nanorods. *J. Phys. Chem. A* **2016**, *120*, 9324−9329.
(369) Bacon, A. D.; Zerner, M. C. An Intermediate Neglect of Differential Overlap Theory for Transition Metal Complexes: Fe, Co and Cu Chlorides. *Theor. Chem. Acc.* **1979**, *53*, 21−54.
(370) Zerner, M. C.; Loew, G. H.; Kirchner, R. F.; Mueller-Westerhoff, U. T. An Intermediate Neglect of Differential Overlap Technique for Spectroscopy of Transition-Metal Complexes. Ferrocene. *J. Am. Chem. Soc.* **1980**, *102*, 589−599.
(371) Cory, M. G.; Köstlmeier, S.; Kotzian, M.; Rösch, N.; Zerner, M. C. An Intermediate Neglect of Differential Overlap Technique for Actinide Compounds. *J. Chem. Phys.* **1994**, *100*, 1353−1365.
(372) Kotzian, M.; Rösch, N.; Zerner, M. Intermediate Neglect of Differential Overlap Spectroscopic Studies on Lanthanide Complexes. *Theor. Chem. Acc.* **1992**, *81*, 201−222.
(373) Voityuk, A. A. INDO/X: A New Semiempirical Method for Excited States of Organic and Biological Molecules. *J. Chem. Theory Comput.* **2014**, *10*, 4950−4958.
(374) Dewar, M. J.; Thiel, W. Ground States of Molecules. 38. The MNDO Method. Approximations and Parameters. *J. Am. Chem. Soc.* **1977**, *99*, 4899−4907.
(375) Dewar, M. J.; Thiel, W. Ground States of Molecules. 39. MNDO Results for Molecules Containing Hydrogen, Carbon, Nitrogen, and Oxygen. *J. Am. Chem. Soc.* **1977**, *99*, 4907−4917.
(376) Stewart, J. J. Optimization of Parameters for Semiempirical Methods I. Method. *J. Comput. Chem.* **1989**, *10*, 209−220.
(377) Stewart, J. J. Optimization of Parameters for Semiempirical Methods II. Applications. *J. Comput. Chem.* **1989**, *10*, 221−264.
(378) Porezag, D.; Frauenheim, T.; Köhler, T.; Seifert, G.; Kaschner, R. Construction of Tight-Binding-Like Potentials on the Basis of Density-Functional Theory: Application to Carbon. *Phys. Rev. B: Condens. Matter Mater. Phys.* **1995**, *51*, 12947.
(379) Elstner, M.; Porezag, D.; Jungnickel, G.; Elsner, J.; Haugk, M.; Frauenheim, T.; Suhai, S.; Seifert, G. Self-Consistent-Charge Density-Functional Tight-Binding Method for Simulations of Complex Materials Properties. *Phys. Rev. B: Condens. Matter Mater. Phys.* **1998**, *58*, 7260−7268.
(380) Wang, F.; Yam, C. Y.; Chen, G.; Wang, X.; Fan, K.; Niehaus, T. A.; Frauenheim, T. Linear Scaling Time-Dependent Density-Functional Tight-Binding Method for Absorption Spectra of Large Systems. *Phys. Rev. B: Condens. Matter Mater. Phys.* **2007**, *76*, 045114.
(381) Chen, G. H.; Mukamel, S. Reduced Electronic Density Matrices, Effective Hamiltonians, and Nonlinear Susceptibilities of Conjugated Polyenes. *J. Chem. Phys.* **1995**, *103*, 9355−9362.
(382) Chen, G. H.; Mukamel, S. Effective Hamiltonian for Conjugated Polyenes Based on the Ground State Single-electron Density Matrix. *Chem. Phys. Lett.* **1996**, *258*, 589−594.
(383) Chen, G. H.; Mukamel, S. Nonlinear Polarizabilities of Donor-Acceptor Substituted Conjugated Polyenes. *J. Phys. Chem.* **1996**, *100*, 11080−11085.
(384) Suzuki, M.; Mukamel, S. Charge and Bonding Redistribution in Octatetraene Driven by a Strong Laser Field: Time-Dependent Hartree-Fock Simulation. *J. Chem. Phys.* **2003**, *119*, 4722−4730.
(385) Campbell, L.; Tanaka, S.; Mukamel, S. Ligand Effects on the X-ray Absorption of a Nickel Porphyrin Complex: A Simulation Study. *Chem. Phys.* **2004**, *299*, 225−231.
(386) Bartell, L. A.; Wall, M. R.; Neuhauser, D. A Time-Dependent Semiempirical Approach to Determining Excited States. *J. Chem. Phys.* **2010**, *132*, 234106.
(387) Ghosh, S.; Andersen, A.; Gagliardi, L.; Cramer, C. J.; Govind, N. Modeling Optical Spectra of Large Organic Systems Using Real-Time Propagation of Semiempirical Effective Hamiltonians. *J. Chem. Theory Comput.* **2017**, *13*, 4410−4420.
(388) Ilawe, N. V.; Oviedo, M. B.; Wong, B. M. Real-Time Quantum Dynamics of Long-Range Electronic Excitation Transfer in Plasmonic Nanoantennas. *J. Chem. Theory Comput.* **2017**, *13*, 3442−3454.
(389) Ilawe, N. V.; Oviedo, M. B.; Wong, B. M. Effect of Quantum Tunneling on the Efficiency of Excitation Energy Transfer in Plasmonic Nanoparticle Chain Waveguides. *J. Mater. Chem. C* **2018**, *6*, 5857−5864.
(390) Oviedo, M. B.; Zarate, X.; Negre, C. F. A.; Schott, E.; Arratia-Perez, R.; Sanchez, C. G. Quantum Dynamical Simulations as a Tool for Predicting Photoinjection Mechanisms in Dye-Sensitized TiO_2 Solar Cells. *J. Phys. Chem. Lett.* **2012**, *3*, 2548−2555.
(391) Negre, C. F. A.; Fuertes, V. C.; Oviedo, M. B.; Oliva, F. Y.; Sanchez, C. G. Quantum Dynamics of Light-Induced Charge Injection in a Model Dye-Nanoparticle Complex. *J. Phys. Chem. C* **2012**, *116*, 14748−14753.
(392) Krause, P.; Klamroth, T.; Saalfrank, P. Molecular Response Properties from Explicitly Time-dependent Configuration Interaction Methods. *J. Chem. Phys.* **2007**, *127*, 034107.
(393) White, A. F.; Heide, C. J.; Saalfrank, P.; Head-Gordon, M.; Luppi, E. Computation of High-harmonic Generation Spectra of the Hydrogen Molecule using Time-dependent Configuration-interaction. *Mol. Phys.* **2016**, *114*, 947−956.
(394) Nest, M.; Klamroth, T.; Saalfrank, P. The Multiconfiguration Time-dependent Hartree−Fock Method for Quantum Chemical Calculations. *J. Chem. Phys.* **2005**, *122*, 124102.
(395) Kato, T.; Kono, H. Time-dependent Multiconfiguration Theory for Electronic Dynamics of Molecules in Intense Laser Fields: A Description in Terms of Numerical Orbital Functions. *J. Chem. Phys.* **2008**, *128*, 184102.

https://dx.doi.org/10.1021/acs.chemrev.0c00223
Chem. Rev. XXXX, XXX, XXX−XXX

(396) Peng, W. T.; Fales, B. S.; Levine, B. G. Simulating Electron Dynamics of Complex Molecules with Time-Dependent Complete Active Space Configuration Interaction. *J. Chem. Theory Comput.* **2018**, *14*, 4129−4138.
(397) Olsen, J.; Roos, B. O.; Jørgensen, P. Determinant Based Configuration Interaction Algorithms for Complete and Restricted Configuration Interaction Spaces. *J. Chem. Phys.* **1988**, *89*, 2185−2192.
(398) Greenman, L.; Ho, P. J.; Pabst, S.; Kamarchik, E.; Mazziotti, D. A.; Santra, R. Implementation of the Time-Dependent Configuration-Interaction Singles Method for Atomic Strong-Field Processes. *Phys. Rev. A: At., Mol., Opt. Phys.* **2010**, *82*, 023406.
(399) Sato, T.; Orimo, Y.; Teramura, T.; Tugs, O.; Ishikawa, K. L. In *Progress in Ultrafast Intense Laser Science XIV*; Yamanouchi, K., Martin, P., Sentis, M., Ruxin, L., Normand, D., Eds.; Springer International Publishing: Cham, 2018; pp 143−171.
(400) Sonk, J. A.; Schlegel, H. B. TD-CI Simulation of the Electronic Optical Response of Molecules in Intense Fields II: Comparison of DFT Functionals and EOM-CCSD. *J. Phys. Chem. A* **2011**, *115*, 11832−11840.
(401) Kato, T.; Kono, H. Time-Dependent Multiconfiguration Theory for Electronic Dynamics of Molecules in an Intense Laser Field. *Chem. Phys. Lett.* **2004**, *392*, 533−540.
(402) Purvis, G. D.; Bartlett, R. J. A Full Coupled-Cluster Singles and Doubles Model: The Inclusion of Disconnected Triples. *J. Chem. Phys.* **1982**, *76*, 1910.
(403) Hoodbhoy, P.; Negele, J. W. Time-Dependent Coupled-Cluster Approximation to Nuclear Dynamics. I. Application to a Solvable Model. *Phys. Rev. C: Nucl. Phys.* **1978**, *18*, 2380−2394.
(404) Kvaal, S. Ab Initio Quantum Dynamics using Coupled-cluster. *J. Chem. Phys.* **2012**, *136*, 194109.
(405) Pedersen, T. B.; Kvaal, S. Symplectic Integration and Physical Interpretation of Time-dependent Coupled-cluster Theory. *J. Chem. Phys.* **2019**, *150*, 144106.
(406) Hoodbhoy, P.; Negele, J. W. Time-Dependent Coupled-Cluster Approximation to Nuclear Dynamics. II. General Formulation. *Phys. Rev. C: Nucl. Phys.* **1979**, *19*, 1971−1982.
(407) Schönhammer, K.; Gunnarsson, O. Time-Dependent Approach to the Calculation of Spectral Functions. *Phys. Rev. B: Condens. Matter Mater. Phys.* **1978**, *18*, 6606−6614.
(408) Köhn, A.; Olsen, J. Orbital-Optimized Coupled-Cluster Theory does not Reproduce the Full Configuration-Interaction Limit. *J. Chem. Phys.* **2005**, *122*, 084116.
(409) Mukherjee, D.; Mukherjee, P. A Response-Function Approach to the Direct Calculation of the Transition-Energy in a Multiple-Cluster Expansion Formalism. *Chem. Phys.* **1979**, *39*, 325−335.
(410) Emrich, K. An Extension of the Coupled Cluster Formalism to Excited States (I). *Nucl. Phys. A* **1981**, *351*, 379−396.
(411) Stanton, J. F.; Bartlett, R. J. The Equation of Motion Coupled-cluster Method. A Systematic Biorthogonal Approach to Molecular Excitation Energies, Transition Probabilities, and Excited State Properties. *J. Chem. Phys.* **1993**, *98*, 7029−7039.
(412) Heller, E. J. Quantum Corrections to Classical Photo-dissociation Models. *J. Chem. Phys.* **1978**, *68*, 2066−2075.
(413) Heller, E. J.; Stechel, E. B.; Davis, M. J. Molecular Spectra, Fermi Resonances, and Classical Motion. *J. Chem. Phys.* **1980**, *73*, 4720−4735.
(414) Mukamel, S. On the Semiclassical Calculation of Molecular Absorption and Fluorescence Spectra. *J. Chem. Phys.* **1982**, *77*, 173−181.
(415) Prasad, M. D. Time-Dependent Coupled Cluster Method: A New Approach to the Calculation of Molecular Absorption Spectra. *J. Chem. Phys.* **1988**, *88*, 7005−7010.
(416) Christiansen, O.; Koch, H.; Jørgensen, P. The Second-order Approximate Coupled Cluster Singles and Doubles Model CC2. *Chem. Phys. Lett.* **1995**, *243*, 409−418.
(417) Ilias, M.; Saue, T. An Infinite-Order Relativistic Hamiltonian by a Simple One-Step Transformation. *J. Chem. Phys.* **2007**, *126*, 064102.
(418) Saue, T. Relativistic Hamiltonians for Chemistry: A Primer. *ChemPhysChem* **2011**, *12*, 3077−3094.
(419) Peng, D.; Middendorf, N.; Weigend, F.; Reiher, M. An Efficient Implementation of Two-Component Relativistic Exact-Decoupling Methods for Large Molecules. *J. Chem. Phys.* **2013**, *138*, 184105.
(420) Kutzelnigg, W.; Liu, W. Quasirelativistic Theory Equivalent to Fully Relativistic Theory. *J. Chem. Phys.* **2005**, *123*, 241102.
(421) Liu, W.; Peng, D. Infinite-Order Quasirelativistic Density Functional Method Based on the Exact Matrix Quasirelativistic Theory. *J. Chem. Phys.* **2006**, *125*, 044102.
(422) Liu, W.; Peng, D. Exact Two-Component Hamiltonians Revisited. *J. Chem. Phys.* **2009**, *131*, 031104.
(423) Peng, D.; Liu, W.; Xiao, Y.; Cheng, L. Making Four- and Two-Component Relativistic Density Functional Methods Fully Equivalent Based on the Idea of From Atoms to Molecule. *J. Chem. Phys.* **2007**, *127*, 104106.
(424) Liu, W. Ideas of Relativistic Quantum Chemistry. *Mol. Phys.* **2010**, *108*, 1679−1706.
(425) Liu, W. Advances in Relativistic Molecular Quantum Mechanics. *Phys. Rep.* **2014**, *537*, 59−89.
(426) Liu, W. The Big Picture of Relativistic Molecular Quantum Mechanics. *Natl. Sci. Rev.* **2016**, *3*, 204−221.
(427) Egidi, F.; Goings, J. J.; Frisch, M. J.; Li, X. Direct Atomic-Orbital-Based Relativistic Two-Component Linear Response Method for Calculating Excited-State Fine Structures. *J. Chem. Theory Comput.* **2016**, *12*, 3711−3718.
(428) Williams-Young, D.; Egidi, F.; Li, X. Relativistic Two-Component Particle-Particle Tamm-Dancoff Approximation. *J. Chem. Theory Comput.* **2016**, *12*, 5379−5384.
(429) Egidi, F.; Sun, S.; Goings, J. J.; Scalmani, G.; Frisch, M. J.; Li, X. Two-Component Non-Collinear Time-Dependent Spin Density Functional Theory for Excited State Calculations. *J. Chem. Theory Comput.* **2017**, *13*, 2591−2603.
(430) Liu, W. *Handbook of Relativistic Quantum Chemistry*; Springer-Verlag Berlin Heidelberg, 2017.
(431) Petrone, A.; Williams-Young, D. B.; Sun, S.; Stetina, T. F.; Li, X. An Efficient Implementation of Two-Component Relativistic Density Functional Theory with Torque-Free Auxiliary Variables. *Eur. Phys. J. B* **2018**, *91*, 169.
(432) Neville, S. P.; Schuurman, M. S. Efficient Solution of the Electronic Eigenvalue Problem Using Wavepacket Propagation. *J. Chem. Theory Comput.* **2018**, *14*, 1433−1441.
(433) Seeger, R.; Pople, J. A. Self-Consistent Molecular Orbital Methods. XVIII. Constraints and Stability in Hartree-Fock Theory. *J. Chem. Phys.* **1977**, *66*, 3045−3050.
(434) Fukutome, H. Unrestricted Hartree−Fock Theory and Its Applications to Molecules and Chemical Reactions. *Int. J. Quantum Chem.* **1981**, *20*, 955−1065.
(435) Stuber, J. L.; Paldus, J. In *Fundamental World of Quantum Chemistry: A Tribute Vol. to the Memory of Per-Olov Löwdin*; Brändas, E. J., S.Kryachko, E., Eds.; Kluwer Academic Publishers, 2003; pp 67−139.
(436) Löwdin, P.-O.; Mayer, I. Some Studies of the General Hartree-Fock Method. *Adv. Quantum Chem.* **1992**, *24*, 79−114.
(437) Yamaki, D.; Shigeta, Y.; Yamanaka, S.; Nagao, H.; Yamaguchi, K. MP2, Tamm-Dancoff, and RPA Methods Based on the Generalized HF Solution. *Int. J. Quantum Chem.* **2000**, *80*, 701−707.
(438) Yamanaka, S.; Yamaki, D.; Shigeta, Y.; Nagao, H.; Yamaguchi, K. Noncollinear Spin Density Functional Theory for Spin-Frustrated and Spin-Degenerate Systems. *Int. J. Quantum Chem.* **2001**, *84*, 670−676.
(439) van Wüllen, C. Spin Densities in Two-Component Relativistic Density Functional Calculations: Noncollinear versus Collinear Approach. *J. Comput. Chem.* **2002**, *23*, 779−785.
(440) Schimpl, J.; Petrilli, H. M.; Blöchl, P. E. Nitrogen Binding to the FeMo-Cofactor of Nitrogenase. *J. Am. Chem. Soc.* **2003**, *125*, 15772−15778.
(441) Kurz, P.; Bihlmayer, G.; Hirai, K.; Blügel, S. Ab Initio Treatment of Noncollinear Magnets with the Full-Potential Linearized Augmented Plane Wave Method. *Phys. Rev. B: Condens. Matter Mater. Phys.* **2004**, *69*, 024415.

https://dx.doi.org/10.1021/acs.chemrev.0c00223
Chem. Rev. XXXX, XXX, XXX−XXX

(442) Sharma, S.; Dewhurst, J.; Ambrosch-Draxl, C.; Kurth, S.; Helbig, N.; Pittalis, S.; Shallcross, S.; Nordström, L.; Gross, E. First-principles Approach to Noncollinear Magnetism: Towards Spin Dynamics. *Phys. Rev. Lett.* **2007**, *98*, 196405.
(443) Peralta, J. E.; Scuseria, G. E.; Frisch, M. J. Noncollinear Magnetism in Density Functional Calculations. *Phys. Rev. B: Condens. Matter Mater. Phys.* **2007**, *75*, 125119.
(444) Armbruster, M. K.; Weigend, F.; van Wullen, C.; Klopper, W. Self-consistent Treatment of Spin−Orbit Interactions with Efficient Hartree−Fock and Density Functional Methods. *Phys. Chem. Chem. Phys.* **2008**, *10*, 1748−1756.
(445) Li, Z.; Liu, W. Spin-Adapted Open-Shell Time-Dependent Density Functional Theory. III. An Even Better and Simpler Formulation. *J. Chem. Phys.* **2011**, *135*, 194106.
(446) Luo, S.; Rivalta, I.; Batista, V.; Truhlar, D. G. Noncollinear Spins Provide a Self-Consistent Treatment of the Low-Spin State of a Biomimetic Oxomanganese Synthetic Trimer Inspired by the Oxygen Evolving Complex of Photosystem II. *J. Phys. Chem. Lett.* **2011**, *2*, 2629−2633.
(447) Scalmani, G.; Frisch, M. J. A New Approach to Noncollinear Spin Density Functional Theory Beyond the Local Density Approximation. *J. Chem. Theory Comput.* **2012**, *8*, 2193−2196.
(448) Bulik, I. W.; Scalmani, G.; Frisch, M. J.; Scuseria, G. E. Noncollinear Density Functional Theory Having Proper Invariance and Local Torque Properties. *Phys. Rev. B: Condens. Matter Mater. Phys.* **2013**, *87*, 035117.
(449) Luo, S.; Truhlar, D. G. Noncollinear Spin States for Density Functional Calculations of Open-Shell and Multi-Configurational Systems: Dissociation of MnO and NiO and Barrier Heights of O3, BeH2, and H4. *J. Chem. Theory Comput.* **2013**, *9*, 5349−5355.
(450) Xu, X.; Yang, K. R.; Truhlar, D. G. Testing Noncollinear Spin-Flip, Collinear Spin-Flip, and Conventional Time-Dependent Density Functional Theory for Predicting Electronic Excitation Energies of Closed-Shell Atoms. *J. Chem. Theory Comput.* **2014**, *10*, 2070−2084.
(451) Hess, B. A. Applicability of the No-Pair Equation with Free-Particle Projection Operators to Atomic and Molecular Structure Calculations. *Phys. Rev. A: At., Mol., Opt. Phys.* **1985**, *32*, 756−763.
(452) Hess, B. A. Relativistic Electronic-Structure Calculations Employing a Two-Component No-Pair Formalism with External-Field Projection Operators. *Phys. Rev. A: At., Mol., Opt. Phys.* **1986**, *33*, 3742−3748.
(453) Peralta, J. E.; Scuseria, G. E. Relativistic All-Electron Two-Component Self-Consistent Density Functional Calculations Including One-Electron Scalar and Spin-Orbit Effects. *J. Chem. Phys.* **2004**, *120*, 5875.
(454) Filatov, M.; Cremer, D. A New Quasi-Relativistic Approach for Density Functional Theory Based on the Normalized Elimination of the Small Component. *Chem. Phys. Lett.* **2002**, *351*, 259−266.
(455) Filatov, M.; Zou, W.; Cremer, D. Spin-Orbit Coupling Calculations with the Two-Component Normalized Elimination of the Small Component Method. *J. Chem. Phys.* **2013**, *139*, 014106.
(456) Chang, C.; Pelissier, M.; Durand, P. Regular Two-Component Pauli-Like Effective Hamiltonians in Dirac Theory. *Phys. Scr.* **1986**, *34*, 394−404.
(457) Faas, S.; Snijders, J. G.; van Lenthe, J. H.; van Lenthe, E.; Baerends, E. J. The ZORA Formalism Applied to the Dirac-Fock Equation. *Chem. Phys. Lett.* **1995**, *246*, 632−640.
(458) Dyall, K. G.; Fægri, Jr., K. *Introduction to Relativistic Quantum Chemistry*; Oxford University Press, 2007.
(459) Reiher, M.; Wolf, A. *Relativistic Quantum Chemistry*, 2nd ed.; Wiley-VCH, 2015.
(460) De Santis, M.; Storchi, L.; Belpassi, L.; Quiney, H. M.; Tarantelli, F. PyBERTHART: A Relativistic Real-Time Four-Component TDDFT Implementation Using Prototyping Techniques Based on Python. *J. Chem. Theory Comput.* **2020**, *16*, 2410−2429.
(461) Amis, E. S. *Solvent Effects on Reaction Rates and Mechanisms*; Academic Press: New York, 1966.
(462) Amis, E. S. *Solvent Effects on Chemical Phenomena*; Academic Press: New York, 1973; Vol. *1*.
(463) Abraham, M. H. Solvent Effects on Reaction Rates. *Pure Appl. Chem.* **1985**, *57*, 1055−1064.
(464) Connors, K. A. *Chemical Kinetics - The Study of Reaction Rates in Solution*; VCH Publishers: Weinheim, 1990.
(465) Wislicenus, W. Ueber die Isomerie der Formylphenylessigester. *Leibigs Ann. Chem.* **1896**, *291*, 147−216.
(466) Stobbe, H.; Werdermann, A. Studien über Tautomerie, Insbesondere an Einem Semicyklischen 1,3-Diketon der Pentamethylenreihe. *Leibigs Ann. Chem.* **1903**, *326*, 347−370.
(467) Reichardt, C. *Solvents and Solvent Effects in Organic Chemistry*; VCH Publishers: Weinheim, 1988.
(468) Coetzee, J. F.; Ritchie, C. D. *Solute-Solvent Interactions*; Dekker: New York, 1969 and 1976; Vol. *1 and 2*.
(469) Abraham, M. H.; Grellier, P. L.; Abboud, J. L. M.; Doherty, R. M.; Taft, R. W. Solvent Effects in Organic Chemistry - Recent Developments. *Can. J. Chem.* **1988**, *66*, 2673−2686.
(470) Miertus, S.; Scrocco, E.; Tomasi, J. Electrostatic Interaction of a Solute with a Continuum. A Direct Utilization of Ab-Initio Molecular Potentials for the Prevision of Solvent Effects. *Chem. Phys.* **1981**, *55*, 117−129.
(471) Cammi, R.; Tomasi, J. Remarks on the use of the Apparent Surface Charges (ASC) Methods in Solvation Problems: Iterative versus Matrix-Inversion Procedures and the Renormalization of the Apparent Charges. *J. Comput. Chem.* **1995**, *16*, 1449−1458.
(472) Cancès, E.; Mennucci, B.; Tomasi, J. A New Integral Equation Formalism for the Polarizable Continuum Model: Theoretical Background and Applications to Isotropic and Anisotropic Dielectrics. *J. Chem. Phys.* **1997**, *107*, 3032−3041.
(473) Barone, V.; Cossi, M.; Tomasi, J. Geometry Optimization of Molecular Structures in Solution by the Polarizable Continuum Model. *J. Comput. Chem.* **1998**, *19*, 404−417.
(474) Tomasi, J.; Mennucci, B.; Cammi, R. Quantum Mechanical Continuum Solvation Models. *Chem. Rev.* **2005**, *105*, 2999−3094.
(475) Lipparini, F.; Scalmani, G.; Mennucci, B.; Cancès, E.; Caricato, M.; Frisch, M. J. A Variational Formulation of the Polarizable Continuum Model. *J. Chem. Phys.* **2010**, *133*, 014106.
(476) Mennucci, B. Polarizable continuum model. *WIREs Comput. Mol. Sci.* **2012**, *2*, 386−404.
(477) Chipman, D. M. Reaction Field Treatment of Charge Penetration. *J. Chem. Phys.* **2000**, *112*, 5558−5565.
(478) Chipman, D. M. Vertical Electronic Excitation with a Dielectric Continuum Model of Solvation Including Volume Polarization. I. Theory. *J. Chem. Phys.* **2009**, *131*, 014103.
(479) Tomasi, J.; Persico, M. Molecular Interactions in Solution: An Overview of Methods Based on Continuous Distributions of the Solvent. *Chem. Rev.* **1994**, *94*, 2027−2094.
(480) Cramer, C.; Truhlar, D. Implicit Solvation Models: Equilibria, Structure, Spectra, and Dynamics. *Chem. Rev.* **1999**, *99*, 2161−2200.
(481) Klamt, A. The COSMO and COSMO−RS Solvation Models. *Wiley Interdiscip. Rev.: Comput. Mol. Sci.* **2011**, *1*, 699−709.
(482) Mennucci, B. Modeling Environment Effects on Spectroscopies through QM/Classical Models. *Phys. Chem. Chem. Phys.* **2013**, *15*, 6583−6594.
(483) Gao, J. Hybrid Quantum and Molecular Mechanics Simulations: An Alternative to Solvent Effects in Organic Chemistry. *Acc. Chem. Res.* **1996**, *29*, 298−305.
(484) Lin, H.; Truhlar, D. G. QM/MM: What Have We Learned, Where Are We, and Where Do We Go from Here? *Theor. Chem. Acc.* **2007**, *117*, 185−199.
(485) Senn, H. M.; Thiel, W. QM/MM Methods for Biomolecular Systems. *Angew. Chem., Int. Ed.* **2009**, *48*, 1198−1229.
(486) Morzan, U. N.; Ramírez, F. F.; Oviedo, M. B.; Sánchez, C. G.; Scherlis, D. A.; González Lebrero, M. C. Electron Dynamics in Complex Environments with Real-Time Time Dependent Density Functional Theory in a QM-MM Framework. *J. Chem. Phys.* **2014**, *140*, 164105.
(487) Rick, S. W.; Stuart, S. J.; Berne, B. J. Dynamical Fluctuating Charge Force Fields: Application to Liquid Water. *J. Chem. Phys.* **1994**, *101*, 6141−6156.

https://dx.doi.org/10.1021/acs.chemrev.0c00223
Chem. Rev. XXXX, XXX, XXX−XXX

(488) Rick, S. W.; Berne, B. J. Dynamical Fluctuating Charge Force Fields: The Aqueous Solvation of Amides. *J. Am. Chem. Soc.* **1996**, *118*, 672−679.
(489) Lipparini, F.; Barone, V. Polarizable Force Fields and Polarizable Continuum Model: A Fluctuating Charges/PCM Approach. 1. Theory and Implementation. *J. Chem. Theory Comput.* **2011**, *7*, 3711−3724.
(490) Lipparini, F.; Cappelli, C.; Barone, V. Linear Response Theory and Electronic Transition Energies for a Fully Polarizable QM/Classical Hamiltonian. *J. Chem. Theory Comput.* **2012**, *8*, 4153−4165.
(491) Day, P. N.; Jensen, J. H.; Gordon, M. S.; Webb, S. P.; Stevens, W. J.; Krauss, M.; Garmer, D.; Basch, H.; Cohen, D. An Effective Fragment Method for Modeling Solvent Effects in Quantum Mechanical Calculations. *J. Chem. Phys.* **1996**, *105*, 1968−1986.
(492) Kairys, V.; Jensen, J. H. QM/MM Boundaries across Covalent Bonds: A Frozen Localized Molecular Orbital-Based Approach for the Effective Fragment Potential Method. *J. Phys. Chem. A* **2000**, *104*, 6656−6665.
(493) Curutchet, C.; Muñoz-Losa, A.; Monti, S.; Kongsted, J.; Scholes, G. D.; Mennucci, B. Electronic Energy Transfer in Condensed Phase Studied by a Polarizable QM/MM Model. *J. Chem. Theory Comput.* **2009**, *5*, 1838−1848.
(494) Caprasecca, S.; Jurinovich, S.; Viani, L.; Curutchet, C.; Mennucci, B. Geometry Optimization in Polarizable QM/MM Models: The Induced Dipole Formulation. *J. Chem. Theory Comput.* **2014**, *10*, 1588−1598.
(495) Caprasecca, S.; Jurinovich, S.; Lagardère, L.; Stamm, B.; Lipparini, F. Achieving Linear Scaling in Computational Cost for a Fully Polarizable MM/Continuum Embedding. *J. Chem. Theory Comput.* **2015**, *11*, 694−704.
(496) Mao, Y.; Demerdash, O.; Head-Gordon, M.; Head-Gordon, T. Assessing Ion-Water Interactions in the AMOEBA Force Field Using Energy Decomposition Analysis of Electronic Structure Calculations. *J. Chem. Theory Comput.* **2016**, *12*, 5422−5437.
(497) Loco, D.; Polack, É.; Caprasecca, S.; Lagardère, L.; Lipparini, F.; Piquemal, J.-P.; Mennucci, B. A QM/MM Approach Using the AMOEBA Polarizable Embedding: From Ground State Energies to Electronic Excitations. *J. Chem. Theory Comput.* **2016**, *12*, 3654−3661.
(498) Boulanger, E.; Thiel, W. Solvent Boundary Potentials for Hybrid QM/MM Computations Using Classical Drude Oscillators: A Fully Polarizable Model. *J. Chem. Theory Comput.* **2012**, *8*, 4527−4538.
(499) Wildman, A.; Donati, G.; Lipparini, F.; Mennucci, B.; Li, X. Nonequilibrium Environment Dynamics in a Frequency-Dependent Polarizable Embedding Models. *J. Chem. Theory Comput.* **2019**, *15*, 43−51.
(500) Nørby, M. S.; Vahtras, O.; Norman, P.; Kongsted, J. Assessing Frequency-Dependent Site Polarisabilities in Linear Response Polarisable Embedding. *Mol. Phys.* **2017**, *115*, 39−47.
(501) Wu, X.; Teuler, J.-M.; Cailliez, F.; Clavaguéra, C.; Salahub, D. R.; de la Lande, A. Simulating Electron Dynamics in Polarizable Environments. *J. Chem. Theory Comput.* **2017**, *13*, 3985−4002.
(502) Kuleff, A. I.; Breidbach, J.; Cederbaum, L. S. Multielectron Wave-Packet Propagation: General Theory and Application. *J. Chem. Phys.* **2005**, *123*, 044111.
(503) Tsolakidis, A.; Sánchez-Portal, D.; Martin, R. M. Calculation of the Optical Response of Atomic Clusters using Time-Dependent Density Functional Theory and Local Orbitals. *Phys. Rev. B: Condens. Matter Mater. Phys.* **2002**, *66*, 235416.
(504) Lian, C.; Guan, M.; Hu, S.; Zhang, J.; Meng, S. Photoexcitation in Solids: First-Principles Quantum Simulations by Real-Time TDDFT. *Adv. Theory Simul* **2018**, *1*, 1800055.
(505) Pemmaraju, C. D.; Vila, F. D.; Kas, J. J.; Sato, S. A.; Rehr, J. J.; Yabana, K.; Prendergast, D. Velocity-Gauge Real-time TDDFT within a Numerical Atomic Orbital Basis Set. *Comput. Phys. Commun.* **2018**, *226*, 30−38.
(506) Yabana, K.; Shinohara, Y.; Otobe, T.; Iwata, J.-I.; Bertsch, G. F. Real-Time and Real-Space Density Functional Calculation for Electron Dynamics in Crystalline Solids. *Procedia Comput. Sci.* **2011**, *4*, 852−859.
(507) Andrade, X.; et al. Real-Space Grids and the Octopus Code as Tools for the Development of New Simulation Approaches for Electronic Systems. *Phys. Chem. Chem. Phys.* **2015**, *17*, 31371−31396.
(508) Kuisma, M.; Sakko, A.; Rossi, T. P.; Larsen, A. H.; Enkovaara, J.; Lehtovaara, L.; Rantala, T. T. Localized Surface Plasmon Resonance in Silver Nanoparticles: Atomistic First-Principles Time-Dependent Density-Functional Theory Calculations. *Phys. Rev. B: Condens. Matter Mater. Phys.* **2015**, *91*, 115431.
(509) Theilhaber, J. Ab Initio Simulations of Sodium using Time-Dependent Density-Functional Theory. *Phys. Rev. B: Condens. Matter Mater. Phys.* **1992**, *46*, 12990−13003.
(510) Walker, B.; Gebauer, R. Ultrasoft Pseudopotentials in Time-Dependent Density-Functional Theory. *J. Chem. Phys.* **2007**, *127*, 164106.
(511) Krishtal, A.; Ceresoli, D.; Pavanello, M. Subsystem Real-Time Time Dependent Density Functional Theory. *J. Chem. Phys.* **2015**, *142*, 154116.
(512) Sander, T.; Kresse, G. Macroscopic Dielectric Function within Time-Dependent Density Functional Theory − Real Time Evolution versus the Casida Approach. *J. Chem. Phys.* **2017**, *146*, 064110.
(513) Draeger, E. W.; Andrade, X.; Gunnels, J. A.; Bhatele, A.; Schleife, A.; Correa, A. A. Massively Parallel First-Principles Simulation of Electron Dynamics in Materials. *J. Parallel Distr. Com.* **2017**, *106*, 205−214.
(514) You, P.; Xu, J.; Lian, C.; Zhang, C.; Li, X.-Z.; Wang, E.-G.; Meng, S. Quantum Dynamics Simulations: Combining Path Integral Nuclear Dynamics and Real-Time TDDFT. *Electron. Struct.* **2019**, *1*, 044005.
(515) Goncharov, V. A.; Varga, K. Multidomain Decomposition Approach to Time-Dependent Density Functional Calculations. *Phys. Rev. B: Condens. Matter Mater. Phys.* **2011**, *83*, 035118.
(516) Varga, K. Multidomain Decomposition Approach to Large-Scale Electronic Structure Calculations. *Phys. Rev. B: Condens. Matter Mater. Phys.* **2010**, *81*, 045109.
(517) Kidd, D.; Pearson, B.; Covington, C.; Varga, K. Accelerated Pseudospectral Basis in Density Functional Calculations. *Int. J. Quantum Chem.* **2018**, *118*, No. e25573.
(518) Lehtovaara, L.; Havu, V.; Puska, M. All-Electron Time-Dependent Density Functional Theory with Finite Elements: Time-Propagation Approach. *J. Chem. Phys.* **2011**, *135*, 154104.
(519) Kanungo, B.; Gavini, V. Real Time Time-Dependent Density Functional Theory using Higher Order Finite-Element Methods. *Phys. Rev. B: Condens. Matter Mater. Phys.* **2019**, *100*, 115148.
(520) Yost, D. C.; Yao, Y.; Kanai, Y. Propagation of Maximally Localized Wannier Functions in Real-time TDDFT. *J. Chem. Phys.* **2019**, *150*, 194113.
(521) Helgaker, T.; Jorgensen, P.; Olsen, J. *Molecular Electronic-Structure Theory*; John Wiley & Sons, 2014.
(522) Stone, M. H. On One-parameter Unitary Groups in Hilbert space. *Appl. Numer. Math.* **1932**, *33*, 643−648.
(523) Butcher, J. C. A. History of Runge-Kutta Methods. *Appl. Numer. Math.* **1996**, *20*, 247−260.
(524) Magnus, W. On the Exponential Solution of Differential Equations for a Linear Operator. *Commun. Pur. Appl. Math.* **1954**, *7*, 649−673.
(525) Blanes, S.; Casas, F.; Oteo, J.; Ros, J. A Pedagogical Approach to the Magnus Expansion. *Eur. J. Phys.* **2010**, *31*, 907−918.
(526) Liang, W.; Chapman, C. T.; Li, X. Efficient First-Principles Electronic Dynamics. *J. Chem. Phys.* **2011**, *134*, 184102.
(527) Blanes, S.; Casas, F. *A Concise Introduction to Geometric Numerical Integration*; CRC Press, 2016; Vol. *23*.
(528) Candy, J.; Rozmus, W. A Symplectic Integration Algorithm for Separable Hamiltonian Functions. *J. Comput. Phys.* **1991**, *92*, 230−256.
(529) McLachlan, R. I.; Atela, P. The Accuracy of Symplectic Integrators. *Nonlinearity* **1992**, *5*, 541−562.
(530) Calvo, M. P.; Sanz-Serna, J. M. The Development of Variable-Step Symplectic Integrators, with Application to the Two-Body Problem. *SIAM J. Sci. Comp.* **1993**, *14*, 936−952.

https://dx.doi.org/10.1021/acs.chemrev.0c00223
Chem. Rev. XXXX, XXX, XXX−XXX

(531) Sanz-Serna, J. M.; Calvo, M. P. Symplectic Numerical Methods for Hamiltonian Problems. *Int. J. Mod. Phys. C* **1993**, *04*, 385−392.
(532) Gray, S. K.; Noid, D. W.; Sumpter, B. G. Symplectic Integrators for Large Scale Molecular Dynamics Simulations: A Comparison of Several Explicit Methods. *J. Chem. Phys.* **1994**, *101*, 4062−4072.
(533) Gray, S. K.; Verosky, J. M. Classical Hamiltonian Structures in Wave Packet Dynamics. *J. Chem. Phys.* **1994**, *100*, 5011−5022.
(534) McLachlan, R. I.; Scovel, C. Equivariant Constrained Symplectic Integration. *J. Nonlinear Sci.* **1995**, *5*, 233−256.
(535) Bigwood, R.; Gruebele, M. Shifted-update Rotation: Simple Integration of the Many-Level Schrödinger Equation to Long Times. *Chem. Phys. Lett.* **1995**, *233*, 383−391.
(536) Manolopoulos, D. E.; Gray, S. K. Symplectic Integrators for the Multichannel Schrödinger Equation. *J. Chem. Phys.* **1995**, *102*, 9214−9227.
(537) Hoover, W. G.; Kum, O.; Owens, N. E. Accurate Symplectic Integrators via Random Sampling. *J. Chem. Phys.* **1995**, *103*, 1530−1532.
(538) Sanz-Serna, J. M.; Portillo, A. Classical Numerical Integrators for Wave Packet Dynamics. *J. Chem. Phys.* **1996**, *104*, 2349−2355.
(539) Gray, S. K.; Manolopoulos, D. E. Symplectic Integrators Tailored to the Time-Dependent Schrödinger Equation. *J. Chem. Phys.* **1996**, *104*, 7099−7112.
(540) Kosloff, R. Time-Dependent Quantum-Mechanical Methods for Molecular Dynamics. *J. Phys. Chem.* **1988**, *92*, 2087−2100.
(541) Gómez Pueyo, A.; Marques, M. A. L.; Rubio, A.; Castro, A. Propagators for the Time-Dependent Kohn-Sham Equations: Multistep, Runge-Kutta, Exponential Runge-Kutta, and Commutator Free Magnus Methods. *J. Chem. Theory Comput.* **2018**, *14*, 3040−3052.
(542) Micha, D. A. Density Matrix Treatment of Electronic Rearrangement. *Adv. Quantum Chem.* **1999**, *35*, 317−337.
(543) Balakrishnan, V. *Mathematical Physics: With Applications, Problems and Solutions*; Ane Books Pvt. Ltd: New Delhi, 2018.
(544) Leforestier, C.; Bisseling, R. H.; Cerjan, C.; Feit, M. D.; Friesner, R.; Guldberg, A.; Hammerich, A.; Jolicard, G.; Karrlein, W.; Meyer, H.-D.; Lipkin, N.; Roncero, O.; Kosloff, R. A Comparison of Different Propagation Schemes for the Time Dependent Schrödinger Equation. *J. Comput. Phys.* **1991**, *94*, 59−80.
(545) Baer, R.; Neuhauser, D. Real-Time Linear Response for Time-Dependent Density-Functional Theory. *J. Chem. Phys.* **2004**, *121*, 9803−9807.
(546) Wang, F.; Yam, C. Y.; Chen, G.; Fan, K. Density Matrix Based Time-dependent Density Functional Theory and the Solution of Its Linear Response in Real Time Domain. *J. Chem. Phys.* **2007**, *126*, 134104.
(547) Barakat, R. Evaluation of the Incomplete Gamma Function of Imaginary Argument by Chebyshev Polynomials. *Math. Comput.* **1961**, *15*, 7−11.
(548) van der Pol, B.; Weijers, T. J. Tchebycheff Polynomials and Their Relation to Circular Functions, Besselfunctions and Lissajous-Figures. *Physica* **1934**, *1*, 78−96.
(549) Oh, H.-S.; Yang, W. S. Comparison of Matrix Exponential Methods for Fuel Burnup Calculations. *J. Kor. Nucl. Soc.* **1999**, *31*, 172−181.
(550) Moler, C.; Van Loan, C. Nineteen Dubious Ways to Compute the Exponential of a Matrix, Twenty-Five Years Later. *SIAM Rev.* **2003**, *45*, 3−49.
(551) Williams-Young, D.; Goings, J. J.; Li, X. Accelerating Real-Time Time-Dependent Density Functional Theory with a Non-Recursive Chebyshev Expansion of the Quantum Propagator. *J. Chem. Theory Comput.* **2016**, *12*, 5333−5338.
(552) Lubich, C. A. Variational Splitting Integrator for Quantum Molecular Dynamics. *Appl. Numer. Math.* **2004**, *48*, 355−368.
(553) Park, T. J.; Light, J. C. Unitary Quantum Time Evolution by Iterative Lanczos Reduction. *J. Chem. Phys.* **1986**, *85*, 5870−5876.
(554) Hofmann, D.; Kümmel, S. Self-Interaction Correction in a Real-Time Kohn-Sham Scheme: Access to Difficult Excitations in Time-Dependent Density Functional Theory. *J. Chem. Phys.* **2012**, *137*, 064117.
(555) Bruner, A.; LaMaster, D.; Lopata, K. Accelerated Broadband Spectra Using Transition Dipole Decomposition and Padé Approximants. *J. Chem. Theory Comput.* **2016**, *12*, 3741−3750.
(556) Mandelshtam, V. A.; Taylor, H. S. Harmonic Inversion of Time Signals and its Applications. *J. Chem. Phys.* **1997**, *107*, 6756−6769.
(557) Wall, M. R.; Neuhauser, D. Extraction, Through Filter-Diagonalization, of General Quantum Eigenvalues or Classical Normal Mode Frequencies from a Small Number of Residues or a Short-Time Segment of a Signal. I. Theory and Application to a Quantum-Dynamics Model. *J. Chem. Phys.* **1995**, *102*, 8011−8022.
(558) Mandelshtam, V. A.; Taylor, H. S. A Low-Storage Filter Diagonalization Method for Quantum Eigenenergy Calculation or for Spectral Analysis of Time Signals. *J. Chem. Phys.* **1997**, *106*, 5085−5090.
(559) Mandelshtam, V. A.; Taylor, H. S.; Shaka, A. Application of the Filter Diagonalization Method to One-and Two-Dimensional NMR Spectra. *J. Magn. Reson.* **1998**, *133*, 304−312.
(560) George, Jr., A. *Essentials of Padé Approximants*; Elsevier, 1975; pp 3−25.
(561) Dey, S.; Mittra, R. Efficient Computation of Resonant Frequencies and Quality Factors of Cavities via a Combination of the Finite-Difference Time-Domain Technique and the Padé Approximation. *IEEE Microw. Guided W.* **1998**, *8*, 415−417.
(562) Wei-Hua Guo; Wei-Jun Li; Yong-Zhen Huang. Computation of Resonant Frequencies and Quality Factors of Cavities by FDTD Technique and Padé Approximation. *IEEE Microw. Wirel. Co.* **2001**, *11*, 223−225.
(563) Makhoul, J. Linear Prediction: A Tutorial Review. *Proc. IEEE* **1975**, *63*, 561−580.
(564) Roy, R.; Sumpter, B.; Noid, D.; Wunderlich, B. Estimation of Dispersion Relations from Short-Duration Molecular Dynamics Simulations. *J. Phys. Chem.* **1990**, *94*, 5720−5729.
(565) Kroes, G.-J.; Wall, M. R.; Pang, J. W.; Neuhauser, D. Avoiding Long Propagation Times in Wave Packet Calculations on Scattering with Resonances: A New Algorithm Involving Filter Diagonalization. *J. Chem. Phys.* **1997**, *106*, 1800−1807.
(566) Liang, W.; Fischer, S. A.; Frisch, M. J.; Li, X. Energy-Specific Linear Response TDHF/TDDFT for Calculating High-Energy Excited States. *J. Chem. Theory Comput.* **2011**, *7*, 3540−3547.
(567) Donati, G.; Lingerfelt, D. B.; Aikens, C.; Li, X. Anisotropic Polarizability-Induced Plasmon Transfer. *J. Phys. Chem. C* **2018**, *122*, 10621−10626.
(568) Oviedo, M. B.; Negre, C. F. A.; Sanchez, C. G. Dynamical Simulation of the Optical Response of Photosynthetic Pigments. *Phys. Chem. Chem. Phys.* **2010**, *12*, 6706−6711.
(569) Oviedo, M. B.; Sanchez, C. G. Transition Dipole Moments of the Qy Band in Photosynthetic Pigments. *J. Phys. Chem. A* **2011**, *115*, 12280−12285.
(570) Stöhr, J. *NEXAFS Spectroscopy*; Springer-Verlag, 2003.
(571) De Groot, F.; Kotani, A. *Core Level Spectroscopy of Solids*; CRC Press, 2008.
(572) Fronzoni, G.; De Francesco, R.; Stener, M. Time Dependent Density Functional Theory of X-ray Absorption Spectroscopy of Alkaline-Earth Oxides. *J. Phys. Chem. B* **2005**, *109*, 10332−10340.
(573) DeBeer George, S.; Petrenko, T.; Neese, F. Time-dependent Density Functional Calculations of Ligand K-edge X-ray Absorption Spectra. *Inorg. Chim. Acta* **2008**, *361*, 965−972.
(574) Peng, B.; Lestrange, P. J.; Goings, J. J.; Caricato, M.; Li, X. Energy-Specific Equation-of-Motion Coupled-Cluster Methods for High-Energy Excited States: Application to K-Edge X-Ray Absorption Spectroscopy. *J. Chem. Theory Comput.* **2015**, *11*, 4146−4153.
(575) Stener, M.; Fronzoni, G.; de Simone, M. Time Dependent Density Functional Theory of Core Electrons Excitations. *Chem. Phys. Lett.* **2003**, *373*, 115−123.
(576) Ray, K.; DeBeer George, S.; Solomon, E. I.; Wieghardt, K.; Neese, F. Description of the Ground-State Covalencies of the Bis(dithiolato) Transition-Metal Complexes From X-ray Absorption Spectroscopy and Time-Dependent Density-Functional Calculations. *Chem. - Eur. J.* **2007**, *13*, 2783−2797.

https://dx.doi.org/10.1021/acs.chemrev.0c00223
Chem. Rev. XXXX, XXX, XXX−XXX

(577) Van Beeumen, R.; Williams-Young, D. B.; Kasper, J. M.; Yang, C.; Ng, E. G.; Li, X. Model Order Reduction Algorithm for Estimating the Absorption Spectrum. *J. Chem. Theory Comput.* **2017**, *13*, 4950−4961.
(578) Wenzel, J.; Wormit, M.; Dreuw, A. Calculating Core-level Excitations and X-ray Absorption Spectra of Medium-sized Closed-shell Molecules with the Algebraic-diagrammatic Construction Scheme for the Polarization Propagator. *J. Comput. Chem.* **2014**, *35*, 1900−1915.
(579) Wenzel, J.; Wormit, M.; Dreuw, A. Calculating X-ray Absorption Spectra of Open-shell Molecules with the Unrestricted Algebraic-diagrammatic Construction Scheme for the Polarization Propagator. *J. Chem. Theory Comput.* **2014**, *10*, 4583−4598.
(580) Wenzel, J.; Holzer, A.; Wormit, M.; Dreuw, A. Analysis and Comparison of CVS-ADC Approaches up to Third Order for the Calculation of Core-excited States. *J. Chem. Phys.* **2015**, *142*, 214104.
(581) Peng, R.; Copan, A. V.; Sokolov, A. Y. Simulating X-ray Absorption Spectra with Linear-Response Density Cumulant Theory. *J. Phys. Chem. A* **2019**, *123*, 1840−1850.
(582) Coriani, S.; Christiansen, O.; Fransson, T.; Norman, P. Coupled-cluster Response Theory for Near-edge X-ray-absorption Fine Structure of Atoms and Molecules. *Phys. Rev. A: At., Mol., Opt. Phys.* **2012**, *85*, 022507.
(583) Fransson, T.; Coriani, S.; Christiansen, O.; Norman, P. Carbon X-ray Absorption Spectra of Fluoroethenes and Acetone: A Study at the Coupled Cluster, Density Functional, and Static-exchange Levels of Theory. *J. Chem. Phys.* **2013**, *138*, 124311.
(584) Josefsson, I.; Kunnus, K.; Schreck, S.; Föhlisch, A.; de Groot, F.; Wernet, P.; Odelius, M. Ab initio Calculations of X-ray Spectra: Atomic Multiplet and Molecular Orbital Effects in a Multiconfigurational SCF Approach to the L-edge Spectra of Transition Metal Complexes. *J. Phys. Chem. Lett.* **2012**, *3*, 3565−3570.
(585) Pinjari, R. V.; Delcey, M. G.; Guo, M.; Odelius, M.; Lundberg, M. Restricted Active Space Calculations of L-edge X-ray Absorption Spectra: From Molecular Orbitals to Multiplet States. *J. Chem. Phys.* **2014**, *141*, 124116.
(586) Roemelt, M.; Neese, F. Excited States of Large Open-Shell Molecules: An Efficient, General, and Spin-Adapted Approach Based on a Restricted Open-Shell Ground State Wave function. *J. Phys. Chem. A* **2013**, *117*, 3069−3083.
(587) Roemelt, M.; Maganas, D.; DeBeer, S.; Neese, F. A Combined DFT and Restricted Open-shell Configuration Interaction Method Including Spin-orbit Coupling: Application to Transition Metal L-edge X-ray Absorption Spectroscopy. *J. Chem. Phys.* **2013**, *138*, 204101.
(588) Bozek, J.; Tan, K.; Bancroft, G.; Tse, J. High Resolution Gas Phase Photoabsorption Spectra of $SiCl_4$ and $Si(CH3)_4$ at the Silicon L Edges: Characterization and Assignment of Resonances. *Chem. Phys. Lett.* **1987**, *138*, 33−42.
(589) Larsen, A. H.; De Giovannini, U.; Rubio, A. *Density-Functional Methods for Excited States*; Springer, 2015; pp 219−271.
(590) Berera, R.; van Grondelle, R.; Kennis, J. T. Ultrafast Transient Absorption Spectroscopy: Principles and Application to Photosynthetic Systems. *Photosynth. Res.* **2009**, *101*, 105−118.
(591) Cronstrand, P.; Christiansen, O.; Norman, P.; Ågren, H. Theoretical Calculations of Excited State Absorption. *Phys. Chem. Chem. Phys.* **2000**, *2*, 5357−5363.
(592) Cronstrand, P.; Christiansen, O.; Norman, P.; Ågren, H. *Ab Initio* Modeling of Excited State Absorption of Polyenes. *Phys. Chem. Chem. Phys.* **2001**, *3*, 2567−2575.
(593) Ruggenthaler, M.; Bauer, D. Rabi Oscillations and Few-Level Approximations in Time-Dependent Density Functional Theory. *Phys. Rev. Lett.* **2009**, *102*, 233001.
(594) Raghunathan, S.; Nest, M. Coherent Control and Time-Dependent Density Functional Theory: Towards Creation of Wave Packets by Ultrashort Laser Pulses. *J. Chem. Phys.* **2012**, *136*, 064104.
(595) Furche, F.; Ahlrichs, R. Adiabatic Time-Dependent Density Functional Methods for Excited State Properties. *J. Chem. Phys.* **2002**, *117*, 7433−7447.
(596) Silverstein, D. W.; Govind, N.; Van Dam, H. J.; Jensen, L. Simulating One-Photon Absorption and Resonance Raman Scattering Spectra using Analytical Excited State Energy Gradients within Time-Dependent Density Functional Theory. *J. Chem. Theory Comput.* **2013**, *9*, 5490−5503.
(597) Marques, M. A. L.; Gross, E. K. U. Time-Dependent Density Functional Theory. *Annu. Rev. Phys. Chem.* **2004**, *55*, 427−455.
(598) Chen, M.; Lopata, K. First-Principles Simulations of X-ray Transient Absorption for Probing Attosecond Electron Dynamics. *J. Chem. Theory Comput.* **2020**, *16*, 4470.
(599) Ghosh, S.; Asher, J. C.; Gagliardi, L.; Cramer, C. J.; Govind, N. A Semiempirical Effective Hamiltonian based Approach for Analyzing Excited State Wave Functions and Computing Excited State Absorption Spectra using Real-Time Dynamics. *J. Chem. Phys.* **2019**, *150*, 104103.
(600) Meng, S.; Kaxiras, E. Electron and Hole Dynamics in Dye-Sensitized Solar Cells: Influencing Factors and Systematic Trends. *Nano Lett.* **2010**, *10*, 1238−1247.
(601) Lopata, K.; Reslan, R.; Kowalska, M.; Neuhauser, D.; Govind, N.; Kowalski, K. Excited-state Studies of Polyacenes: A Comparative Picture using EOMCCSD, CR-EOMCCSD(T), Range-Separated (LR/RT)-TDDFT, TD-PM3, and TD-ZINDO. *J. Chem. Theory Comput.* **2011**, *7*, 3686−3693.
(602) Moore, J. E.; Morton, S. M.; Jensen, L. Importance of Correctly Describing Charge-Transfer Excitations for Understanding the Chemical Effect in SERS. *J. Phys. Chem. Lett.* **2012**, *3*, 2470−2475.
(603) Govind, N.; Valiev, M.; Jensen, L.; Kowalski, K. Excitation Energies of Zinc Porphyrin in Aqueous Solution using Long-Range Corrected Time-Dependent Density Functional Theory. *J. Phys. Chem. A* **2009**, *113*, 6041−6043.
(604) Klamroth, T.; Nest, M. Ultrafast electronic excitations of small sodium clusters and the onset of electron thermalization. *Phys. Chem. Chem. Phys.* **2009**, *11*, 349−357.
(605) Donati, G.; Lingerfelt, D. B.; Petrone, A.; Rega, N.; Li, X. Watching" Polaron Pair Formation from First-Principles Electron-Nuclear Dynamics. *J. Phys. Chem. A* **2016**, *120*, 7255−7261.
(606) Franken, P. A.; Hill, A. E.; Peters, C. W.; Weinreich, G. Generation of Optical Harmonics. *Phys. Rev. Lett.* **1961**, *7*, 118−119.
(607) Antoine, P.; L'Huillier, A.; Lewenstein, M. Attosecond Pulse Trains Using High-Order Harmonics. *Phys. Rev. Lett.* **1996**, *77*, 1234−1237.
(608) Corkum, P. Plasma Perspective on Strong-field Multiphoton Ionization. *Phys. Rev. Lett.* **1993**, *71*, 1994−1997.
(609) Lewenstein, M.; Balcou, P.; Ivanov, M.; L'Huillier, A.; Corkum, P. Theory of High-harmonic Generation by Low-frequency Laser Fields. *Phys. Rev. A: At., Mol., Opt. Phys.* **1994**, *49*, 2117−2132.
(610) Butcher, P. N.; Cotter, D. *The Elements of Nonlinear Optics*; Cambridge University Press, 1990.
(611) Wang, F.; Yam, C. Y.; Chen, G. Time-Dependent Density-Functional Theory/Localized Density Matrix Method for Dynamic Hyperpolarizability. *J. Chem. Phys.* **2007**, *126*, 244102.
(612) Bandrauk, A. D.; Chelkowski, S.; Diestler, D. J.; Manz, J.; Yuan, K.-J. Quantum Simulation of High-order Harmonic Spectra of the Hydrogen Atom. *Phys. Rev. A: At., Mol., Opt. Phys.* **2009**, *79*, 023403.
(613) Davidson, E. R.; Eichinger, B. E.; Robinson, B. H. Hyperpolarizability: Calibration of Theoretical Methods for Chloroform, Water, Acetonitrile, and p-Nitroaniline. *Opt. Mater.* **2006**, *29*, 360−364.
(614) Chu, X.; Chu, S.-I.; Laughlin, C. Spectral and Temporal Structures of High-order Harmonic Generation of Na in Intense Mid-IR Laser Fields. *Phys. Rev. A: At., Mol., Opt. Phys.* **2001**, *64*, 013406.
(615) Ding, F.; Liang, W.; Chapman, C. T.; Isborn, C. M.; Li, X. On the Gauge Invariance of Nonperturbative Electronic Dynamics Using the Time-Dependent Hartree-Fock and Time-Dependent Kohn-Sham. *J. Chem. Phys.* **2011**, *135*, 164101.
(616) Castro, A.; Rubio, A.; Gross, E. K. U. Enhancing and Controlling Single-atom High-harmonic Generation Spectra: A Time-dependent Density-functional Scheme. *Eur. Phys. J. B* **2015**, *88*, 191.

https://dx.doi.org/10.1021/acs.chemrev.0c00223
Chem. Rev. XXXX, XXX, XXX−XXX

(617) Schönborn, J. B.; Saalfrank, P.; Klamroth, T. Controlling the High Frequency Response of H_2 by Ultra-short Tailored Laser Pulses: A Time-dependent Configuration Interaction Study. *J. Chem. Phys.* **2016**, *144*, 044301.
(618) Mukamel, S. *Principles of Nonlinear Optical Spectroscopy*; Oxford University Press, 1999.
(619) Mukamel, S.; Healion, D.; Zhang, Y.; Biggs, J. D. Multidimensional Attosecond Resonant X-ray Spectroscopy of Molecules: Lessons from the Optical Regime. *Annu. Rev. Phys. Chem.* **2013**, *64*, 101−127.
(620) Bennett, K.; Zhang, Y.; Kowalewski, M.; Hua, W.; Mukamel, S. Multidimensional Resonant Nonlinear Spectroscopy with Coherent Broadband X-ray Pulses. *Phys. Scr.* **2016**, *T169*, 014002−17.
(621) Bennett, K.; Rouxel, J. R.; Mukamel, S. Linear and Nonlinear Frequency- and Time-Domain Spectroscopy with Multiple Frequency Combs. *J. Chem. Phys.* **2017**, *147*, 094304.
(622) Cho, D.; Rouxel, J. R.; Kowalewski, M.; Saurabh, P.; Lee, J. Y.; Mukamel, S. Phase Cycling RT-TDDFT Simulation Protocol for Nonlinear XUV and X-ray Molecular Spectroscopy. *J. Phys. Chem. Lett.* **2018**, *9*, 1072−1078.
(623) Cho, D.; Rouxel, J. R.; Kowalewski, M.; Lee, J. Y.; Mukamel, S. Attosecond X-ray Diffraction Triggered by Core or Valence Ionization of a Dipeptide. *J. Chem. Theory Comput.* **2018**, *14*, 329−338.
(624) Bruner, A.; Cavaletto, S. M.; Govind, N.; Mukamel, S. Resonant X-ray Sum-Frequency-Generation Spectroscopy of K-Edges in Acetyl Fluoride. *J. Chem. Theory Comput.* **2019**, *15*, 6832−6839.
(625) Nascimento, D. R.; Zhang, Y.; Bergmann, U.; Govind, N. Near-Edge X-ray Absorption Fine Structure Spectroscopy of Heteroatomic Core-Hole States as a Probe for Nearly Indistinguishable Chemical Environments. *J. Phys. Chem. Lett.* **2020**, *11*, 556−561.
(626) Pople, J. Molecular-Orbital Theory of Diamagnetism. I. An Approximate LCAO Scheme. *J. Chem. Phys.* **1962**, *37*, 53−59.
(627) Hameka, H. Calculation of Magnetic Susceptibilities of Diatomic Molecules: I. General Theory. *Physica* **1962**, *28*, 908−916.
(628) Hameka, H. On Pople's Molecular-Orbital Theory of Diamagnetism. *J. Chem. Phys.* **1962**, *37*, 3008−3009.
(629) Pople, J. Reply to Letter by HF Hameka. *J. Chem. Phys.* **1962**, *37*, 3009−3010.
(630) Tellgren, E. I.; Helgaker, T.; Soncini, A. Non-Perturbative Magnetic Phenomena in Closed-Shell Paramagnetic Molecules. *Phys. Chem. Chem. Phys.* **2009**, *11*, 5489−5498.
(631) Sun, S.; Williams-Young, D.; Stetina, T. F.; Li, X. Generalized Hartree-Fock with Non-perturbative Treatment of Strong Magnetic Field: Application to Molecular Spin Phase Transition. *J. Chem. Theory Comput.* **2019**, *15*, 348−356.
(632) Barron, L. D. *Molecular Light Scattering and Optical Activity*; Cambridge University Press, 2004.
(633) Grimme, S.; Harren, J.; Sobanski, A.; Vögtle, F. Structure/Chiroptics Relationships of Planar Chiral and Helical Molecules. *Eur. J. Org. Chem.* **1998**, *1998*, 1491−1509.
(634) Furche, F.; Ahlrichs, R.; Wachsmann, C.; Weber, E.; Sobanski, A.; Vögtle, F.; Grimme, S. Circular Dichroism of Helicenes Investigated by Time-Dependent Density Functional Theory. *J. Am. Chem. Soc.* **2000**, *122*, 1717−1724.
(635) Stephens, P.; Devlin, F.; Cheeseman, J.; Frisch, M.; Rosini, C. Determination of Absolute Configuration using Optical Rotation Calculated using Density Functional Theory. *Org. Lett.* **2002**, *4*, 4595−4598.
(636) Diedrich, C.; Grimme, S. Systematic Investigation of Modern Quantum Chemical Methods to Predict Electronic Circular Dichroism Spectra. *J. Phys. Chem. A* **2003**, *107*, 2524−2539.
(637) Stephens, P.; Devlin, F.; Cheeseman, J.; Frisch, M.; Bortolini, O.; Besse, P. Determination of Absolute Configuration using Ab Initio Calculation of Optical Rotation. *Chirality* **2003**, *15*, S57−S64.
(638) Tam, M. C.; Russ, N. J.; Crawford, T. D. Coupled Cluster Calculations of Optical Rotatory Dispersion of (S)-Methyloxirane. *J. Chem. Phys.* **2004**, *121*, 3550−3557.
(639) Crawford, T. D. Ab Initio Calculation of Molecular Chiroptical Properties. *Theor. Chem. Acc.* **2006**, *115*, 227−245.
(640) Helgaker, T.; Coriani, S.; Jørgensen, P.; Kristensen, K.; Olsen, J.; Ruud, K. Recent Advances in Wave Function-based Methods of Molecular-property Calculations. *Chem. Rev.* **2012**, *112*, 543−631.
(641) Crawford, T. D. High-Accuracy Quantum Chemistry and Chiroptical Properties. *Comprehensive Chiroptical Spectroscopy: Instrumentation, Methodologies, and Theoretical Simulations* **2012**, *1*, 675−697.
(642) Zhang, Y.; Rouxel, J. R.; Autschbach, J.; Govind, N.; Mukamel, S. X-ray Circular Dichroism Signals: a Unique Probe of Local Molecular Chirality. *Chem. Sci.* **2017**, *8*, 5969−5978.
(643) Norman, P.; Bishop, D. M.; Jorgen Aa. Jensen, H.; Oddershede, J. Near-Resonant Absorption in the Time-Dependent Self-Consistent Field and Multiconfigurational Self-Consistent Field Approximations. *J. Chem. Phys.* **2001**, *115*, 10323−10334.
(644) Jiemchooroj, A.; Norman, P. Electronic Circular Dichroism Spectra from the Complex Polarization Propagator. *J. Chem. Phys.* **2007**, *126*, 134102.
(645) Pedersen, T. B.; Koch, H. Coupled Cluster Response Functions Revisited. *J. Chem. Phys.* **1997**, *106*, 8059−8072.
(646) Condon, E. U. Theories of Optical Rotatory Power. *Rev. Mod. Phys.* **1937**, *9*, 432−457.
(647) Barron, L. D. *Molecular Light Scattering and Optical Activity*; Cambridge University Press, 2009.
(648) Coriani, S.; Jørgensen, P.; Rizzo, A.; Ruud, K.; Olsen, J. Ab initio Determinations of Magnetic Circular Dichroism. *Chem. Phys. Lett.* **1999**, *300*, 61−68.
(649) Solheim, H.; Ruud, K.; Coriani, S.; Norman, P. Complex Polarization Propagator Calculations of Magnetic Circular Dichroism Spectra. *J. Chem. Phys.* **2008**, *128*, 094103.
(650) Krykunov, M.; Seth, M.; Ziegler, T.; Autschbach, J. Calculation of the Magnetic Circular Dichroism B Term from the Imaginary Part of the Verdet Constant Using Damped Time-Dependent Density Functional Theory. *J. Chem. Phys.* **2007**, *127*, 244102.
(651) Solheim, H.; Ruud, K.; Coriani, S.; Norman, P. The A and B Terms of Magnetic Circular Dichroism Revisited. *J. Phys. Chem. A* **2008**, *112*, 9615−9618.
(652) Seth, M.; Ziegler, T. Formulation of Magnetically Perturbed Time-Dependent Density Functional Theory. *J. Chem. Phys.* **2007**, *127*, 134108.
(653) Seth, M.; Krykunov, M.; Ziegler, T.; Autschbach, J.; Banerjee, A. Application of Magnetically Perturbed Time-Dependent Density Functional Theory to Magnetic Circular Dichroism: Calculation of B Terms. *J. Chem. Phys.* **2008**, *128*, 144105.
(654) Seth, M.; Krykunov, M.; Ziegler, T.; Autschbach, J. Application of Magnetically Perturbed Time-Dependent Density Functional Theory to Magnetic Circular Dichroism. II. Calculation of A Terms. *J. Chem. Phys.* **2008**, *128*, 234102.
(655) Honda, Y.; Hada, M.; Ehara, M.; Nakatsuji, H.; Downing, J.; Michl, J. Relativistic Effects on Magnetic Circular Dichroism Studied by GUHF/SECI Method. *Chem. Phys. Lett.* **2002**, *355*, 219−225.
(656) Honda, Y.; Hada, M.; Ehara, M.; Nakatsuji, H.; Michl, J. Theoretical Studies on Magnetic Circular Dichroism by the Finite Perturbation Method with Relativistic Corrections. *J. Chem. Phys.* **2005**, *123*, 164113.
(657) Ganyushin, D.; Neese, F. First-Principles Calculations of Magnetic Circular Dichroism Spectra. *J. Chem. Phys.* **2008**, *128*, 114117.
(658) Gendron, F.; Fleischauer, V. E.; Duignan, T. J.; Scott, B. L.; Löble, M. W.; Cary, S. K.; Kozimor, S. A.; Bolvin, H.; Neidig, M. L.; Autschbach, J. Magnetic Circular Dichroism of UCl^{6-} in the Ligand-to-Metal Charge-Transfer Spectral Region. *Phys. Chem. Chem. Phys.* **2017**, *19*, 17300−17313.
(659) Heit, Y. N.; Sergentu, D.-C.; Autschbach, J. Magnetic Circular Dichroism Spectra of Transition Metal Complexes Calculated from Restricted Active Space Wavefunctions. *Phys. Chem. Chem. Phys.* **2019**, *21*, 5586−5597.
(660) Coriani, S.; Hättig, C.; Jørgensen, P.; Helgaker, T. Gauge-Origin Independent Magneto-Optical Activity within Coupled Cluster Response Theory. *J. Chem. Phys.* **2000**, *113*, 3561−3572.

https://dx.doi.org/10.1021/acs.chemrev.0c00223
Chem. Rev. XXXX, XXX, XXX−XXX

(661) Jansik, B.; Jørgensen, P.; Coriani, S.; Michl, J. Gauge-Origin-Independent Coupled Cluster Singles and Doubles Calculation of Magnetic Circular Dichroism of Azabenzenes and Phosphabenzene Using London Orbitals. *J. Phys. Chem. A* **2007**, *111*, 11278−11286.
(662) Krykunov, M.; Banerjee, A.; Ziegler, T.; Autschbach, J. Calculation of Verdet Constants with Time-Dependent Density Functional Theory: Implementation and Results for Small Molecules. *J. Chem. Phys.* **2005**, *122*, 074105.
(663) Kjærgaard, T.; Jørgensen, P.; Thorvaldsen, A. J.; Sałek, P.; Coriani, S. Gauge-Origin Independent Formulation and Implementation of Magneto-Optical Activity within Atomic-Orbital-Density Based Hartree- Fock and Kohn- Sham Response Theories. *J. Chem. Theory Comput.* **2009**, *5*, 1997−2020.
(664) Sun, S.; Williams-Young, D.; Li, X. An Ab Initio Linear Response Method for Computing Magnetic Circular Dichroism Spectra with Nonperturbative Treatment of Magnetic Field. *J. Chem. Theory Comput.* **2019**, *15*, 3162−3169.
(665) Helgaker, T.; Taylor, P. R. In *Modern Electronic Structure Theory*; Yarkony, D. R., Ed.; World Scientific Publishing Co. Pte. Ltd.: Singapore, 1995; Chapter 12, pp 725−856.
(666) Lestrange, P. J.; Egidi, F.; Li, X. The Consequences of Improperly Describing Oscillator Strengths Beyond the Electric Dipole Approximation. *J. Chem. Phys.* **2015**, *143*, 234103.
(667) Epstein, S. T. Gauge Invariance of the Hartree-Fock Approximation. *J. Chem. Phys.* **1965**, *42*, 2897−2898.
(668) Epstein, S. Gauge Invariance, Current Conservation, and GIAO's. *J. Chem. Phys.* **1973**, *58*, 1592−1595.
(669) Gauss, J.; Stanton, J. F. Electron-Correlated Approaches for the Calculation of NMR Chemical Shifts. *Adv. Chem. Phys.* **2003**, *123*, 355−422.
(670) Schindler, M.; Kutzelnigg, W. Theory of Magnetic Susceptibilities and NMR Chemical Shifts in Terms of Localized Quantities. II. Application to Some Simple Molecules. *J. Chem. Phys.* **1982**, *76*, 1919−1933.
(671) Kutzelnigg, W. Theory of Magnetic Susceptibilities and NMR Chemical Shifts in Terms of Localized Quantities. *Isr. J. Chem.* **1980**, *19*, 193−200.
(672) London, F. Théorie Quantique des Courants Interatomiques dans les Combinaisons Aromatiques. *J. Phys. Radium* **1937**, *8*, 397−409.
(673) Ditchfield, R. Molecular Orbital Theory of Magnetic Shielding and Magnetic Susceptibility. *J. Chem. Phys.* **1972**, *56*, 5688−5691.
(674) Wolinski, K.; Hinton, J. F.; Pulay, P. Efficient Implementation of the Gauge-Independent Atomic Orbital Method for NMR Chemical Shift Calculations. *J. Am. Chem. Soc.* **1990**, *112*, 8251−8260.
(675) Bouten, R.; Baerends, E.; Van Lenthe, E.; Visscher, L.; Schreckenbach, G.; Ziegler, T. Relativistic Effects for NMR Shielding Constants in Transition Metal Oxides Using the Zeroth-Order Regular Approximation. *J. Phys. Chem. A* **2000**, *104*, 5600−5611.
(676) Krykunov, M.; Autschbach, J. Calculation of Origin-Independent Optical Rotation Tensor Components in Approximate Time-Dependent Density Functional Theory. *J. Chem. Phys.* **2006**, *125*, 034102.
(677) Autschbach, J. Analyzing NMR Shielding Tensors Calculated with Two-Component Relativistic Methods Using Spin-Free Localized Molecular Orbitals. *J. Chem. Phys.* **2008**, *128*, 164112.
(678) Helgaker, T.; Jaszuński, M.; Ruud, K. Ab initio Methods for the Calculation of NMR Shielding and Indirect Spin-Spin Coupling Constants. *Chem. Rev.* **1999**, *99*, 293−352.
(679) Brabec, T., Ed. *Strong Field Laser Physics*; Springer: New York, 2008.
(680) Suzuki, M.; Mukamel, S. Many-Body Effects in Molecular Photoionization in Intense Laser Fields; Time-Dependent Hartree-Fock Simulations. *J. Chem. Phys.* **2004**, *120*, 669−676.
(681) Krause, P.; Schlegel, H. B. Strong-Field Ionization Rates of Linear Polyenes Simulated with Time-Dependent Configuration Interaction with an Absorbing Potential. *J. Chem. Phys.* **2014**, *141*, 174104.
(682) Sissay, A.; Abanador, P.; Mauger, F.; Gaarde, M.; Schafer, K. J.; Lopata, K. Angle-Dependent Strong-Field Molecular Ionization Rates with Tuned Range-Separated Time-Dependent Density Functional Theory. *J. Chem. Phys.* **2016**, *145*, 094105.
(683) Sándor, P.; Sissay, A.; Mauger, F.; Abanador, P. M.; Gorman, T. T.; Scarborough, T. D.; Gaarde, M. B.; Lopata, K.; Schafer, K. J.; Jones, R. R. Angle Dependence of Strong-Field Single and Double Ionization of Carbonyl Sulfide. *Phys. Rev. A: At., Mol., Opt. Phys.* **2018**, *98*, 043425.
(684) Kosloff, R.; Kosloff, D. Absorbing Boundaries for Wave Propagation Problems. *J. Comput. Phys.* **1986**, *63*, 363−376.
(685) Krause, J. L.; Schafer, K. J.; Kulander, K. C. Calculation of Photoemission from Atoms Subject to Intense Laser Fields. *Phys. Rev. A: At., Mol., Opt. Phys.* **1992**, *45*, 4998−5010.
(686) Muga, J.; Palao, J.; Navarro, B.; Egusquiza, I. Complex Absorbing Potentials. *Phys. Rep.* **2004**, *395*, 357−426.
(687) Tao, L.; Vanroose, W.; Reps, B.; Rescigno, T. N.; McCurdy, C. W. Long-Time Solution of the Time-Dependent Schrödinger Equation for an Atom in an Electromagnetic Field using Complex Coordinate Contours. *Phys. Rev. A: At., Mol., Opt. Phys.* **2009**, *80*, 063419.
(688) Scrinzi, A. Infinite-Range Exterior Complex Scaling as a Perfect Absorber in Time-Dependent Problems. *Phys. Rev. A: At., Mol., Opt. Phys.* **2010**, *81*, 053845.
(689) Telnov, D. A.; Sosnova, K. E.; Rozenbaum, E.; Chu, S.-I. Exterior Complex Scaling Method in Time-Dependent Density-Functional Theory: Multiphoton Ionization and High-Order-Harmonic Generation of Ar Atoms. *Phys. Rev. A: At., Mol., Opt. Phys.* **2013**, *87*, 053406.
(690) Grobe, R.; Haan, S.; Eberly, J. A Split-Domain Algorithm for Time-Dependent Multi-Electron Wave Functions. *Comput. Phys. Commun.* **1999**, *117*, 200−210.
(691) De Giovannini, U.; Varsano, D.; Marques, M. A.; Appel, H.; Gross, E. K.; Rubio, A. Ab Initio Angle-and Energy-Resolved Photoelectron Spectroscopy with Time-Dependent Density-Functional Theory. *Phys. Rev. A: At., Mol., Opt. Phys.* **2012**, *85*, 062515.
(692) Martín, F. Ionization and Dissociation using B-Splines: Photoionization of the Hydrogen Molecule. *J. Phys. B: At., Mol. Opt. Phys.* **1999**, *32*, R197−R231.
(693) Madsen, L. B.; Nikolopoulos, L.; Kjeldsen, T. K.; Fernández, J. Extracting Continuum Information from $\Psi(t)$ in Time-Dependent Wave-Packet Calculations. *Phys. Rev. A: At., Mol., Opt. Phys.* **2007**, *76*, 063407.
(694) Moiseyev, N. *Non-Hermitian Quantum Mechanics*; University Press: Cambridge, 2011.
(695) Sándor, P.; Sissay, A.; Mauger, F.; Gordon, M. W.; Gorman, T.; Scarborough, T.; Gaarde, M. B.; Lopata, K.; Schafer, K.; Jones, R. Angle-Dependent Strong-Field Ionization of Halomethanes. *J. Chem. Phys.* **2019**, *151*, 194308.
(696) Tellgren, E. I.; Teale, A. M.; Furness, J. W.; Lange, K.; Ekström, U.; Helgaker, T. Non-Perturbative Calculation of Molecular Magnetic Properties within Current-Density Functional Theory. *J. Chem. Phys.* **2014**, *140*, 034101.
(697) Reimann, S.; Borgoo, A.; Austad, J.; Tellgren, E. I.; Teale, A. M.; Helgaker, T.; Stopkowicz, S. Kohn−Sham Energy Decomposition for Molecules in a Magnetic Field. *Mol. Phys.* **2019**, *117*, 97−109.
(698) Reimann, S.; Borgoo, A.; Tellgren, E. I.; Teale, A. M.; Helgaker, T. Magnetic-Field Density-Functional Theory (BDFT): Lessons from the Adiabatic Connection. *J. Chem. Theory Comput.* **2017**, *13*, 4089−4100.
(699) Zhao, L.; Tao, Z.; Pavošević, F.; Wildman, A.; Hammes-Schiffer, S.; Li, X. Real-Time Time-Dependent Nuclear-Electronic Orbital Approach: Dynamics Beyond the Born-Oppenheimer Approximation. *J. Phys. Chem. Lett.* **2020**, *11*, 4052−4058.
(700) Pavošević, F.; Culpitt, T.; Hammes-Schiffer, S. Multicomponent Quantum Chemistry: Integrating Electronic and Nuclear Quantum Effects via the Nuclear-Electronic Orbital Method. *Chem. Rev.* **2020**, *120*, 4222−4253.
(701) Feynman, R. P. Simulating Physics with Computers. *Int. J. Theor. Phys.* **1982**, *21*, 467−488.
(702) Lloyd, S. Universal Quantum Simulators. *Science* **1996**, *273*, 1073−1078.

https://dx.doi.org/10.1021/acs.chemrev.0c00223
Chem. Rev. XXXX, XXX, XXX−XXX